Alikhanov Institute for Theoretical and Experimental Physics
Russian Federation State scientific center

Dense Cold Matter

1. Motivation
2. Dense Cold Matter
3. Kinematical trigger
4. Experimental status
5. Detector for DCM study
6. Perspectives

1. Motivation(1)

Strong interacting QGP is one of the most remarkable discovery for the last 10 years.
Important itself this discovery also
1)Show the importance of collective phenomena.
2)Provides new energy scale for physics ~200MeV(the temperature of the plasma).
3)Break the tendency of the study of particle interaction at the maximum available energy.

1. Motivation(2)

The theory of electrodynamics has been tested and found correct to a few parts in a trillion. The theory of weak interactions has been tested and found correct to a few parts in a thousand. Perturbative aspects of QCD have been tested to a few percent. In contrast, **non-perturbative aspects of QCD** (such as **confinement or deconfinement**) have barely been tested. The study of the **QGP** is part of this effort to consolidate the grand theory of **particle physics.** In particle physics, **hadronization** is the process of the formation of hadrons out of quarks and gluons. Due to postulated colour **confinement**, these cannot exist individually. In the Standard Model they combine with quarks and antiquarks spontaneously created from the vacuum to form hadrons. The QCD (Quantum Chromodynamics) dynamics of the hadronization process are not yet fully understood, but are modeled and parameterized in a number of phenomenological studies, including the Lund **string** model and in various long-range QCD approximation schemes

Hadronization a) in vacuum (particle physics)
b) in artificial gluon matter (See, also ***Gluodynamics**)
c) in quark matter → **dense baryonic matter**

1. Motivation(3)

~Forty years ago [1], T.D. Lee suggested that it would be interesting to explore new phenomena “by distributing high energy **or high nucleon density** over a relatively large volume”. In this way one could
1)temporarily restore broken symmetries of the physical vacuum and
2)possibly create novel abnormal dense states of nuclear matter [2].

W. Greiner and collaborators pointed out that the required high densities could be achieved via relativistic heavy ion collisions [3]. Concurrently, Collins and Perry and others [4] realized that the asymptotic freedom property of quantum chromodynamics (QCD) implies the existence of an ultra-dense form of matter with deconfined quarks and gluons, called later the quark–gluon plasma (QGP) [5].

[1] Report of the workshop on BeV/nucleon collisions of heavy ions—how and why, Bear Mountain, New York, 29 November–1 December, 1974, BNL-AUI, 1975;
G. Baym, Nucl. Phys. A 698 (2002) 23, hep-ph/0104138.
[2] T.D. Lee, G.C. Wick, Phys. Rev. D 9 (1974) 2291.
[3] J. Hofmann, H. Stocker,W. Scheid,W. Greiner, in: Bear Mountain Workshop, New York, December 1974;
H.G. Baumgardt, et al., Z. Phys. A 273 (1975) 359.
[4] J.C. Collins, M.J. Perry, Phys. Rev. Lett. 34 (1975) 1353;
G. Baym, S.A. Chin, Phys. Lett. B 62 (1976) 241;
B.A. Freedman, L.D. McLerran, Phys. Rev. D 16 (1977) 1169;
G. Chapline, M. Nauenberg, Phys. Rev. D 16 (1977) 450.
[5] E.V. Shuryak, Sov. Phys. JETP 47 (1978) 212–219, Zh. Eksp. Teor. Fiz. 74 (1978) 408–420 (in Russian);
E.V. Shuryak, Phys. Lett. B 78 (1978) 150;
E.V. Shuryak, Phys. Rep. 61 (1980) 71–158;
O.K. Kalashnikov, V.V. Klimov, Phys. Lett. B 88 (1979) 328;
J.I. Kapusta, Nucl. Phys. B 148 (1979) 461.

Phase diagram of nuclear matter

*current region of the experiments

**ρ/ρ_0»1,

T/T_0«1(DenseColdMatter): rich structure of the QCD phase diagram - new phenomena are expected

***Diagram study not finished- additional new phenomena can be found

See, for example L.McLerran, “Happy Island”, arXiv:1105.4103 [hep-ph] and ref. therein.

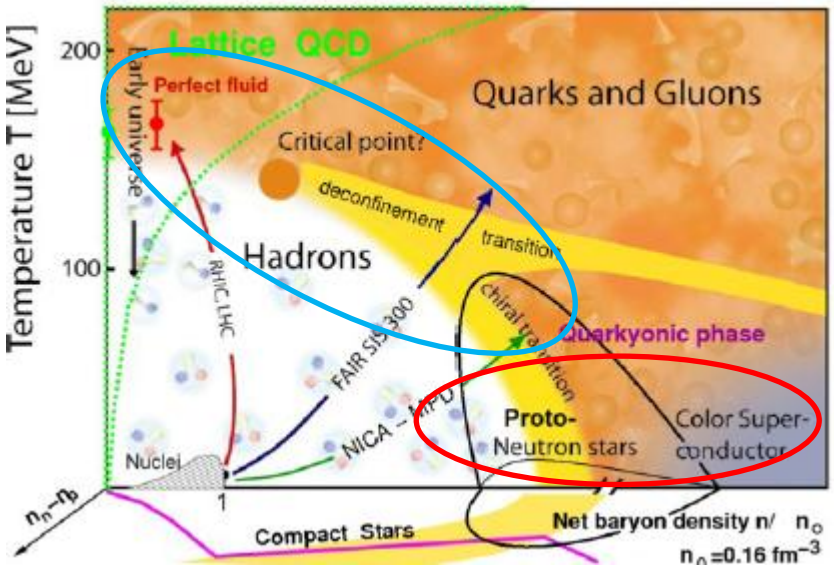

*NICA

2. Dense Cold Matter(1)

Different ways to Dense Cold Matter:

1) $m \to \infty$ (neutron(compact) stars)

2) $T \to 0$ (condensed matter)

3) $V \to 0$ (nuclear physics)

2. Dense Cold Matter(2)

An example of dense cold matter: Neutron star

Under the effect of the gravitational collapse of a core heavier than 1.4 solar masses, the matter is forced into a degenerate state: electrons are unable to remain in their orbits around the nuclei (they would have to traver faster than light in order to obey the Pauli exclusion principle) and they are forced to penetrate the atomic nuclei. So they fuse with protons, and form neutrons. Pauli's principle, that we've seen before, forbids two neutrons having the same state to stay in the same place . This principle creates a degeneracy pressure fighting against gravity, and so allows the remnant of the star to find an equilibrium state.The result of this process is a so called 'neutron star', whose diameter is about 10 to 20 kilometers, weighting as much as the Sun. Its surface is like a hard and smooth ball, where the highest mountain is less than one micrometer. The surface of the star is mainly iron.

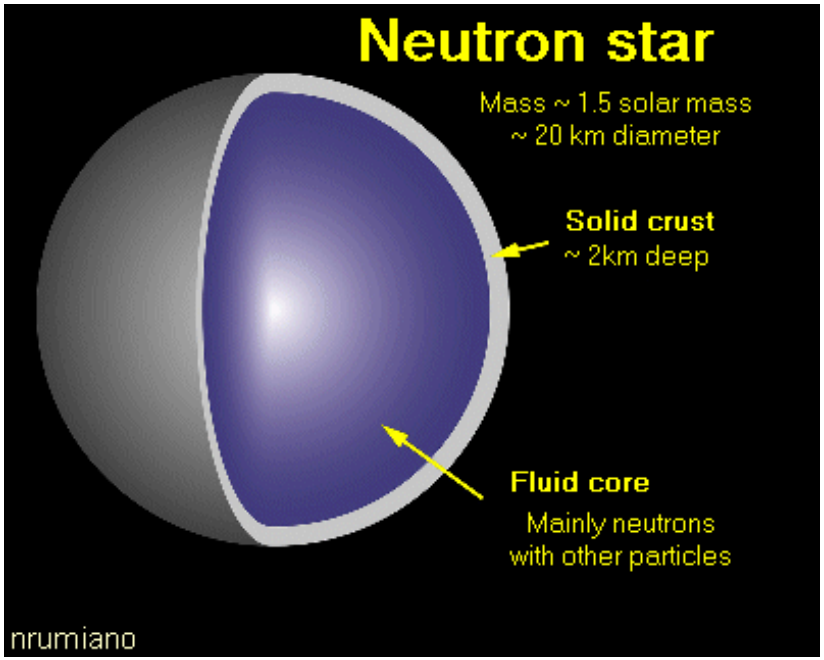

2. Dense Cold Matter(3)

Only in the most primitive conception, a neutron star is constituted from neutrons. At the densities that exist in the interiors of neutron stars, the neutron chemical potential, μ_n, easily exceeds the mass of the so that neutrons would be replaced with hyperons. From the threshold relation $\mu_n = \mu$ it follows that this would happen for neutron Fermi momenta greater than $k_{Fn} \sim 3$ fm^{-1}. Such Fermi momenta correspond to densities of just $\sim 2\rho_0$, with $\rho_0 = 0.16$ fm^{-3} the baryon number density of infinite nuclear matter.(F.Weber et.al.,astro-ph/0604422)

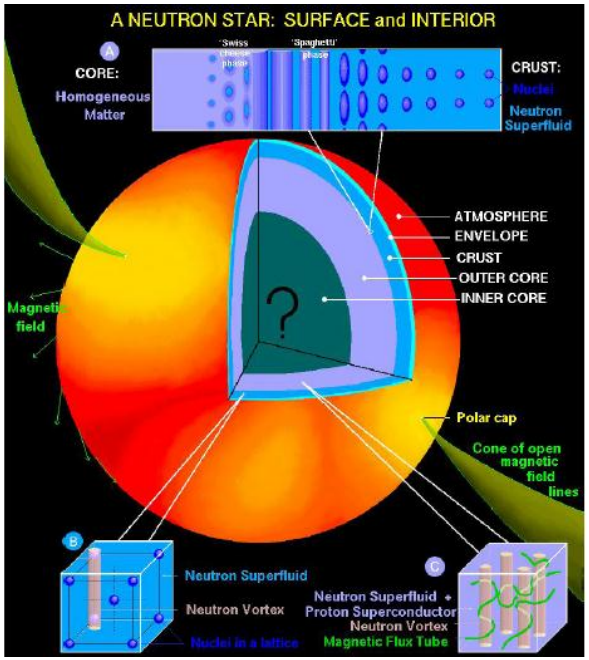

A rendition of the structure and phases of a neutron star (courtesy of Dany Page) nucl-th/0901.4475

*strangeness enhancement in DCM
**exotic(dibaryons, pentaquarks,…)

2. Dense Cold Matter(4)

Condensed matter(not an analog in the state of matter but for the statistical properties of the system):

Advances in atom cooling and detection have led to the observation and full characterisation of the atomic analogue of the HBT effect

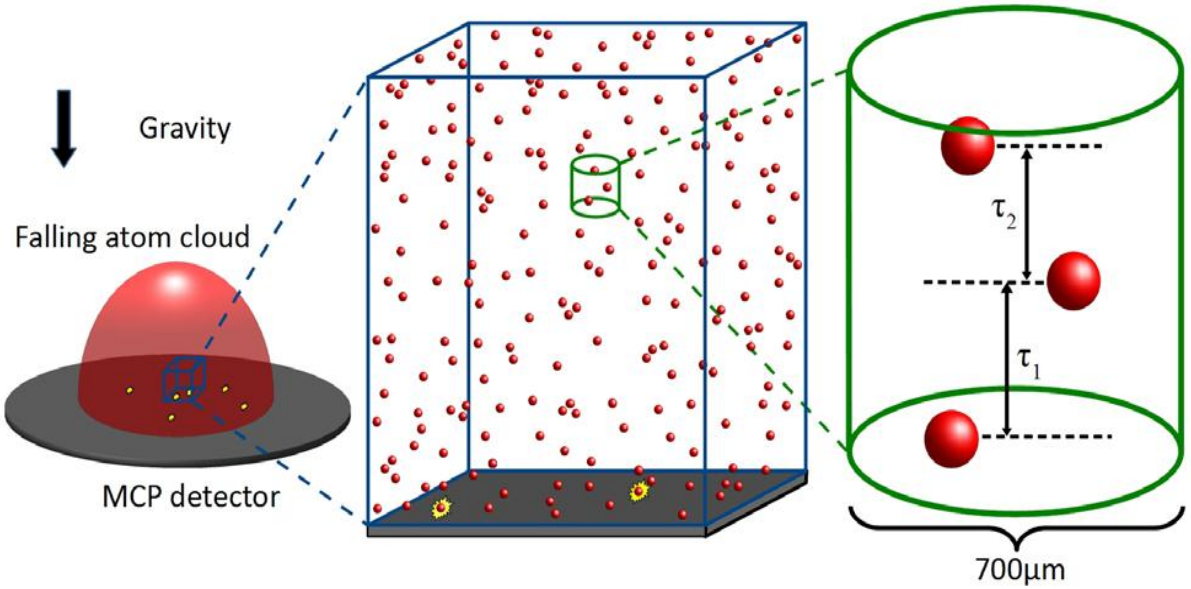

Fig.2-K.G.H. Baldwin, *Contemp. Phys.* **46**, 105 (2005).

Caption for figure 1: The experimental setup. A cold cloud of metastable helium atoms is released at the switch-off of a magnetic trap. The cloud expands and falls under the effect of gravity onto a time resolved and position sensitive detector (micro-channel plate and delay-line anode), that detects single atoms. The inset shows conceptually the two 2-particle amplitudes (in black or grey) that interfere to give bunching or antibunching: S1 and S2 refer to the initial positions of two identical atoms jointly detected at D1 and D2.

T.Jeltes et al., Nature,**445**,402(2007)

2. Dense Cold Matter(5)

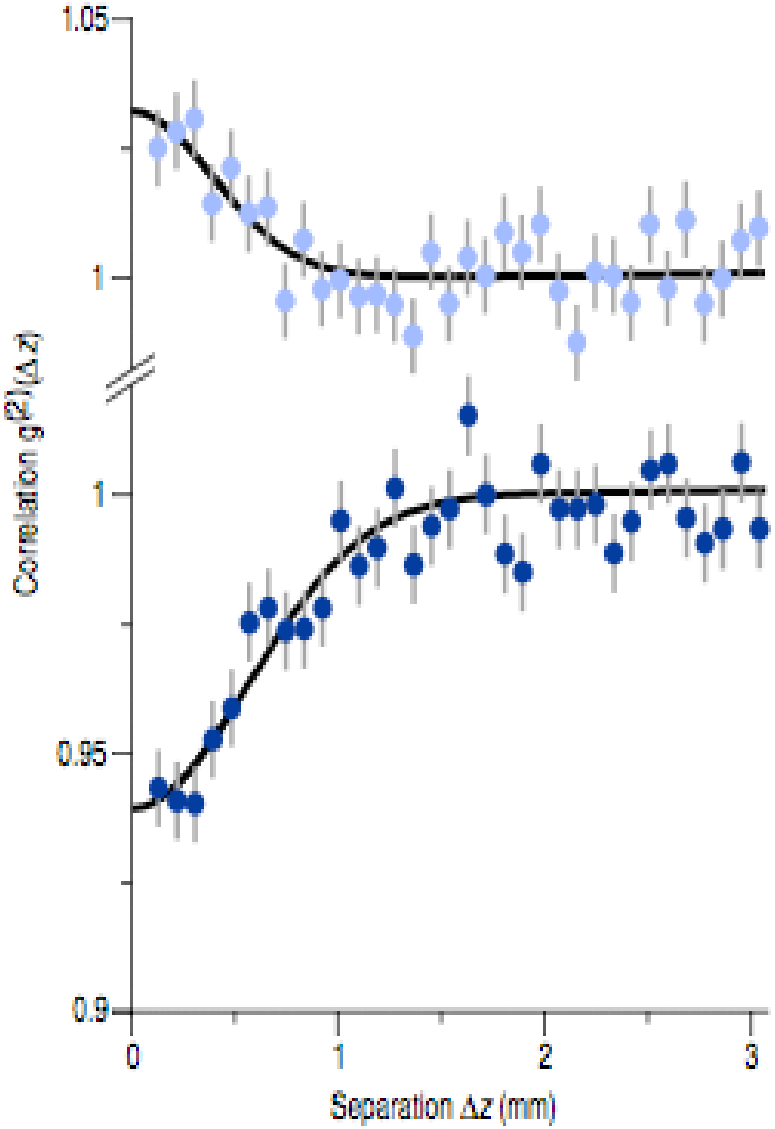

Caption for figure 2: Normalised correlation functions for 4He* (bosons) in the upper graph, and 3He* (fermions) in the lower graph. Both functions are measured at the same cloud temperature (0.5 μK), and with identical trap parameters. Error bars correspond to the root of the number of pairs in each bin. The line is a fit to a Gaussian function. The bosons show a bunching effect; the fermions anti-bunching. The correlation length for 3He* is expected to be 33% larger than that for 4He* due to the smaller mass. We find 1/e values for the correlation lengths of 0.75±0.07 mm and 0.56±0.08 mm for fermions and bosons respectively.

T.Jeltes et al.,Nature,**445**,402(2007)

2. Dense Cold Matter(6)

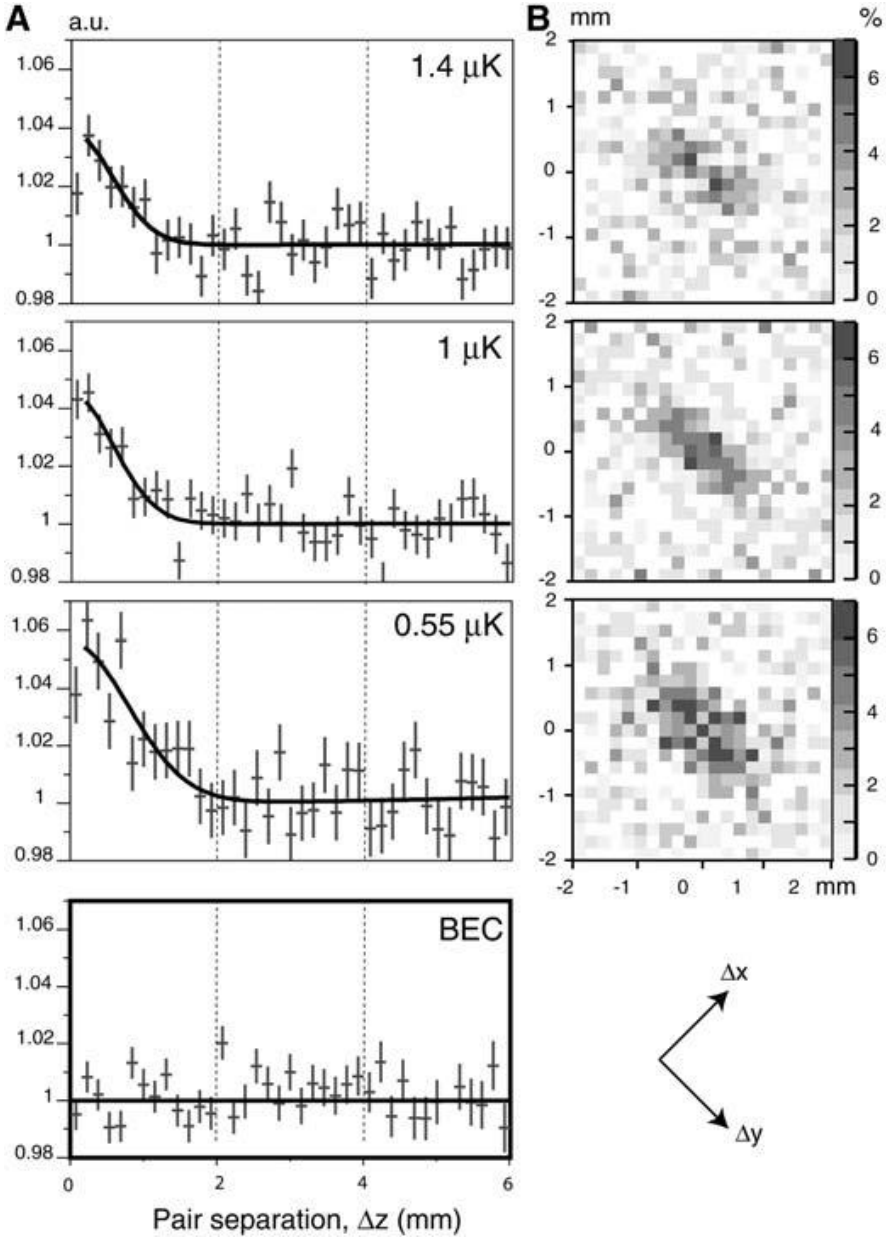

Hanbury Brown Twiss Effect for Ultracold Quantum Gases

M. Schellekens,R. Hoppeler,A. Perrin,J. Viana Gomes,D. Boiron, A. Aspect, C. I. Westbrook

We have studied two-body correlations of atoms in an expanding cloud above and below the Bose-Einstein condensation threshold. The observed correlation function for a thermal cloud shows a bunching behavior, whereas the correlation is flat for a coherent sample. These quantum correlations are the atomic analog of the Hanbury Brown Twiss effect.

Fig. 2. (A) Normalized correlation functions along the vertical (z) axis for thermal gases at three different temperatures and for a BEC. For the thermal clouds, each plot corresponds to the average of a large number of clouds at the same temperature. Error bars correspond to the square root of the number of pairs. a.u., arbitrary units. (B) Normalized correlation functions in the Dx j Dy plane for the three thermal gas runs. The arrows at the bottom show the 45- rotation of our coordinate system with respect to the axes of the detector. The inverted ellipticity of the correlation function relative to the trapped cloud is visible.

Science,v.310,p.648(2005)

3.Kinematical trigger-1

How the new state of matter is created in the lab?

Y. Ivanov, V. Russkikh, V.Toneev,
Phys. Rev. C73 (2006) 044904

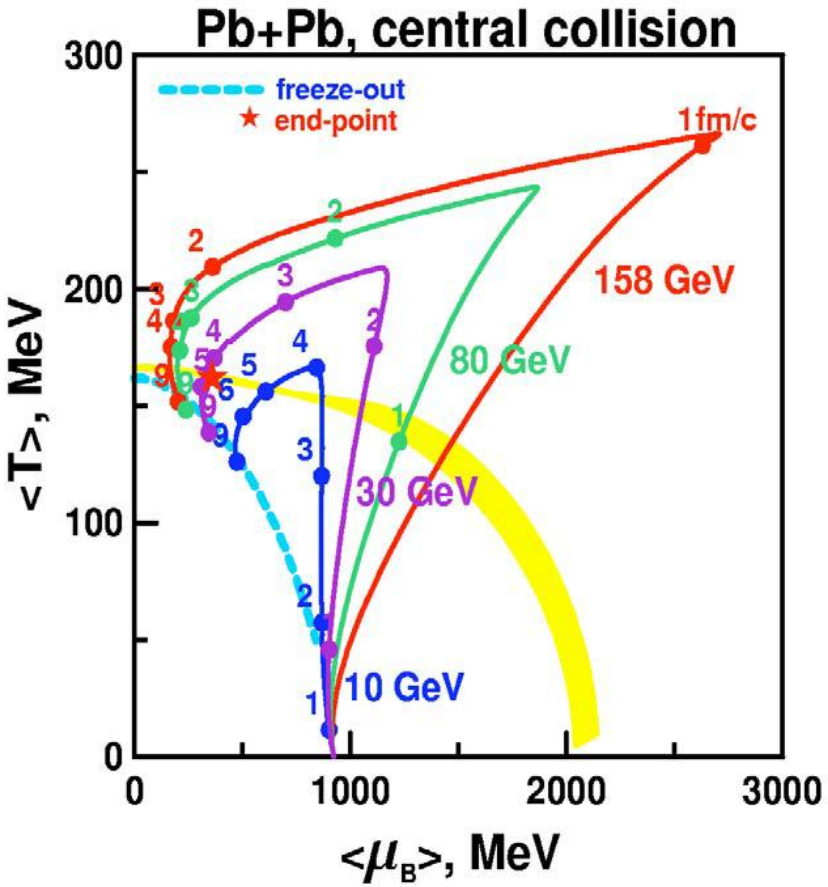

The QGP can be created by heating matter up to a temperature of 2×10^{12} K, which amounts to 175 MeV per particle. This can be accomplished by colliding two large nuclei at high energy (note that 175 MeV is not the energy of the colliding beam). Lead and gold nuclei have been used for such collisions at CERN and BNL, respectively. The nuclei are accelerated to ultrarelativistic speeds and slammed into each other. When they do collide, the resulting hot volume called a "fireball" is created after a head-on collision. Once created, this fireball is expected to expand under its own pressure, and cool while expanding. By carefully studying this flow, experimentalists put the theory to test.

*Region ρ/ρ_0»1, T/T_0«1(DenseColdMatter) hardly accessible experimentally by standard way

4. Kinematical trigger -2

Phase diagram*

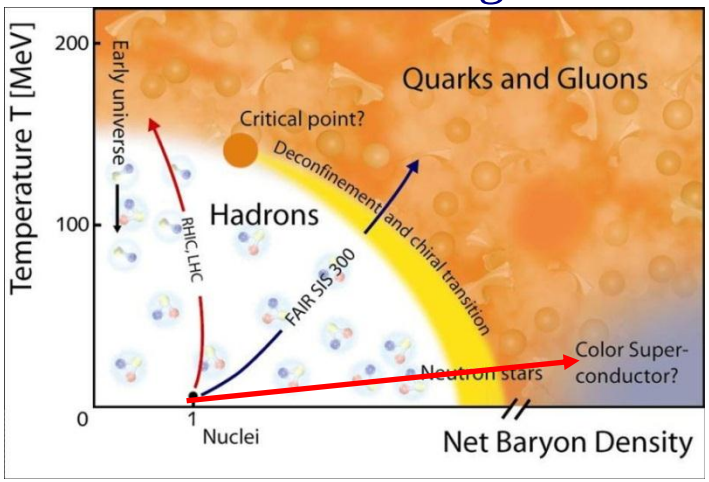

*http://www.gsi.de/forschung/fair_experiments/CBM/

Scheme of process

High p_T trigger $\gamma,\gamma(\pi^o),\pi^{\pm},K^{\pm}\ldots$

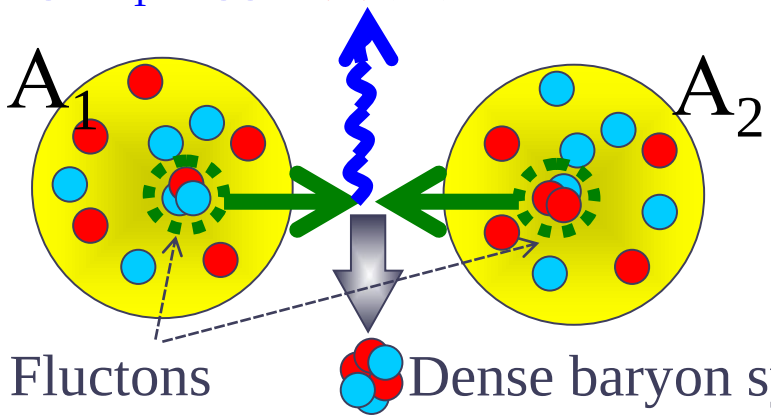

Kinematical limits for γ from different subprocesses: 1N+1N(black line)
1N+Flucton(2N,3N,4N)&
Flucton+1N(blue lines)
Flucton+Flucton(red lines)

He+He @ 6 AGeV

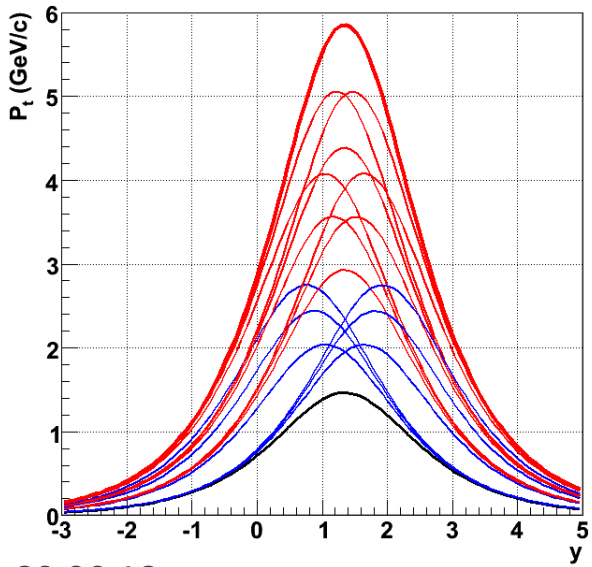

4. Kinematical trigger -3

J. Arrington, 2004

~~Crazy~~ New ideas: Probe even higher densities

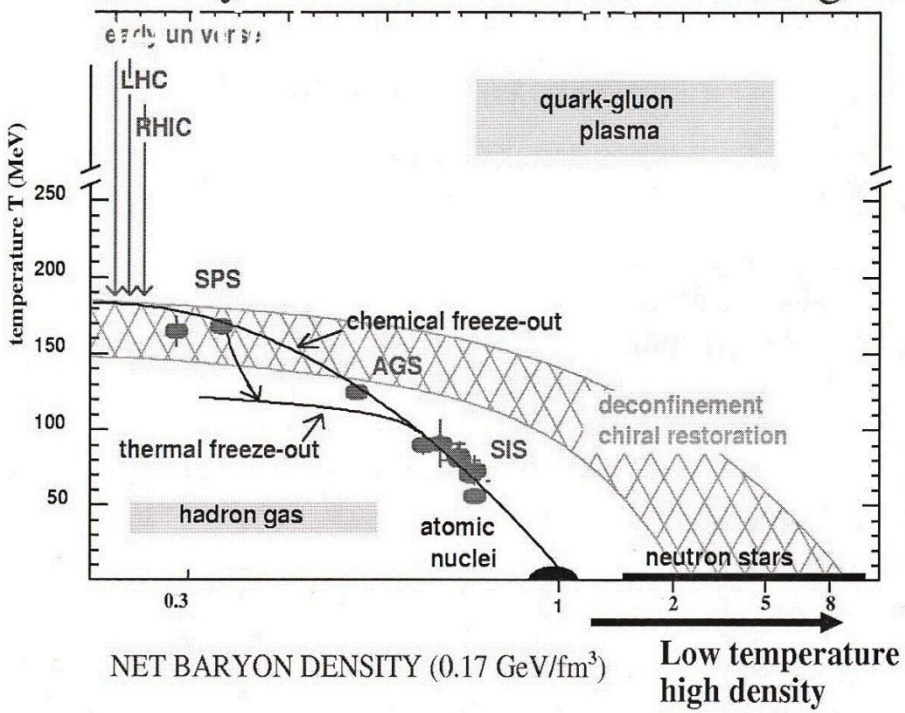

Average nuclear density is a few times smaller than the critical density

A nucleus is a dynamic system, with local fluctuations in density

These fluctuations provide a small high-density component (short-range correlations)

* This may be origin of EMC effect, medium modifications
* We can try to isolate SRCs to probe high density matter

If SRCs are the source of the EMC effect, why probe nuclei? ***Probe SRCs instead!***

4. Kinematical trigger -4

The Study of Cold, Dense Nuclear Matter at BNL

Yousef Makdisi, Brookhaven National Laboratory
Eli Piasetzky, Tel Aviv University
John Watson, Kent State University
Mark Strikman, Pennsylvania State University

Neutrons and protons, known collectively as nucleons, attract each other strongly, which is why we have atomic nuclei. However, when nucleons get very close at distances shorter than 0.4 fm = $4x10^{-16}$ m, they repel each other strongly, which is why nuclei do not collapse to a point. This repulsion between nucleons at small distances causes all heavy nuclei to have a maximum density at their centers of about 0.18 nucleons/fm^3. "Dense nuclear matter" is then a system of nucleons with density higher than this central density. The repulsive inter-nucleon force at small distances has not been investigated enough to exclude the possibility that the repulsive barrier is penetrable and new kinds of dense nuclear matter may exist under special conditions.

3.Kinematical trigger-5

CLAS $e^-A \rightarrow e^-X$ @~4 AGeV

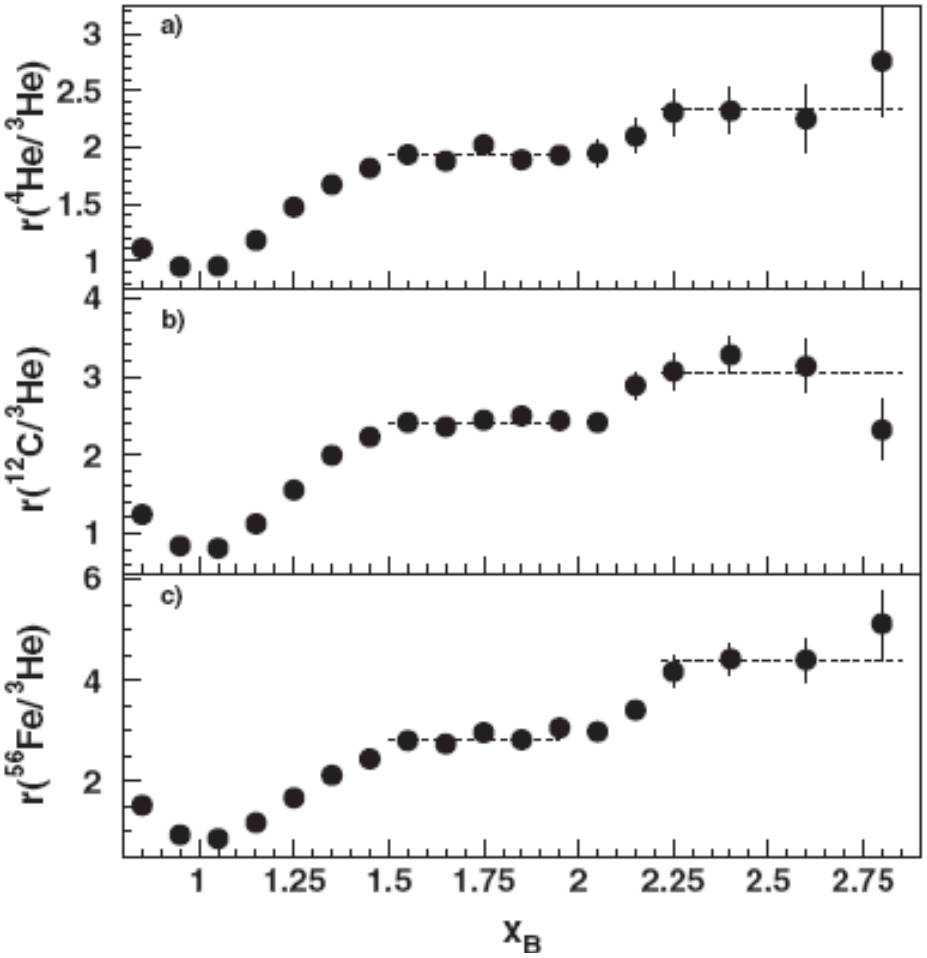

K.S. Egiyan et al. Phys. Rev. Lett. 96, 082501 (2006)

- No rescattering

	a_{2N}, %	a_{3N}, %	$(a_{2N})^2$, %
^{3}He	8.0±1.6	0.18±0.06	0.64
^{4}He	15.4±3.3	0.42±0.14	2.4
^{12}C	19.3±4.1	0.55±0.17	3.7

dramatic decreasing of the cross sections with N

$$x_B = Q^2/2m_N U$$

4. Kinematical trigger -6

^{12}C – structure

RNP – program at JINR

V.V.B., V.K.Lukyanov, A.I.Titov, PLB, 67, 46(1977)

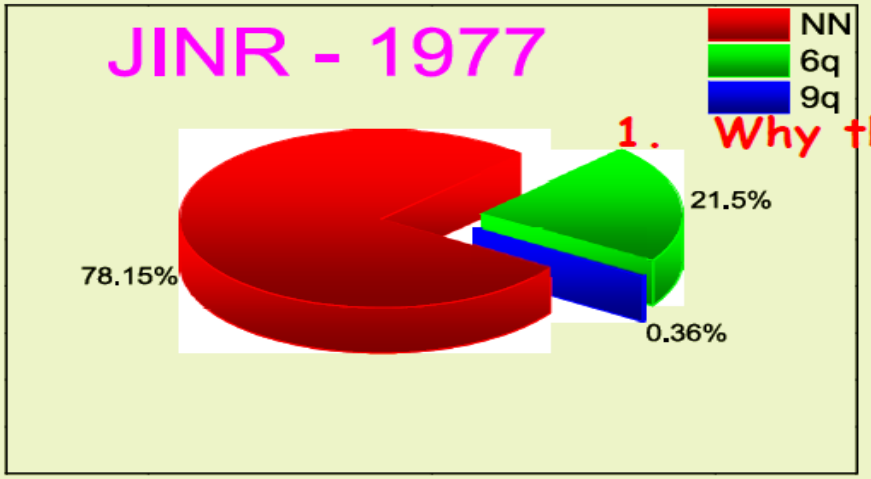

eA – program at JLab

R.Subedi et al., Science 320 (2008) 1476-1478
e-Print: arXiv:0908.1514 [nucl-ex]

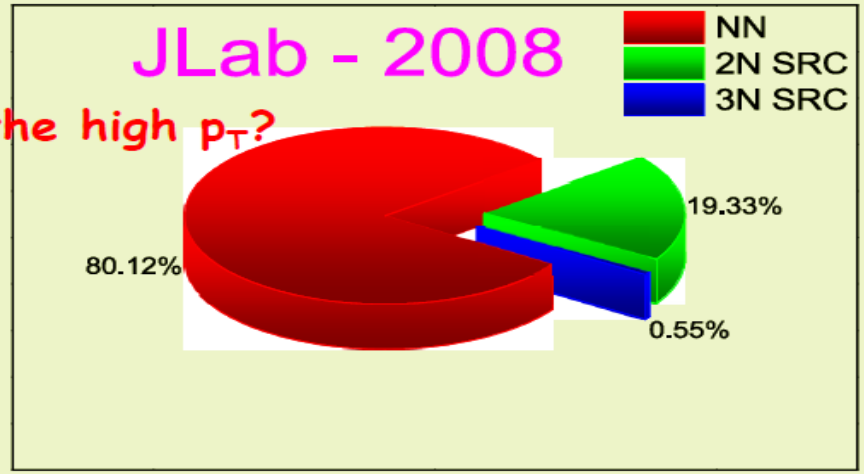

1. Why the high p_T?

"Experimental study the cold dense baryon matter in high p_T processes"

S.S. Shimanskiy (JINR, Dubna)

Лукьянов, Титов, т.10, вып.4, 815-849(1979);
Буров и др. том.15,вып.6, 1249-1295(1984).

3.Kinematical trigger-7

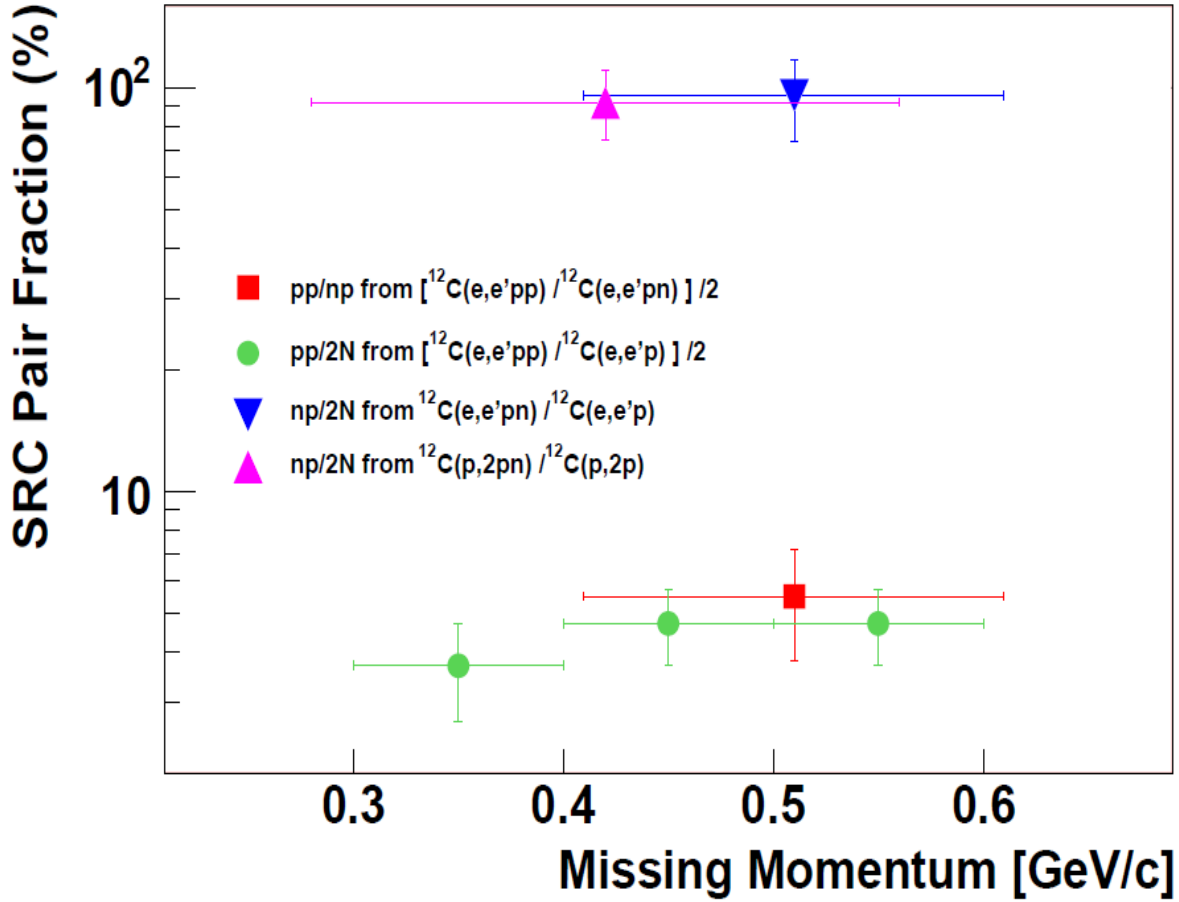

Figure 2: The fractions of correlated pair combinations in carbon as obtained from the (e,e'pp) and (e,e'pn) reactions, as well as from previous (p,2pn) data. The results and references are listed in Table 1.

R. Subedi et al., Probing Cold Dense Nuclear Matter, arXiv:0908.1514v1 [nucl-ex] 11 Aug 2009{http://arxiv.org/abs/0908.1514v1}.
See also preprint ITEP,11-89,1989

3.Kinematical trigger-8

1) K.S. Egiyan et al. Phys. Rev. Lett. 96, 082501 (2006): $W_3/(W_2)2 \sim 1/(6\pm2)$
2) R. Subedi et al., Probing Cold Dense Nuclear Matter, arXiv:0908.1514v1 [nucl-ex] 11 Aug 2009: W(pp+nn)/W(np) ~ 1/(10±2)

Our estimate $\mathbf{W_n \sim (W_2)^{(n-1)} (1/8)^{(n-2)}}$

σ (3N+3N(He+He)) ~ σ(He+He)*$(W_3)^2$ ~2*10^{-6}b
σ (4N+4N(He+He)) ~ σ(He+He)*$(W_4)^2$ ~2*10^{-9}b

"DCM": baryonic droplet with $<P_{NDCM}> < 0.4$GeV/c in the droplet rest frame

T_0=2GeV/nucleon, p_N~0.80GeV/c, $(P_{NDCM}/ P_N)^{3(n-1)}$~3*10^{-5},(n=6) σ(DCM-6N)~60pb

Beam(He): 10^{9}sec $^{-1}$; target(He):0.1; run:1000hours
6n droplet- 2*10^5 events($<P_{NDCM}> <$ 0.3 GeV/c- 6000 events)

Kinematical cooling for cumulative trigger

$dS=d^4p_1 \ldots d^4p_n \delta(p_i^2-m_i^2)\delta^4(\sum_1^n p_i - P_n) ɱ^2$

Nonrelativistic n particles:
$dS \sim T_n^{(3n-5)/2} ɱ^2$

Cumulative trigger:
$ɱ^2 \sim \exp\{-T_n/T_*\}$(neglecting for dramatic decreasing of the cross sections with N)

$T_0 \sim (3n-5)T^*/2n \rightarrow 3T^*/2 \sim 60$MeV, p~300-400MeV/c

4. Experimental status-1

Simplest experimental setup

A_1-projectale nucleus with energy per nucleon E_0, A_2 target nucleus;
a-high p_t (duble)cumulative trigger,
$B_1,\ldots B_n$-dense baryonic system,
$D_{1,2}$-detectors

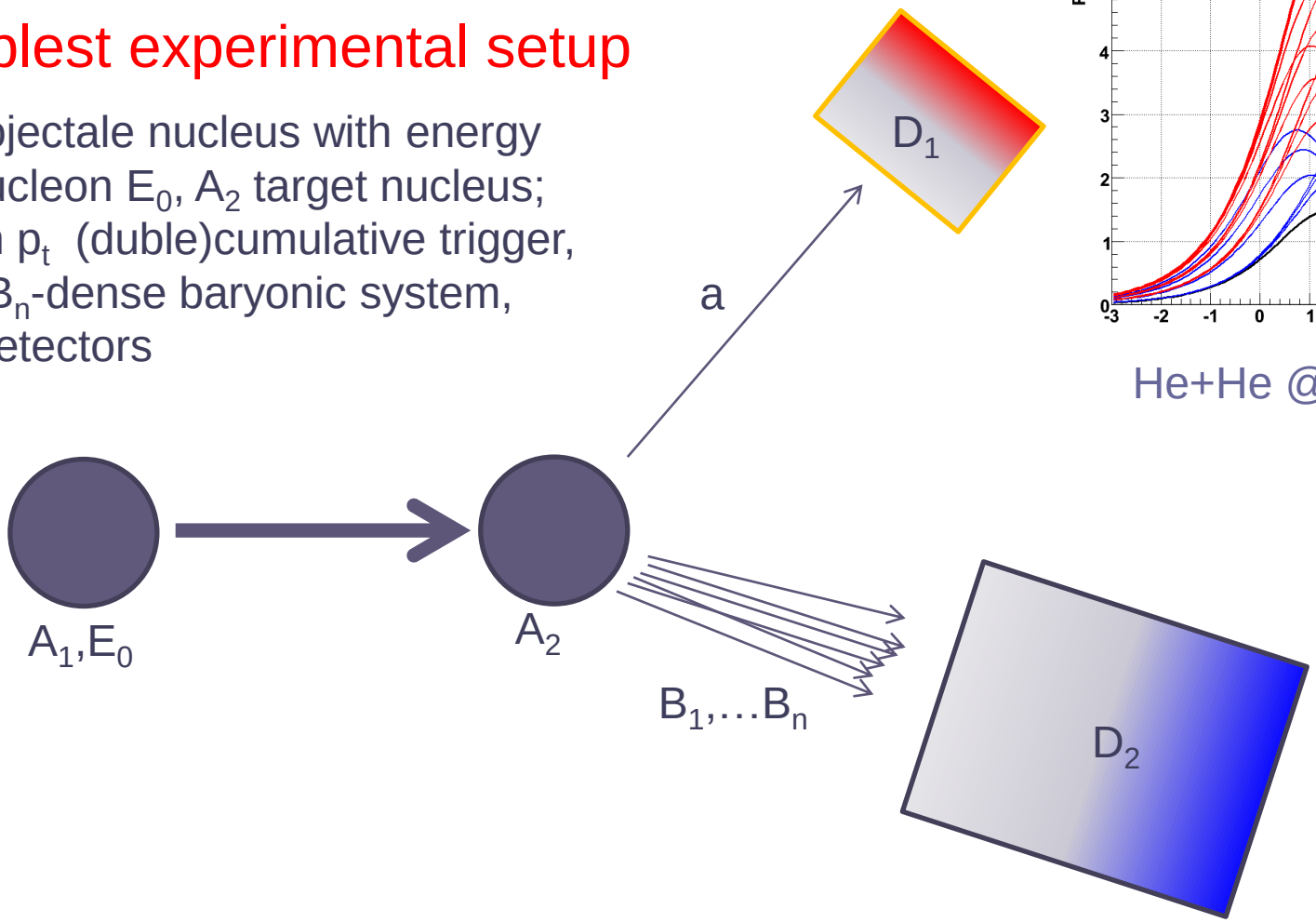

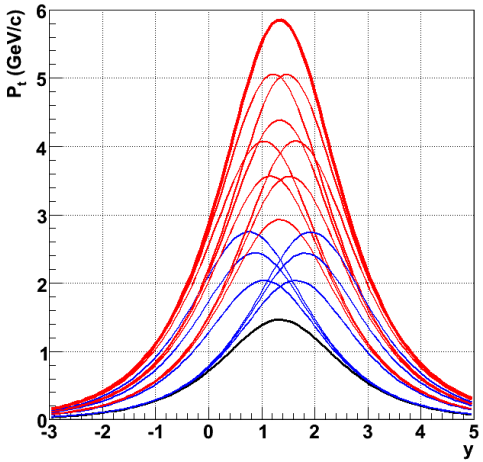

He+He @ 6 AGeV

4. Experimental status-2

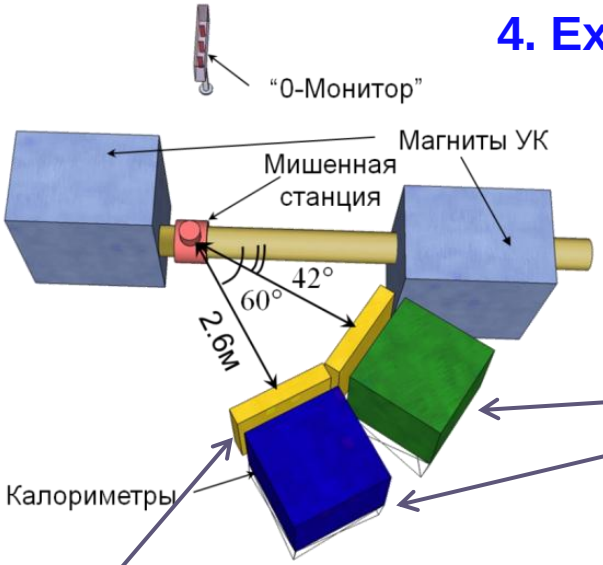

FLINT electromagnetic calorimeters

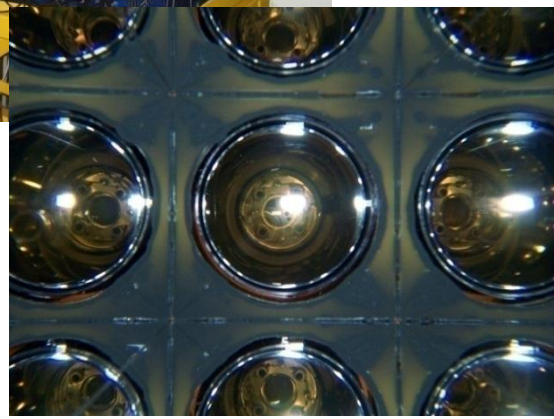

FLINT VETO

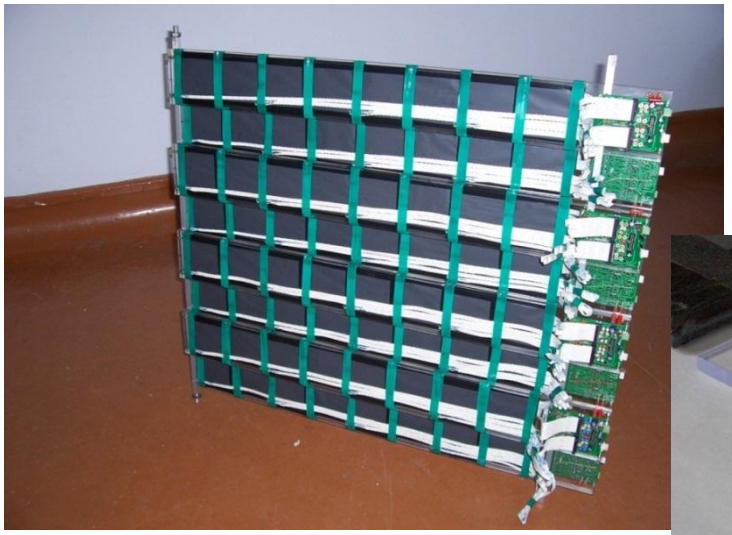

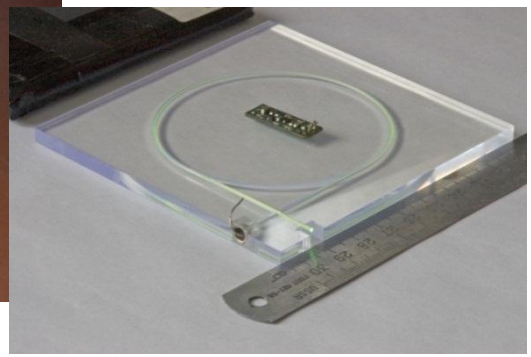

4. Experimental status-3

FLINT DATA: Photon spectra CBe→γX

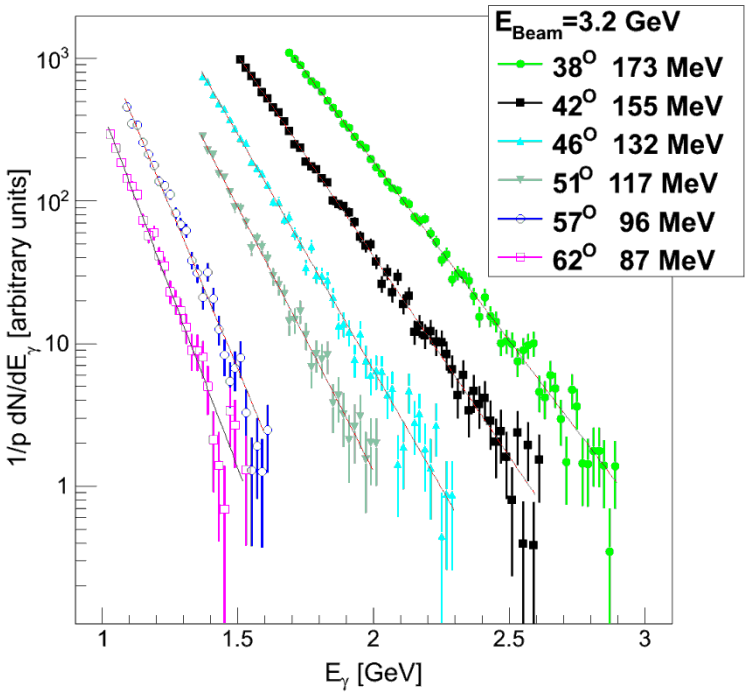

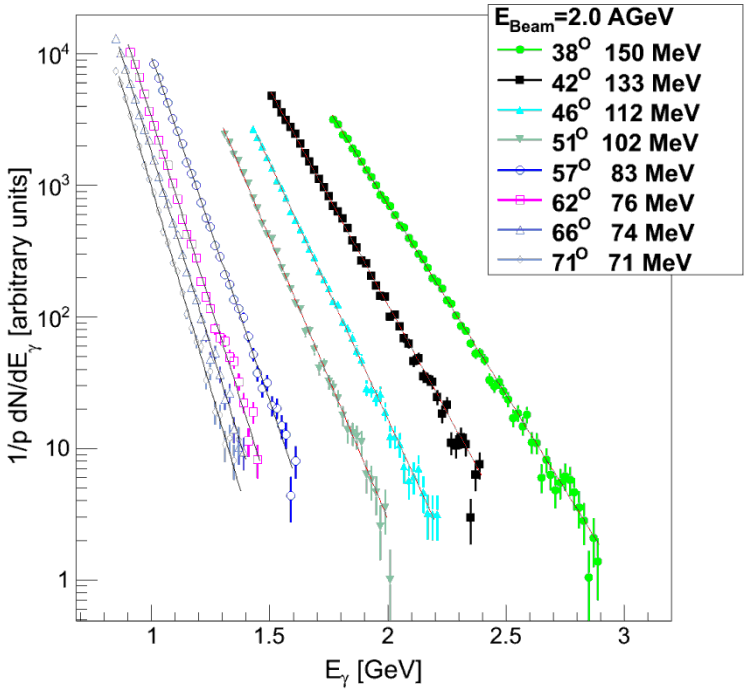

FLINT have got data for fluctonfluctoninteraction up to 6 nucleonskinematicalregion, which cannot be explained neither p+Be nor C+p interactions

Six nucleons system: n!n¡p!p¡+??

Does we already see phase transition?

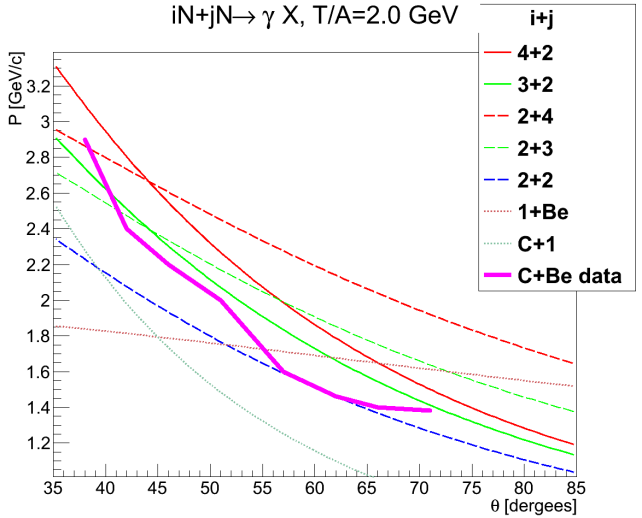

4. Experimental status-5

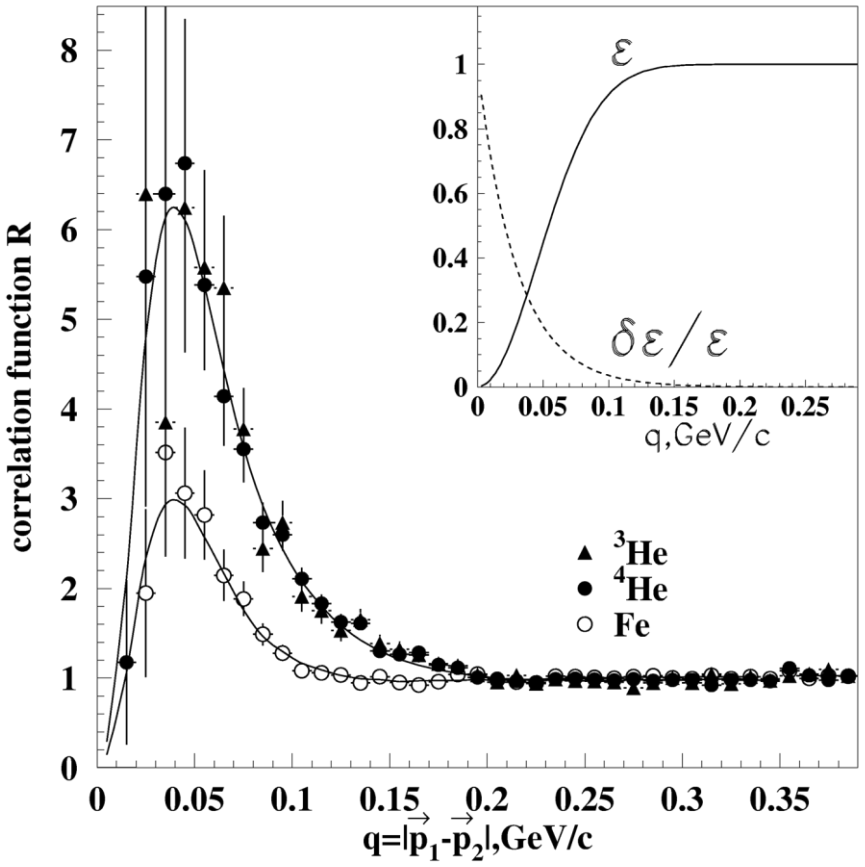

r_f~1-1.5fm

A.S.et al., Phys.Rev.Lett. 93,192301 (2004)

An estimate of baryon density

r_f~1.5fm

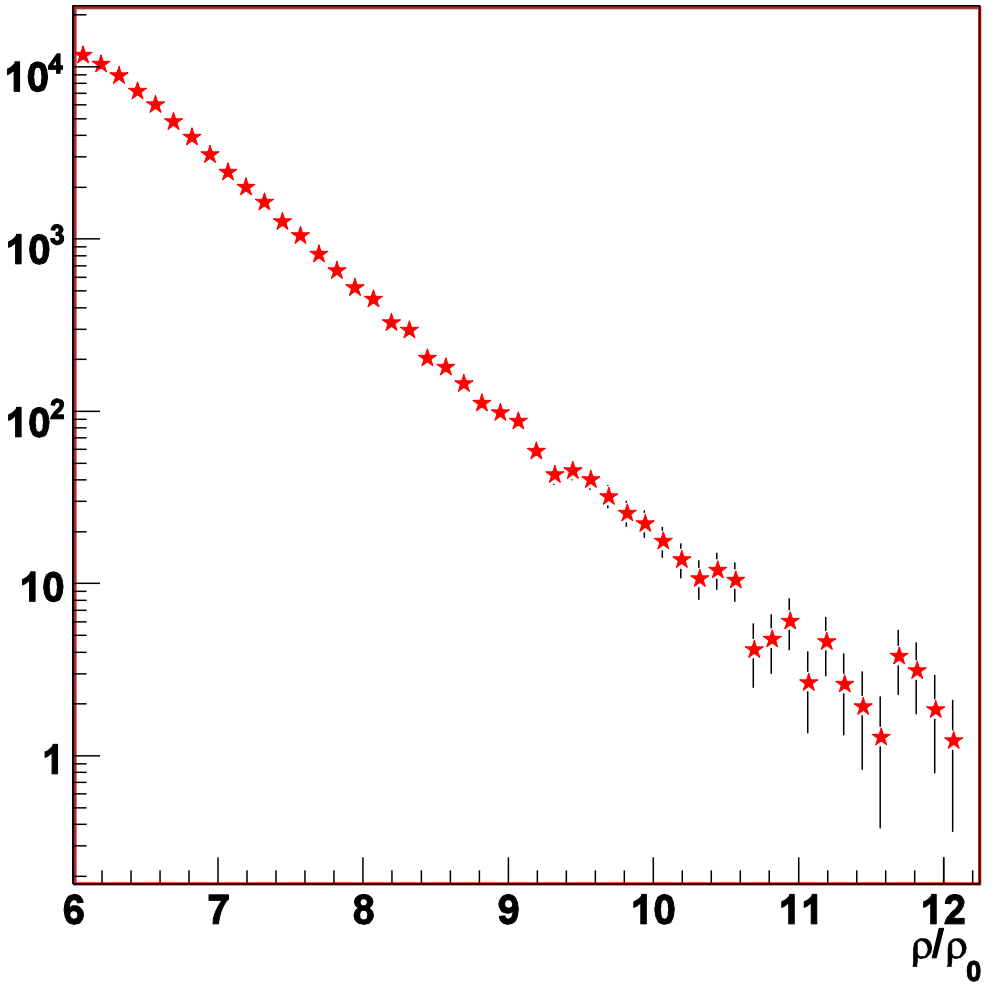

4. Experimental status-7

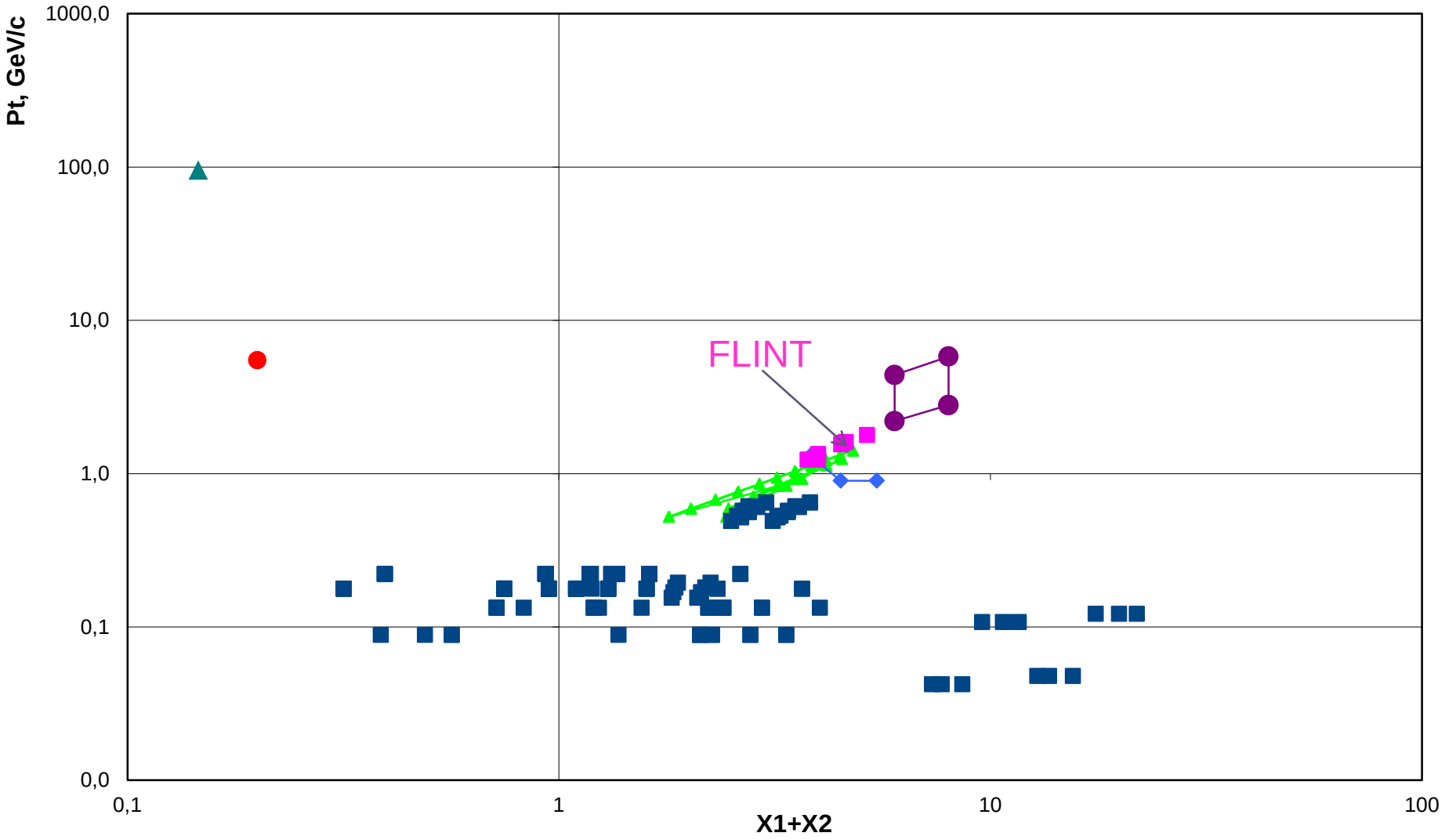

4. Experimental status-8

FHS, ITEP, S.Boyarinov et al.

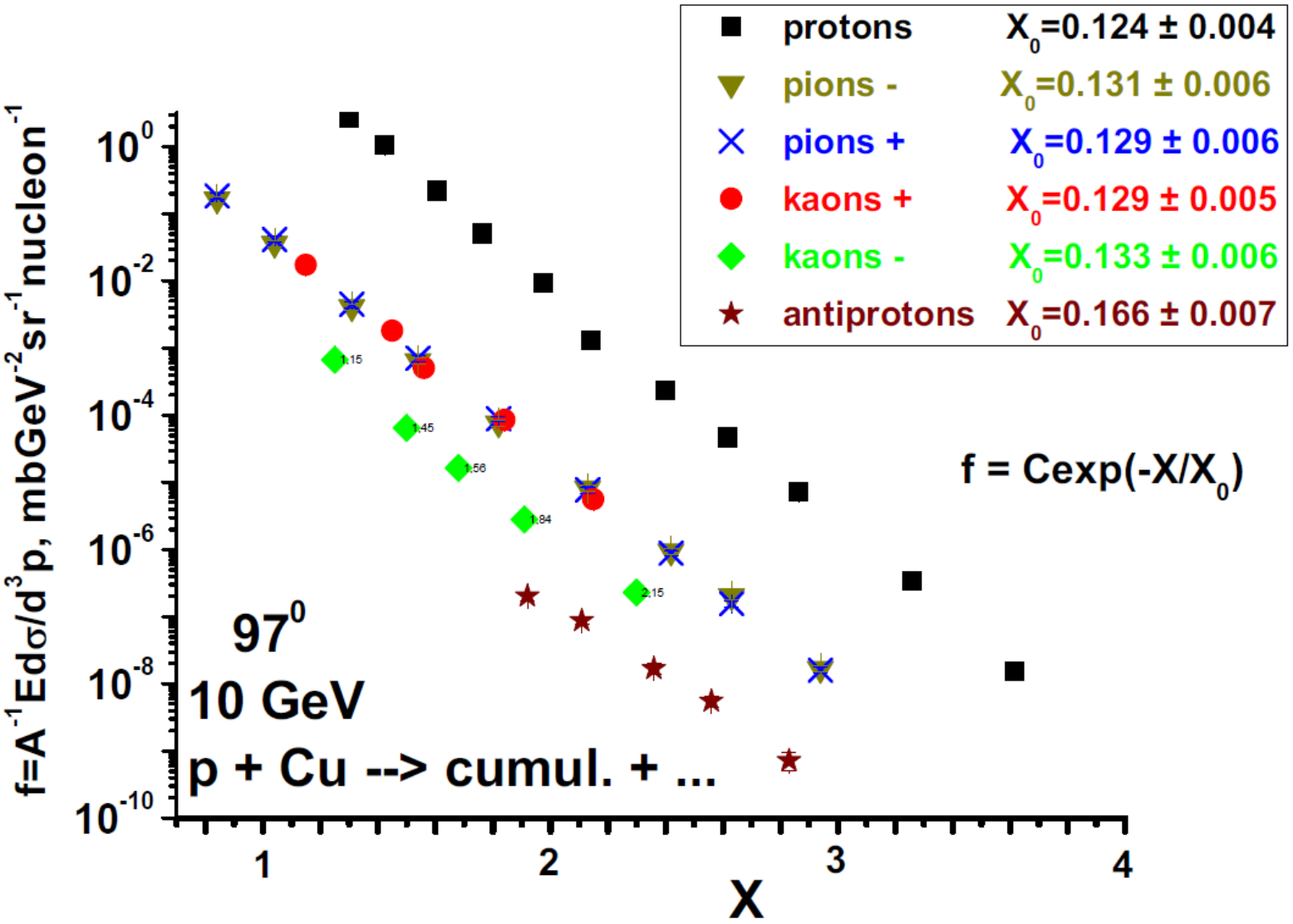

4. Experimental status-9

TAPS $^{12}C+^{12}C \rightarrow \pi^{\circ}(\eta)X$ @ 0.8, 1.0 & 2.0 AGeV

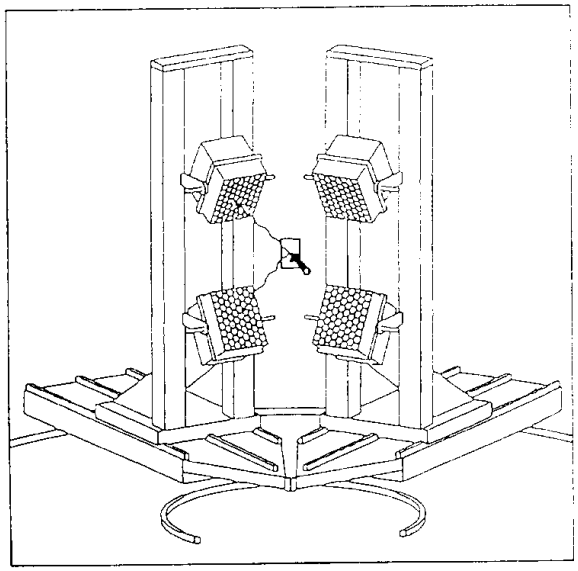

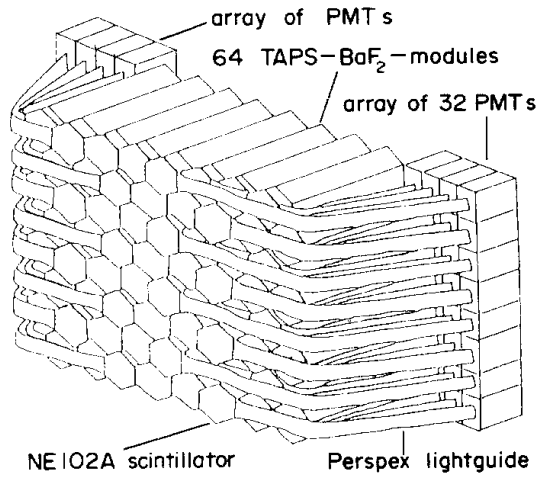

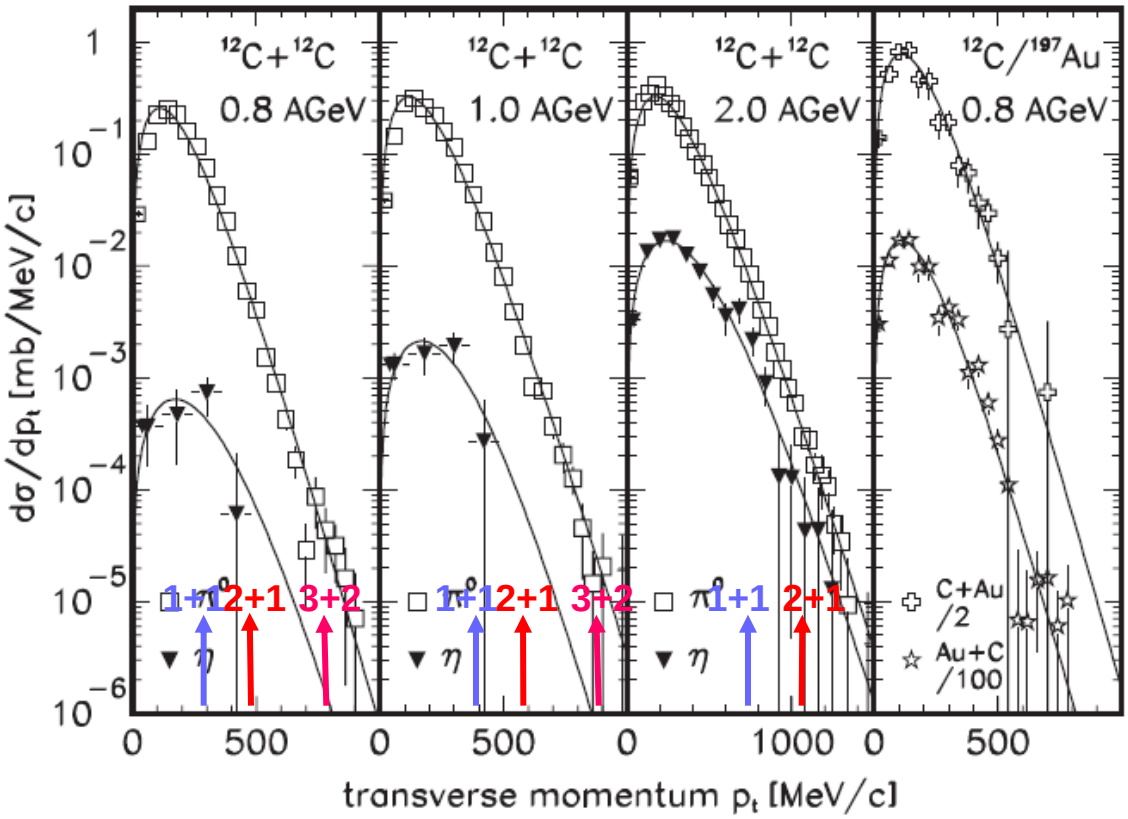

Z. Phys. A 359, 65–73 (1997)

Search for and study of cold dense baryonic matter
(Letter of intent)

O.A.Chernishov [1],A.A.Golubev[1], V.S.Goryachev[1], A.G.Dolgolenko[1], M.M.Kats[1], B.O.Kerbikov[1], S.M.Kiselev[1], Yu.T.Kiselev[1], A.Kogevnikov [1], K.R.Mikhailov[1], N.A.Pivnyuk[1], P.A.Polozov[1], M.S.Prokudin[1], D.V.Romanov[1], V.K.Semyachkin[1], A.V.Stavinskiy[1], V.L.Stolin[1], G.B.Sharkov[1] , N.M.Zhigareva[1], Yu.M.Zaitsev[1], A.Andronenkov[2], A.Ya. Berdnikov[2] , Ya.A. Berdnikov[6], M.A. Braun[2], V.V. Vechernin[2], L. Vinogradov[2], V. Gerebchevskiy[2], S. Igolkin[2], A.E. Ivanov[6], V.T. Kim[3,6], A. Koloyvar[2], V.Kondrat'ev[2], V.A.Murzin[3], V.A. Oreshkin[3], D.P. Suetin[6] , G. Feofilov[2],A.A.Baldin[4], V.S.Batovskaya[4], Yu.T. Borzunov[4], A.V. Kulikov[4], A.V. Konstantinov[4], L.V.Malinina[4,7],G.V.Mesheryakov[4],A.P.Nagaitsev[4], V.K. Rodionov[4], S.S.Shimanskiy[4], O.Yu.Shevchenko[4] , A.V.Gapienko[5], V.I.Krishkin[5] , I.N.Dorofeeva[7], M.M.Merkin[7], AA.Ershov[7], N.P.Zotov[7]

1). ITEP NRC KI , Moscow, 2). SPbSU, S.Peterburg, 3). PINP NRC KI, S.Peterburg, 4). LPHE,JINR,Dubna, 5). IHEP NRC KI, Protvino , 6). SPbSPU, S.Peterburg, 7).MSU,Moscow

Experimental program:

1). Search for and the study of new state of matter at high density and low temperature corner of phase diagram

- search for the dense baryonic droplet in correlation measurements with high p_t cumulative trigger
- femtoscopy measurements for the dense baryonic droplet
- izotopic properties of the droplet
- strangeness production in the droplet
- fluctuations
- search for an exotic in the droplet

2) Dense cold matter contribution in ordinary nuclear matter and its nature SRC,flucton,…

- nuclear fragmentation
- hard scattering

3) Modification of particles properties in nuclear matter

Proposed measurements:

1.Trigger's particles: γ, π, K^-,K^+,p, d, …(p_t /E_0~1)

2. Recoil particles: nucleon, multinucleon systems, nuclear fragments, exotic states

3. Measurement values: <N(p_t ,y)> vs X_{trig} and E_0(2-6GeV/nucleon); -ratios(p/n, ^{3}He/t,…);correlations between recoil particles

Simulations (S.M.Kiselev,ITEP)

Our goal: using the high momentum π^0 as a trigger, study the baryon system produced in 4N+4N → π^0+8N

An instrument: collisions of light nuclei (e.g. ^{4}He+^{4}He and C+Be at T/A=2.0 GeV)

An idea to estimate the background:

- select events with the number of nucleon-participants, $N_{prod} \geq 8$
- among N_{prod} find 8N with minimal momentum, p_{min}
- select events with $p^{8N}_{min} < p_{cut}$ (=100 MeV/c)
- remove this 8N from each event, rest nucleons - background
- add the π^0+8N system, these 8N – signal
- momentum of a nucleon from the signal is smearing with a parameter σ_{smear}: $\sigma_x=\sigma_y=\sigma_z=\sigma_{smear}$= 170 MeV/c. momentum non conservation ΔP due to the removing+adding procedure should be close to zero.

Input info

UrQMD1.3 generator

• 10^6 min. bias ^{4}He+^{4}He and 10^5 C+Be events at T/A=2 GeV ($b<R_1 + R_2$)

4N+4N ↔ π^0+8N in an ^{4}He+^{4}He or C+Be event:

• π^0 will be detected at $\theta_{c.m.}=90^0$ → p_{cumul} = 2.78 GeV/c for T/A=2.0,
(p_x =0, p_y = - p_{cumul} , p_z =0)

• the momentum of every N of the 8N system,
(p_x =0, p_y = p_{cumul} /8, p_z =0)
is smearing with $\sigma_x = \sigma_y = \sigma_z = \sigma_{smear}$ (= 170 MeV/c)
Do N_{cycles} (= 1000) to select the 8N system with minimal ΔP

•our "detector" covers the cone with 45^0 around the y axis

Background and signal 3N+3N

$^4He+^4He$

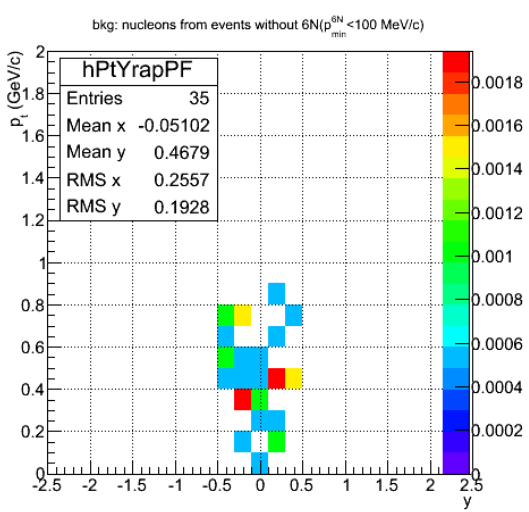

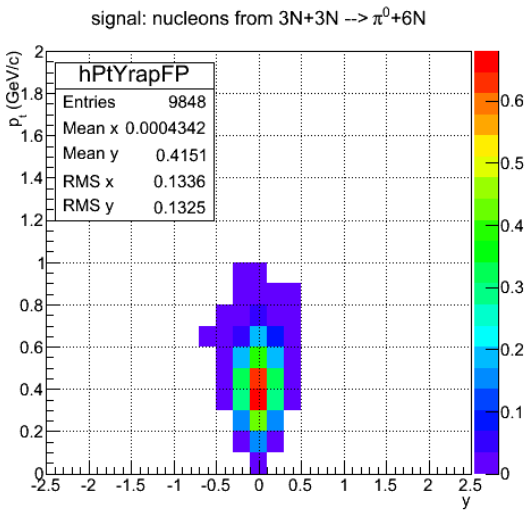

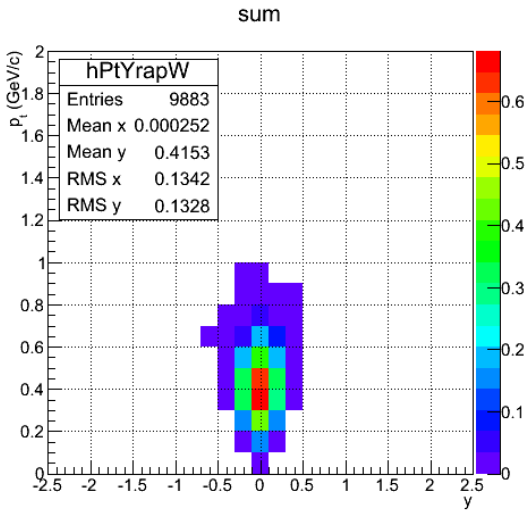

C+Be

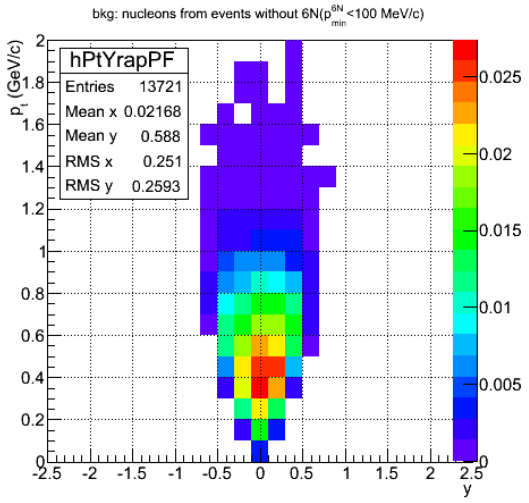

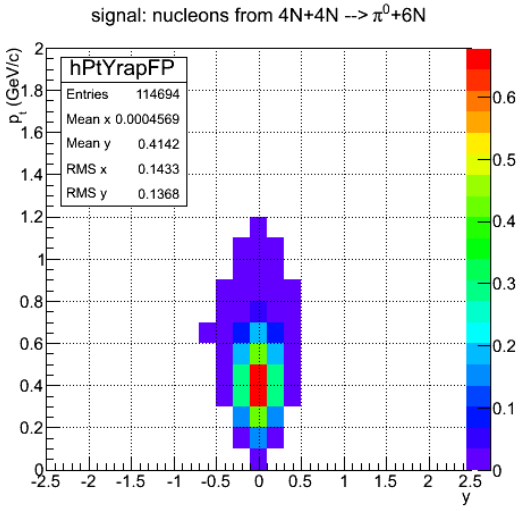

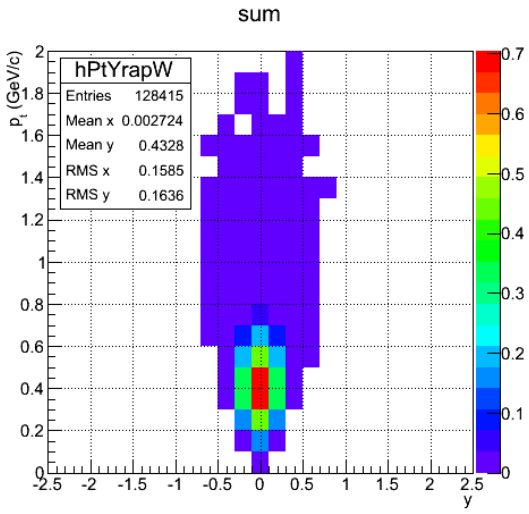

Background and signal 4N+4N

^{4}He+^{4}He

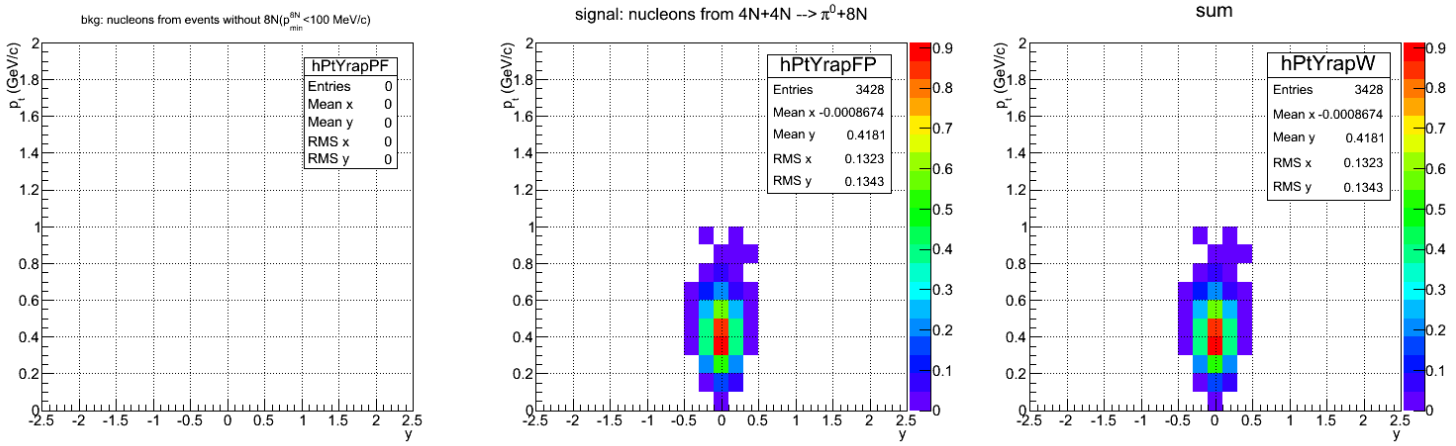

C+Be

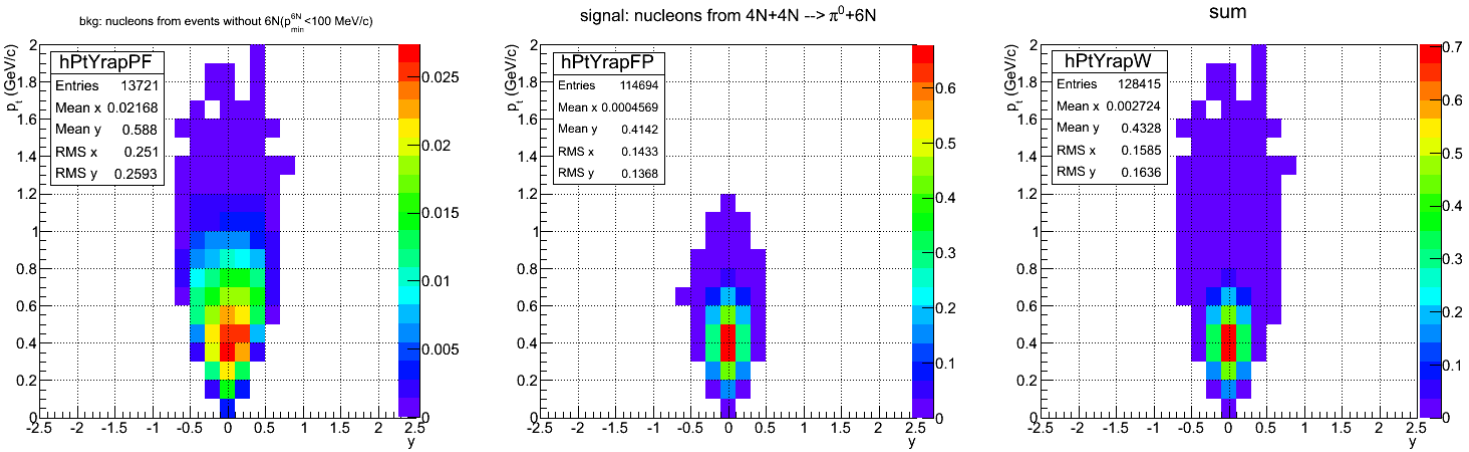

reminder: for 3N + 3N

select the 'signal area':
$y = 0 \pm 0.3$,
$p_t = 0.4 \pm 0.2$ GeV/c

system	$\langle N_{sig} \rangle / \langle N_{bkg} \rangle$
^{4}He+^{4}He	$5.33/0 = \infty$
C+B	$5.25/0.22 = 24$

system	$\langle N_{sig} \rangle / \langle N_{bkg} \rangle$
^{4}He+^{4}He	$4.043/0.0077 = 525$
C+B	$4.56/0.75 = 6$

En example:

search for the dense baryonic droplet in correlation measurements with high p_t cumulative trigger

α-angle between trigger particle and baryon (cms);

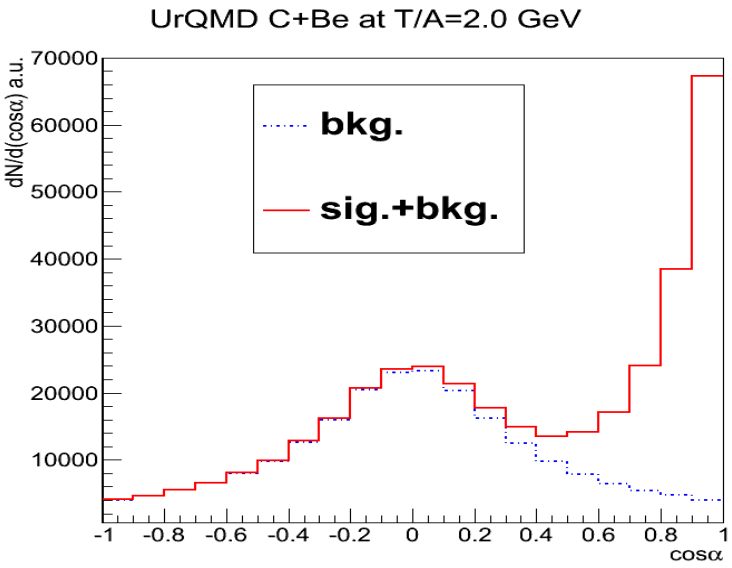

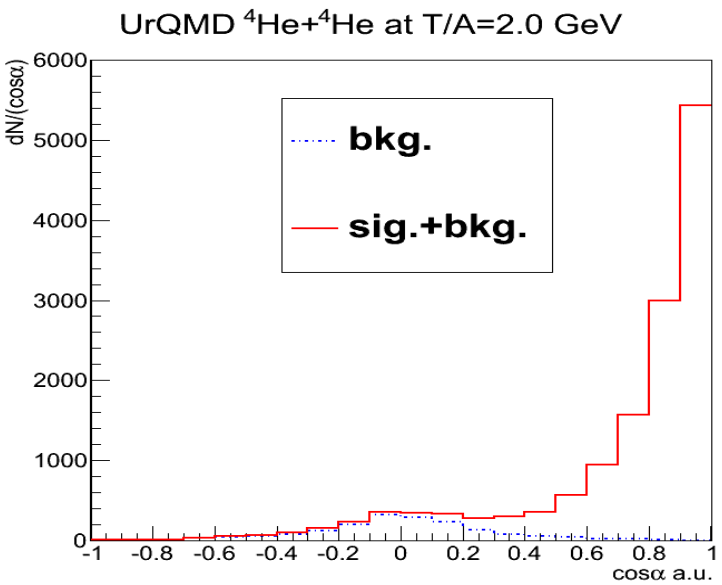

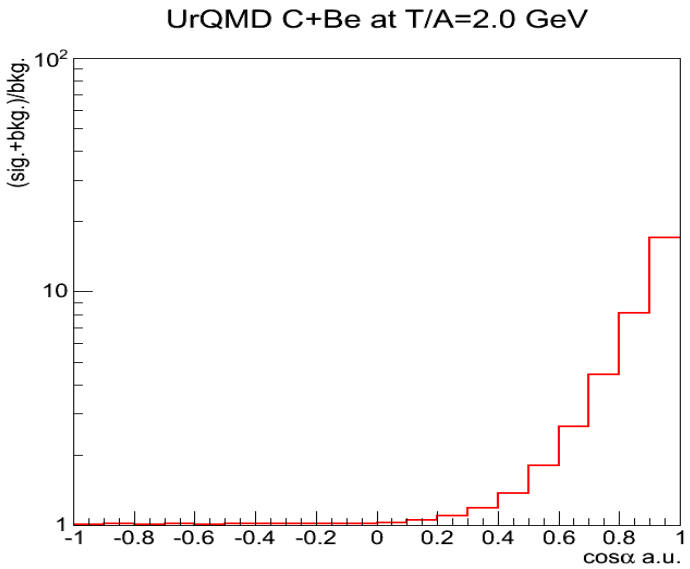

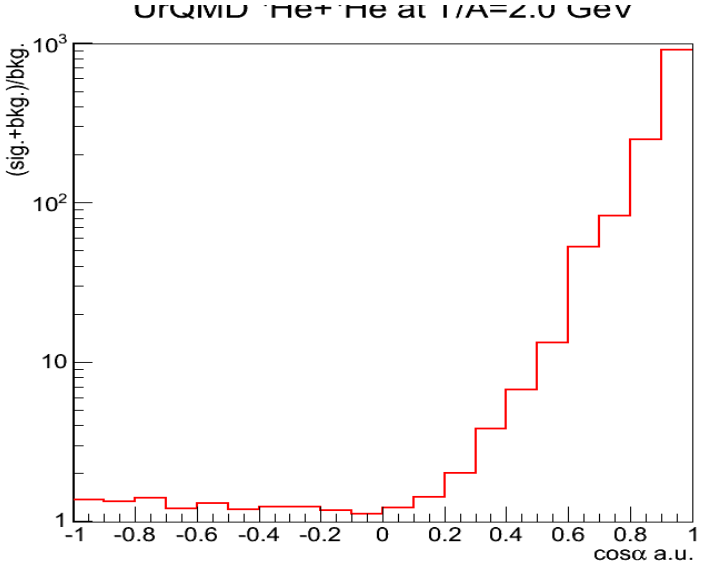

Detector for DCM study-8

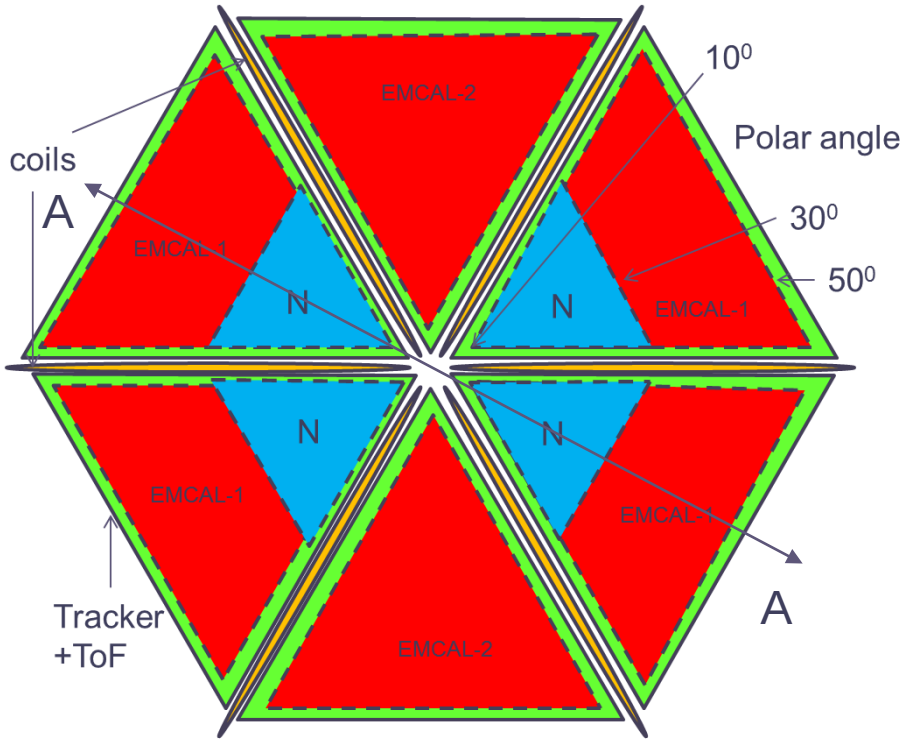

View from target

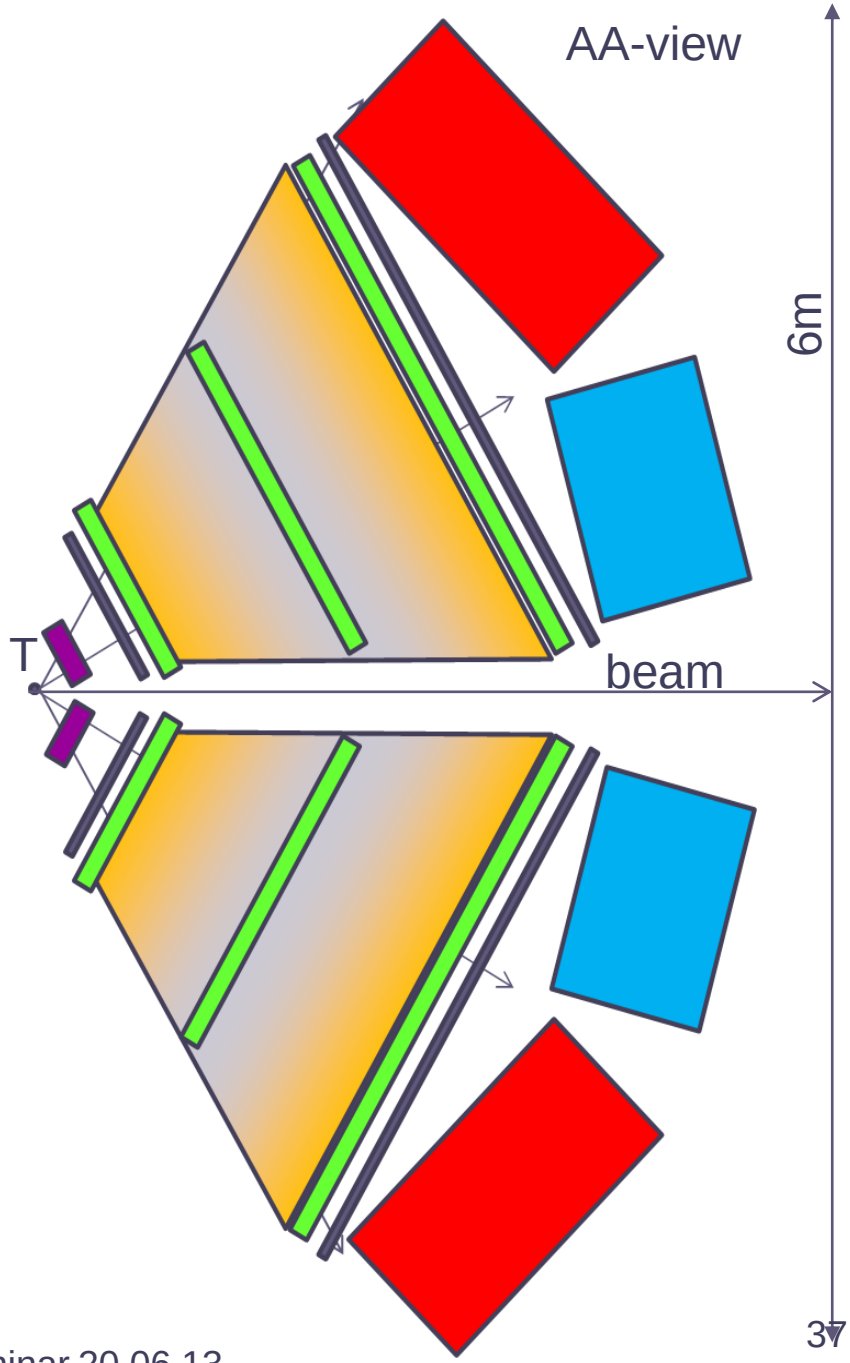

HADES@GSI

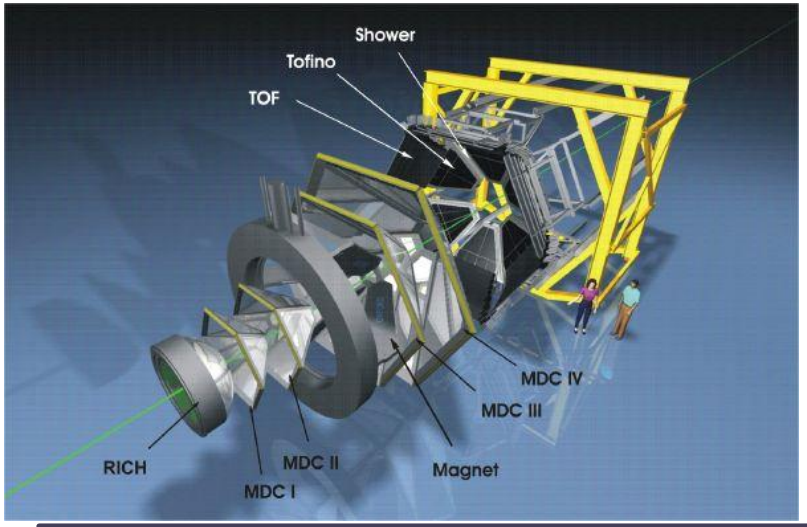

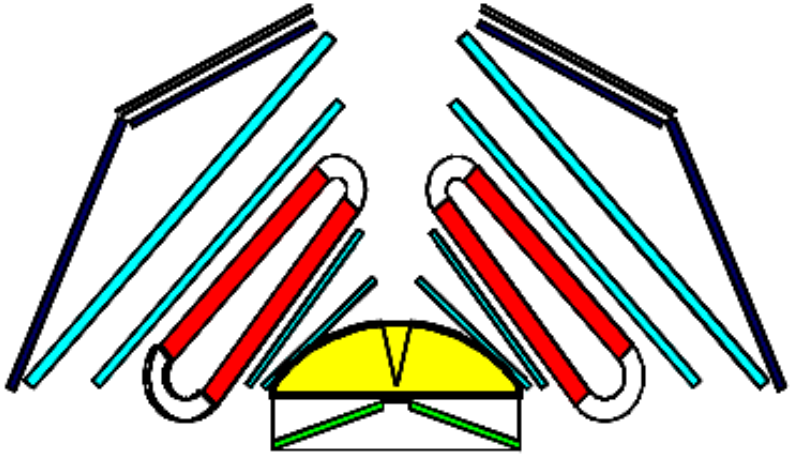

Shown above is a schematic view of the HADES detector system. The system is divided into 6 identical sectors surrounding the beam axis; the picture above shows a two-dimensional slice to demonstrate HADES' large angular acceptance, which stretches between 16 and 88 degrees. HADES is comprised of the following components:
A diamond START detector, composed of two identical 8-strip diamond detectors of octagonal shape placed 75 cm downstream respectively 75 cm upstream of the HADES target.

A Ring Imaging Cherenkov (RICH) gas radiator for electron identification, covering the full azimuthal range. The high angular resolution of a RICH is needed to assure that the lepton identification can be assigned to the corresponding lepton track.

Two sets of Multiwire Drift Chambers (MDC) before and after the magnetic field region for tracking. Besides precise determination of lepton trajectories, event characterization via charged particle momentum and angular distributions is obtained from these detectors.

A superconducting toroidal magnet with 6 coils in separate vacuum chambers. The coil cases are aligned with the frames of the MDC's to reduce dead space in the spectrometer. The magnet provides the momentum kick necessary to obtain charged particle momenta with a resolution of about 1%.

A multiplicity/electron trigger array consisting of granular pre-shower detectors at forward angles below 45° and two walls of scintillators: the time-of-flight wall (TOF) at angles above 45° and the TOFINO wall at angles below 45°.

CLAS

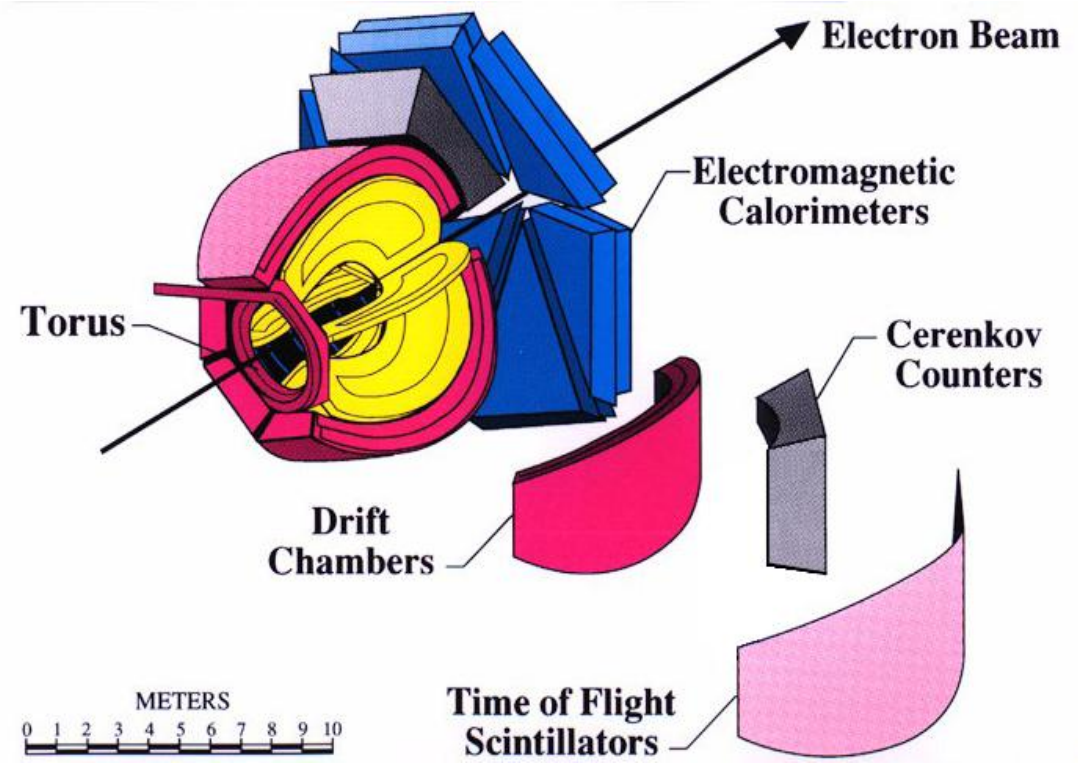

Performance

- $L = 10^{34}\ cm^{-2}\ s^{-1}$
- $B\,dl = 2.5\ T\ m$
- $\delta p/p \sim 0.5\text{–}1\ \%$
- $\sim 4\pi$ acceptance
- Best suited for multiparticle final states
- Bremsstrahlung Photon Tagger ($\delta E_\gamma/E_\gamma \sim 10^{-3}$)

*search for an exotic in the droplet

Reaction: $^4He(2GeV/nucleon)+^4He \rightarrow K^- BX$

Trigger's particle: K^- ($p>2GeV/c$, $30^0<\vartheta<60^0$)

$B \rightarrow B_1 \ldots B_{n-1}\Theta^+$; $\Theta^+ \rightarrow K_s p$; $K_s \rightarrow \pi^+\pi^-$

1event=1fb, (CLAS Upper limit for Θ^+ - 0.7nb(PRD74(2006)032001),

see also I.G.Alekseev et al.,preprint ITEP 2-05,2005(EPECUR))

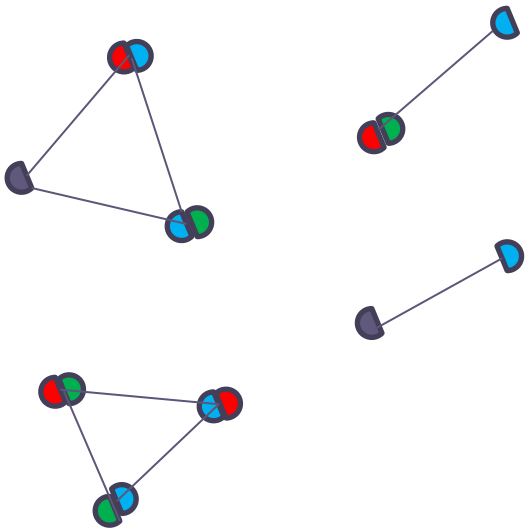

$\rho \gg \rho_0$(Dense Cold Matter)

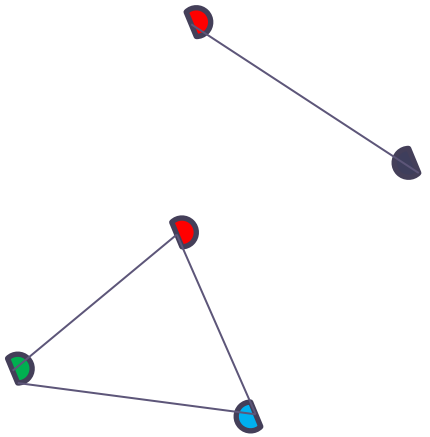

$\rho_0 \geq \rho$

* nuclear fragments

Coalescence model: Sato&Yazaki,PL98(1981),see also
Dover,Heinz,Schedemann&Zimanyi,PRD44(1991),Schibl&Heinz,PRC59(1999)

$\sigma_d \sim \sigma_p \sigma_n R_{np} K(r)$

Gavrilov,Kornienko,Leksin,Semenov,Sov.J
.Nucl.Phys. 41(1Apr.1985)p.540

Z. Phys. A – Atomic Nuclei 323, 391–398 (1986)

Measurements of $n-p$ Correlations in the Reaction of Relativistic Neon with Uranium

K. Frankel, W. Schimmerling, J.O. Rasmussen, K.M. Crowe, J. Bistirlich, H. Bowman, O. Hashimoto, D.L. Murphy, J. Ridout, J.P. Sullivan*, and E. Yoo
Lawrence Berkeley Laboratory, University of California, Berkeley, California, USA

W.J. McDonald
University of Alberta, Edmonton, Canada

M. Salomon
University of British Columbia, Vancouver, Canada

J.-S. Xu
Fudan University, Shanghai, Peoples Republic of China

Received July 1, 1985; revised version November 19, 1985

reasonable to assume that correlated $n-p$ pairs in the triplet state emerge as bound deuterons and that deuteron breakup is negligible and, hence, that the majority of the observed correlated $n-p$ pairs (if real) are due to virtual singlet deuterons. Such an assump-

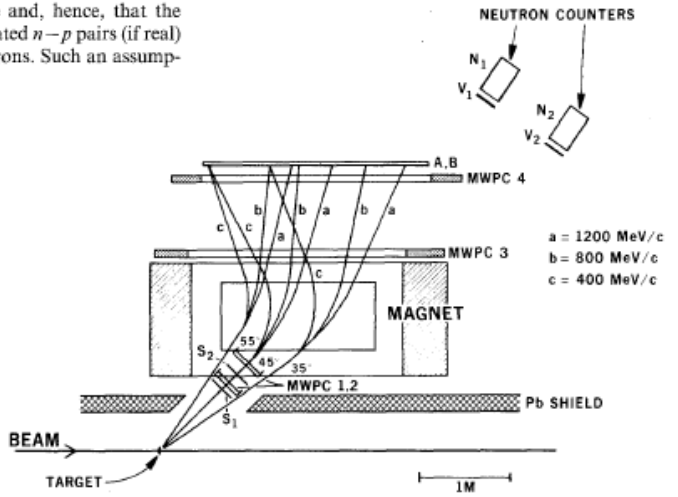

Fig. 1. Schematic layout of JANUS spectrometer system for the $n-p$ correlation experiment. Magnet and detector sizes are to scale, but the positions are only approximately to scale. Trajectories for protons of three different momenta are shown. Time of flight is determined between coincident scintillators S_1-S_2 and coincident scintillators $A-B$ for charged particles and between S_1-S_2 and N_1 for neutron particles. The four multiwire proportional counters MWPC1–4 define the charged particle trajectories through the magnet. V_1 and V_2 are thin scintillators used to veto events with a charged particle incident on N_1 and N_2

*modification of particle properties in baryon environment

Yu.T.Kiselev,S.M.Kiselev&M.M.Chumakov
Yad.Fiz,73(2010),p.154 and ref.therein

1) inverse kinematics
2) different decay modes, including lepton's one(to be confirmed)
   $\omega \to \pi^0\gamma(8.9*10^{-2})$, $\omega \to e+e-(7.1*10^{-5})$
3) semi-exclusive reaction

Криогенная мишень

Ю.Т. Борзунов, А.В. Константинов, ЛФВЭ

Предполагается использовать в эксперименте СОВА криогенную мишень разрабатываемую в ЛФВЭ ОИЯИ.

Материалы используемые при изготовлении мишеней

По результатам многочисленных экспериментов было установлено, что наиболее подходящими материалами для изготовления основных узлов мишеней являются пенопласт и лавсановая пленка. Эти материалы ввиду своей малой плотности позволили добиться оптимального соотношения между рабочим веществом и веществом, окружающим рабочую область.

Внутренний сосуд мишени в сборке с вакуумным кожухом

Внутренний сосуд мишени

Subdetectors. Large angle ECAL(lead glass F8) supermodule

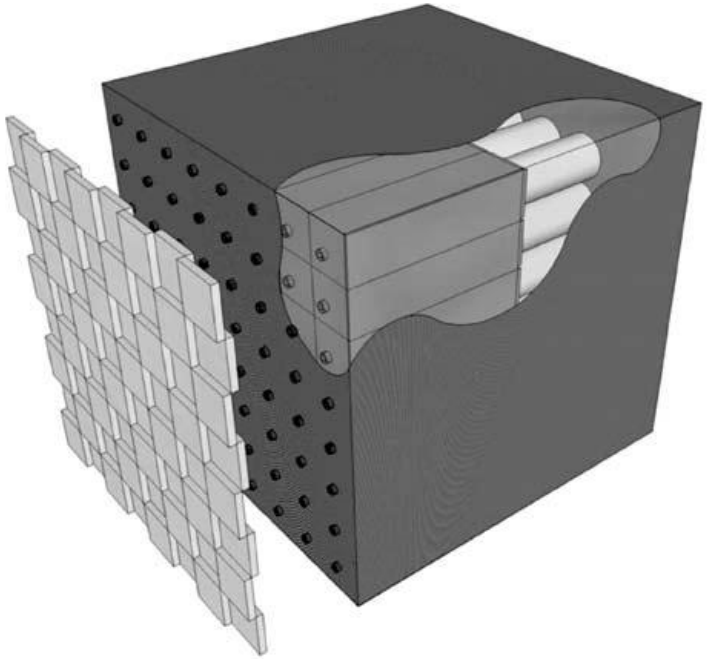

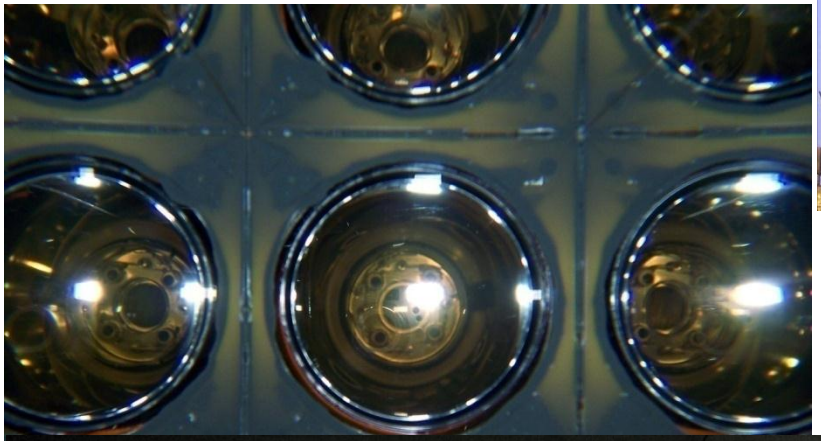

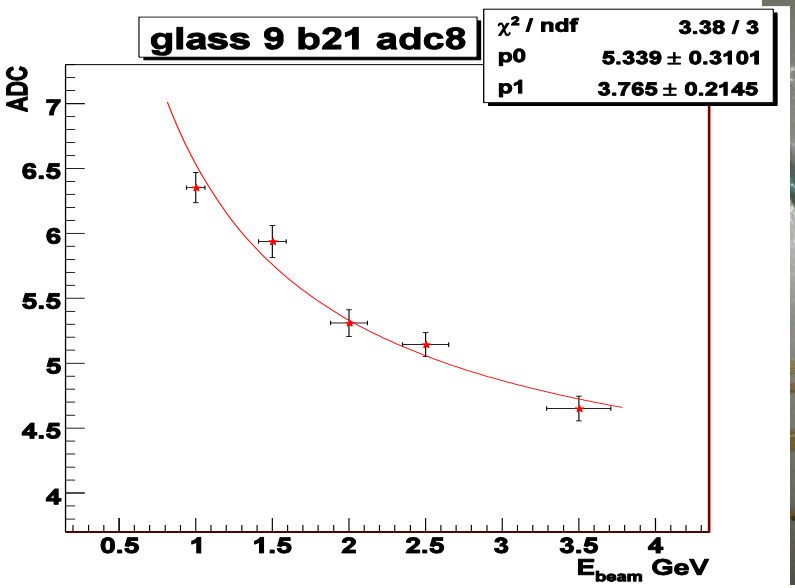

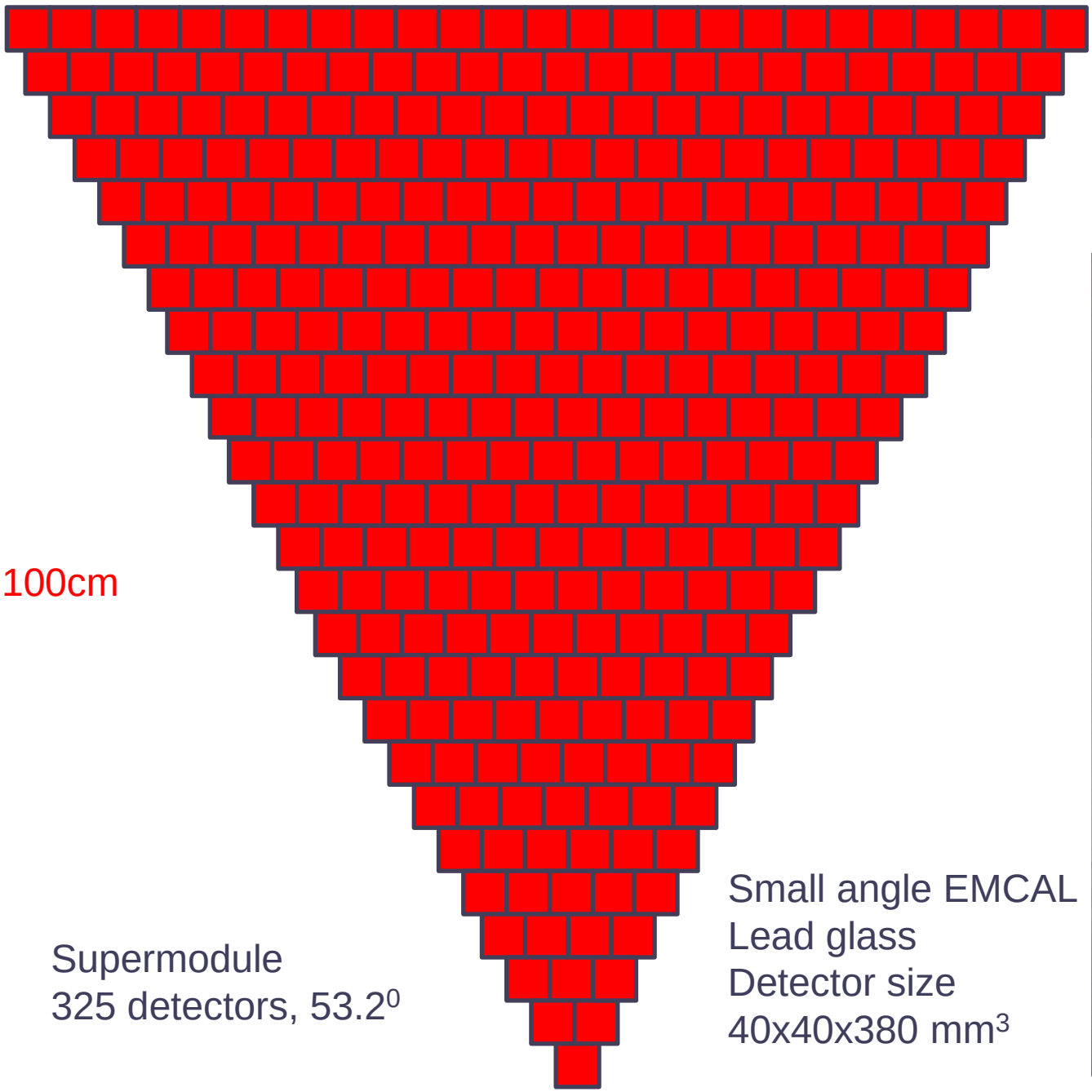

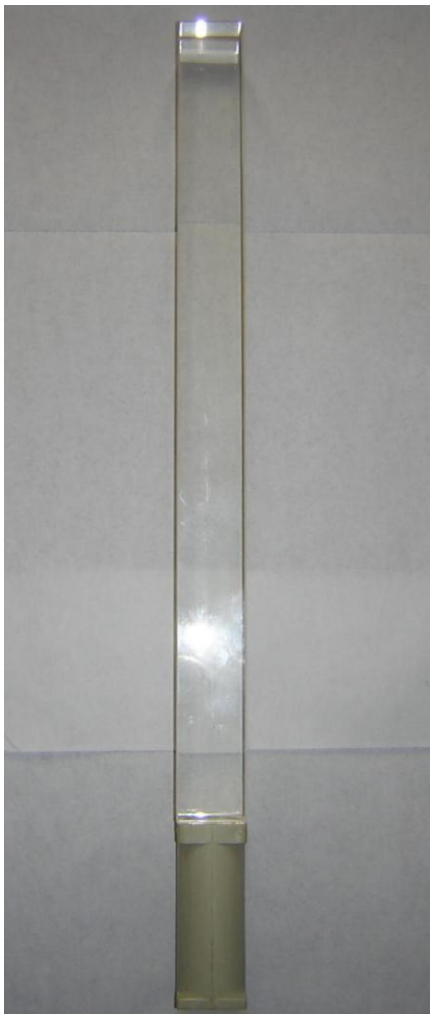

Supermodule
325 detectors, 53.2^0

Small angle EMCAL
Lead glass
Detector size
$40x40x380\ mm^3$

Plastic Scintillator 105*100*5 mm^3

Fiber: KYRARAY, Y-11,d =1mm, wavelength shift

MRS APD & Amplifier - CPTA(Golovin)

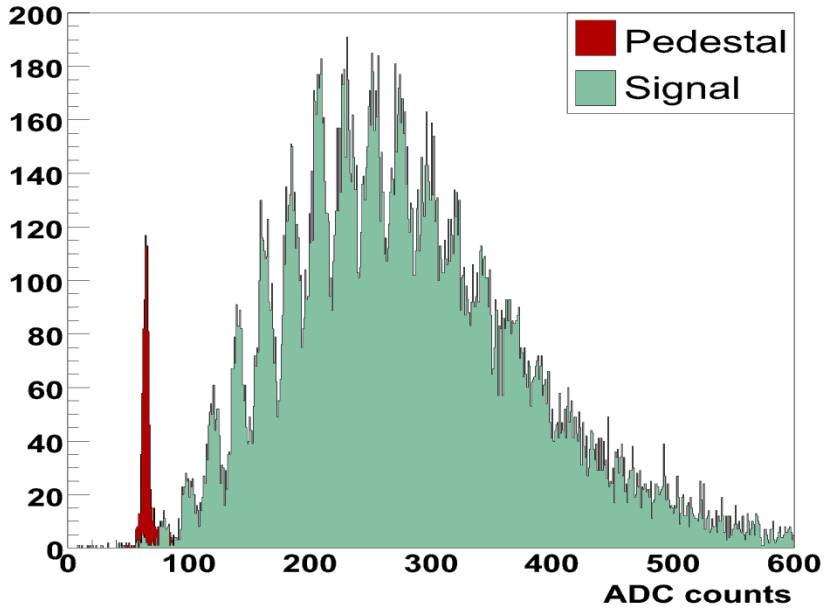

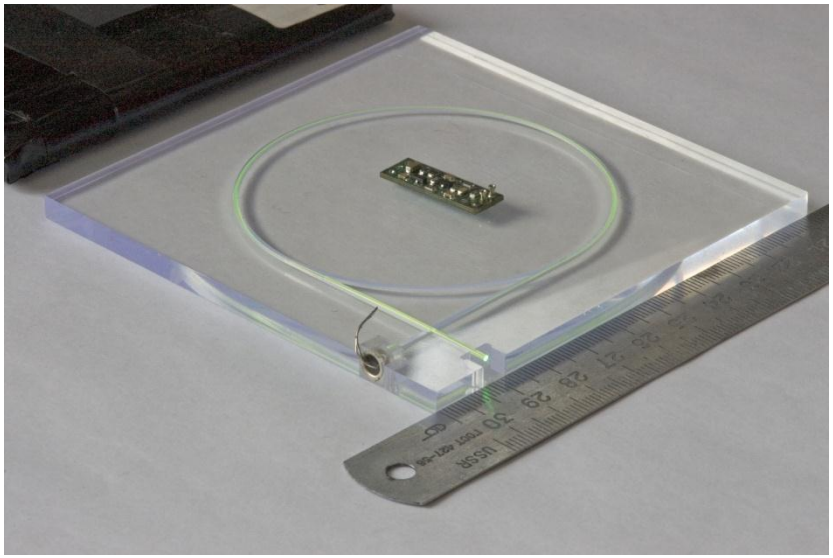

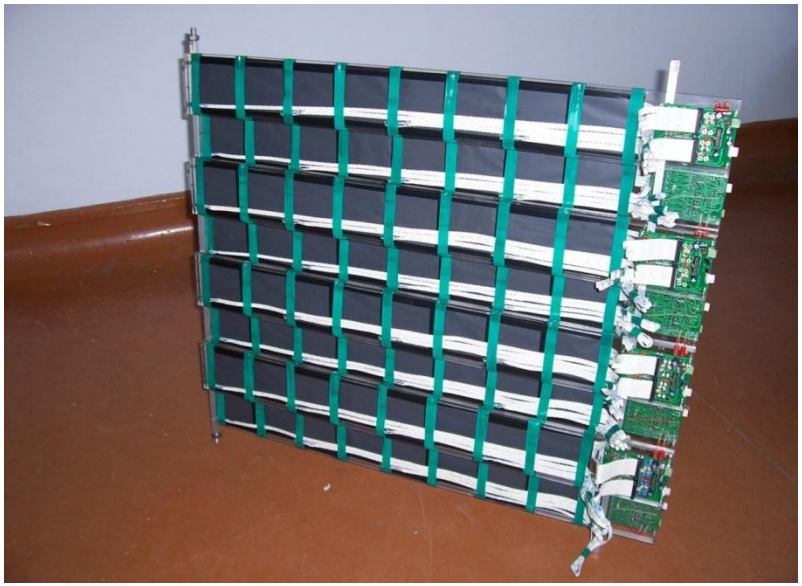

Концептуальный проект радиационно-прозрачного (X\Xo < 0.3-0.5% на детектирующий слой) Вершинного трекового детектора.

СПбГУ, Санкт-Петербург

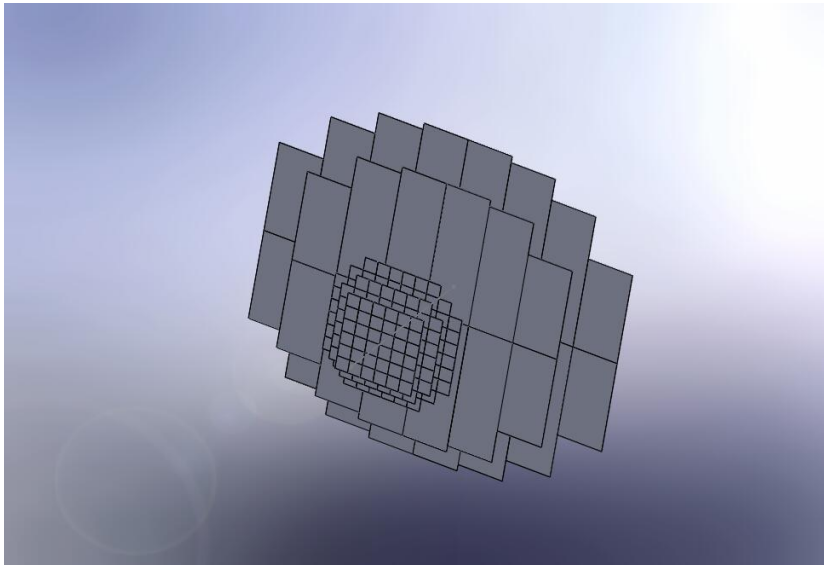

SPD EXPERIMENT AT NICA.

SPD.Torrid magnet.

- 8 coils
- ~100 x 40 cm coils
- average integrated field: ~ 0.8 - 1.0 Tm
- acceptance ~ 80 %

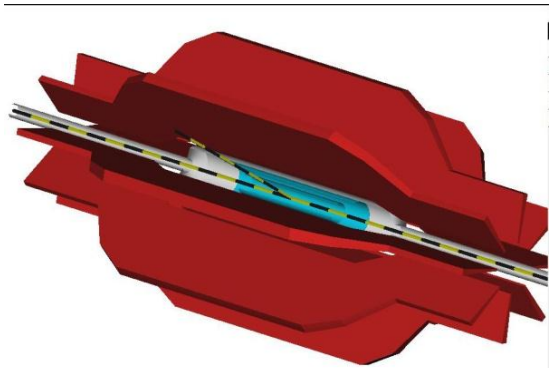

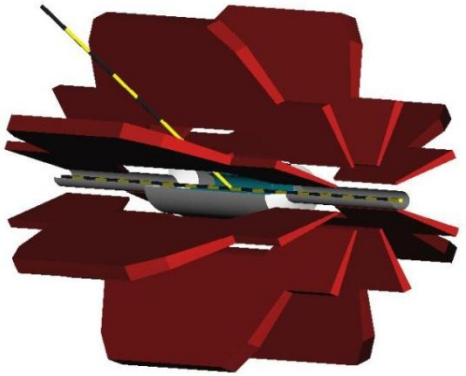

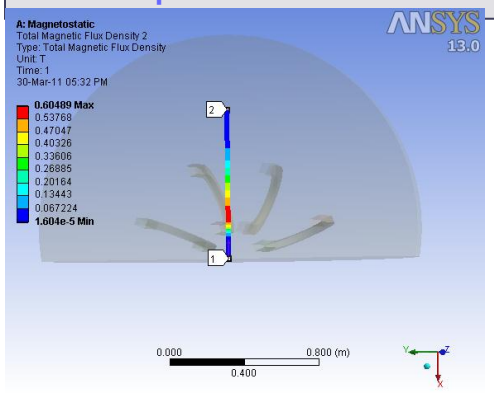

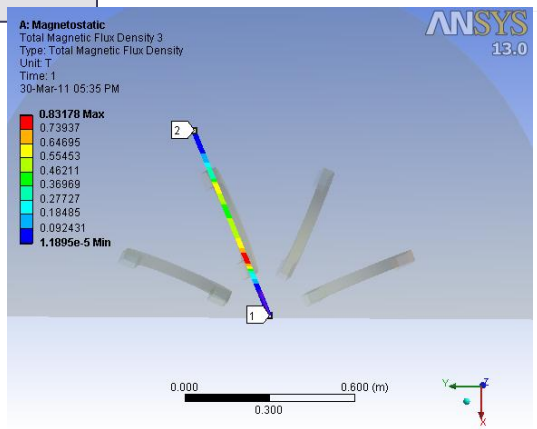

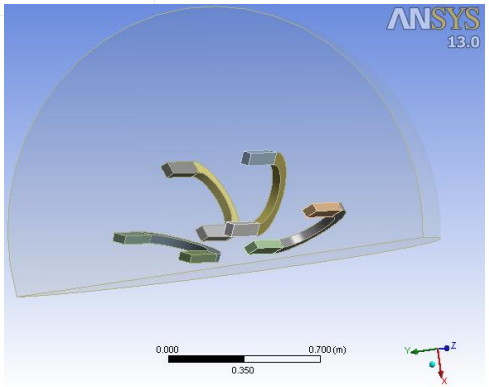

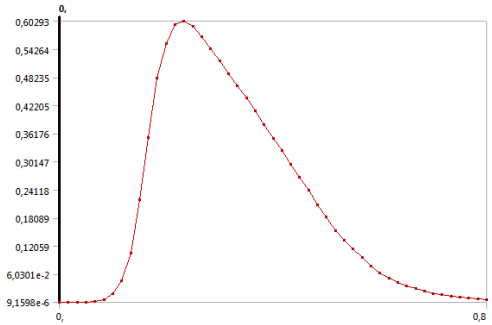

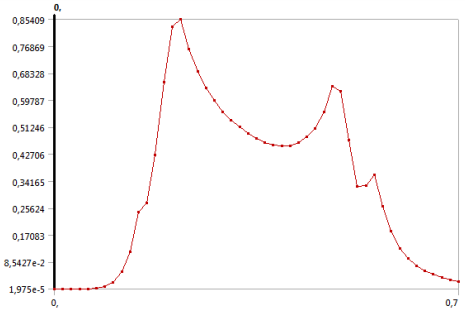

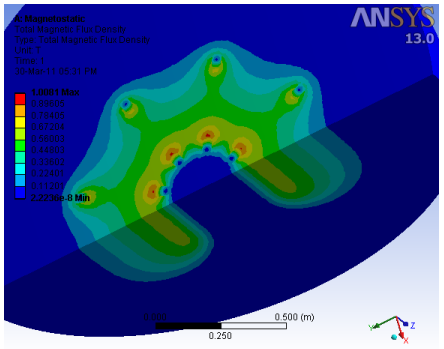

Done by Pivin R.

5. Detector for DCM study-4

Neutron detector supermodule(78 detectors)

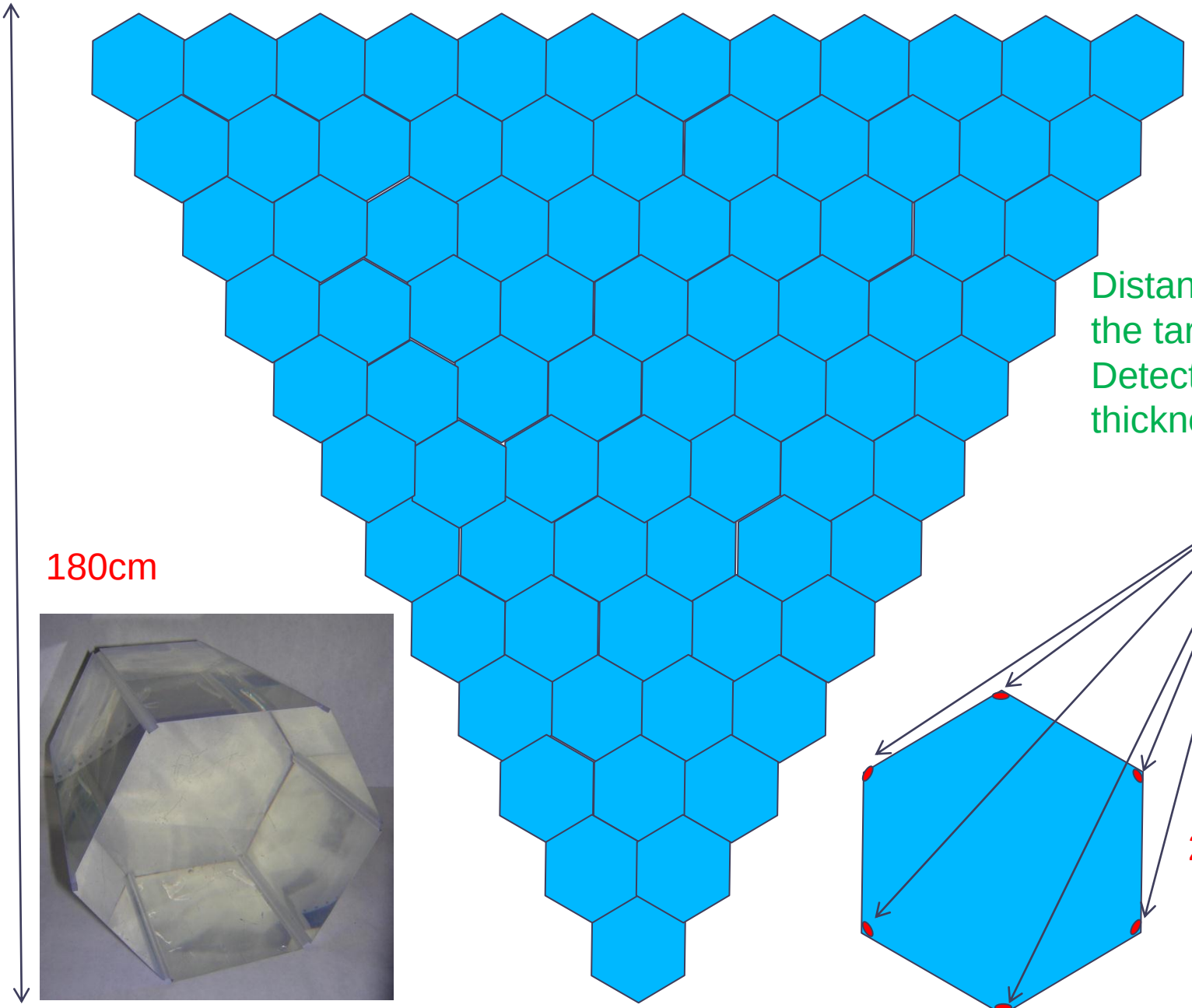

Distance from the target 240cm; Detector thickness 20cm

180cm

5. Detector for DCM study-5

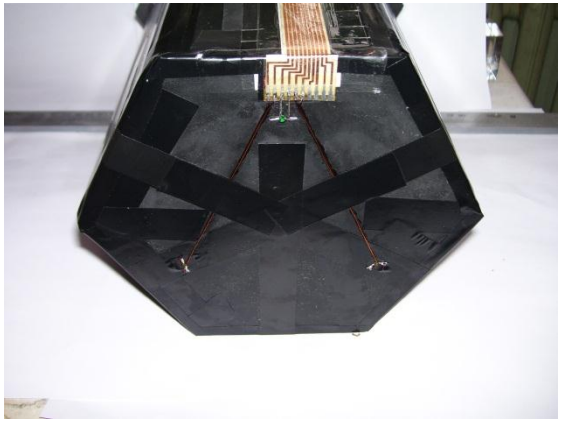

Front

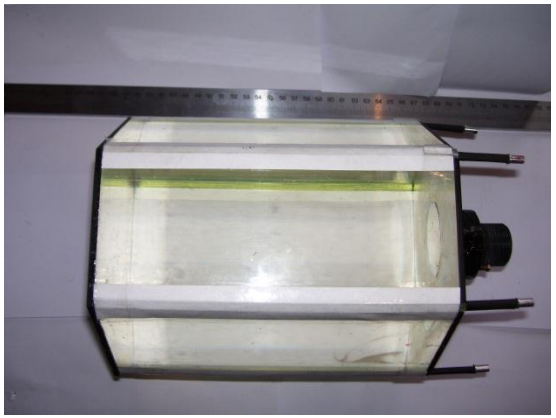

Side

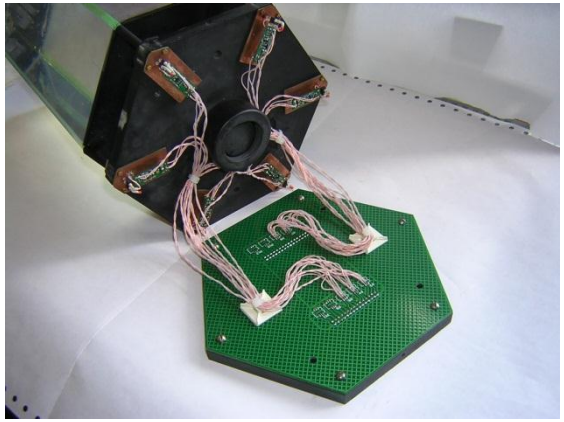

Back

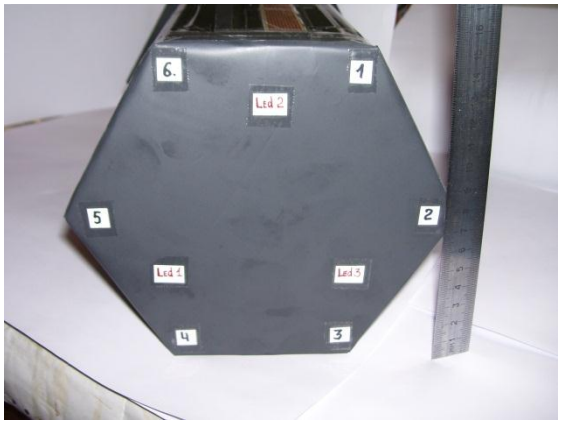

Neutron Beam test of prototype@Nuclotron(dec.2012)

$$d + C \rightarrow (pn) + X$$

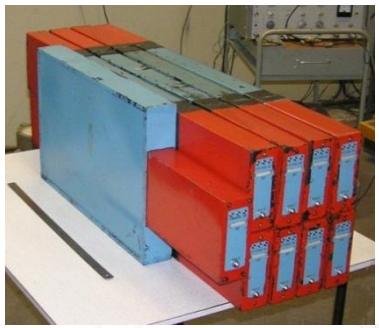

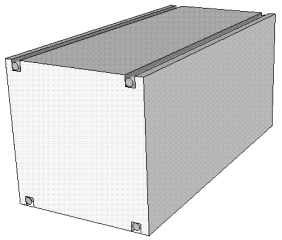

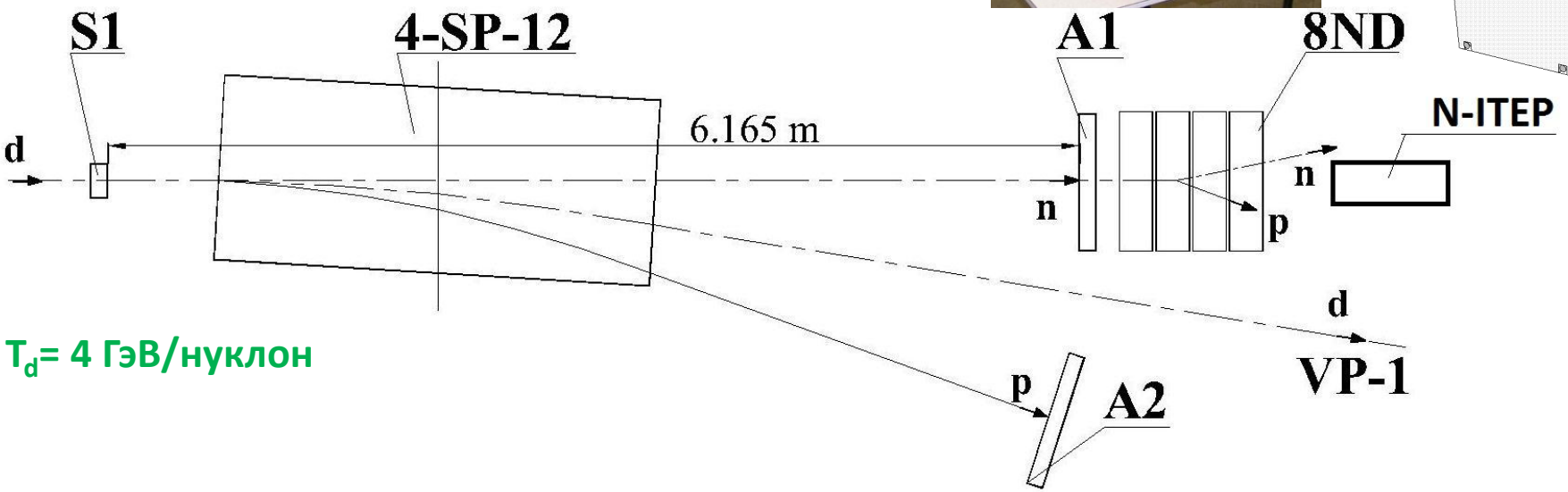

T_d= 4 ГэВ/нуклон

N-ITEP нейтронный детектор ИТЭФ, использован в триггере:

(A2)·(N-ITEP(≥4))· $\overline{A1}$

μB extended range in STAR due to fixed target program

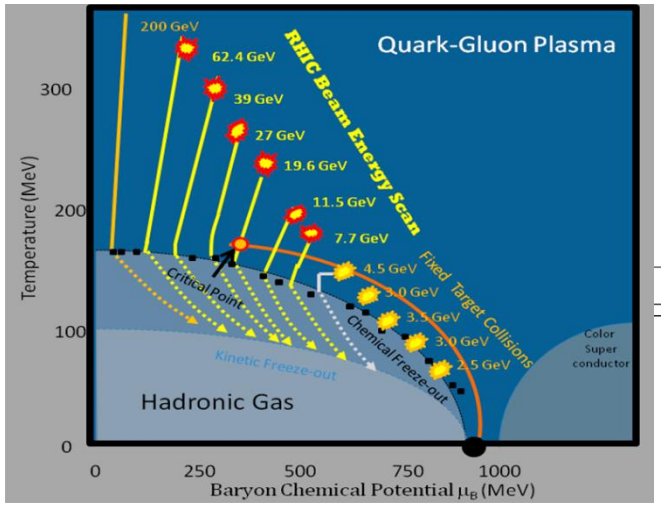

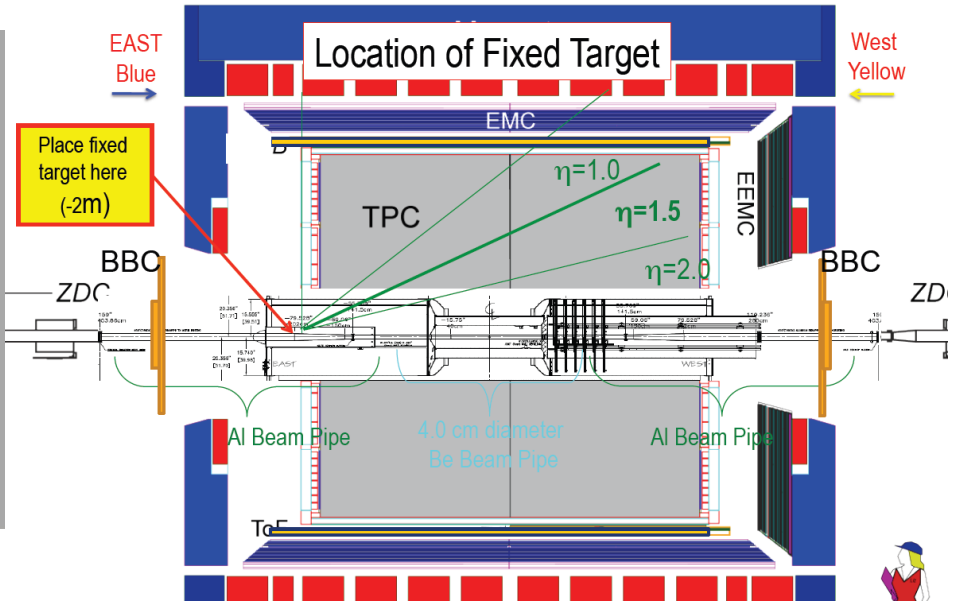

2.8 AGeV Au+Al: Spectra π^+ and π^-

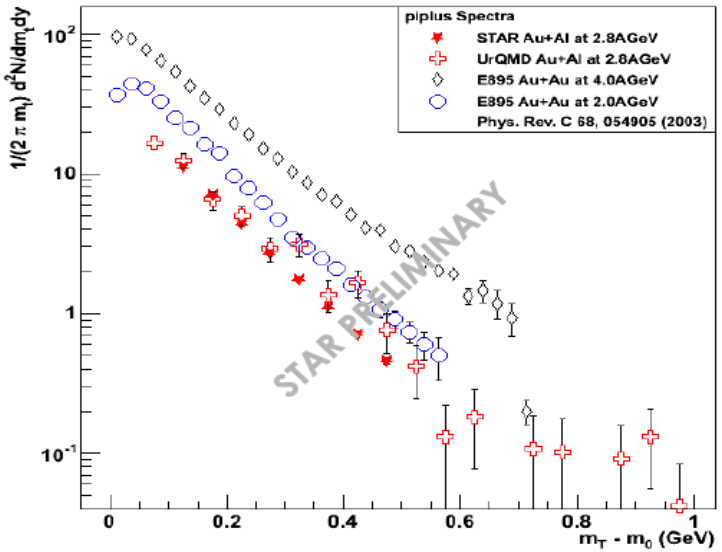

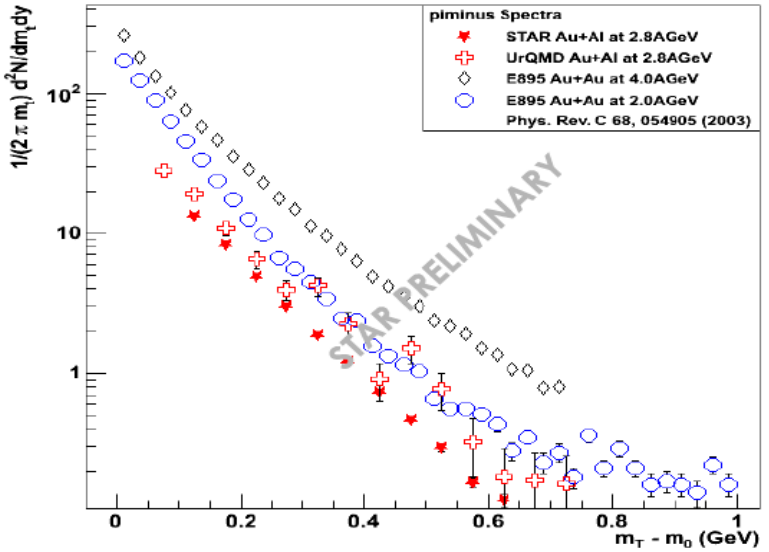

BM@N

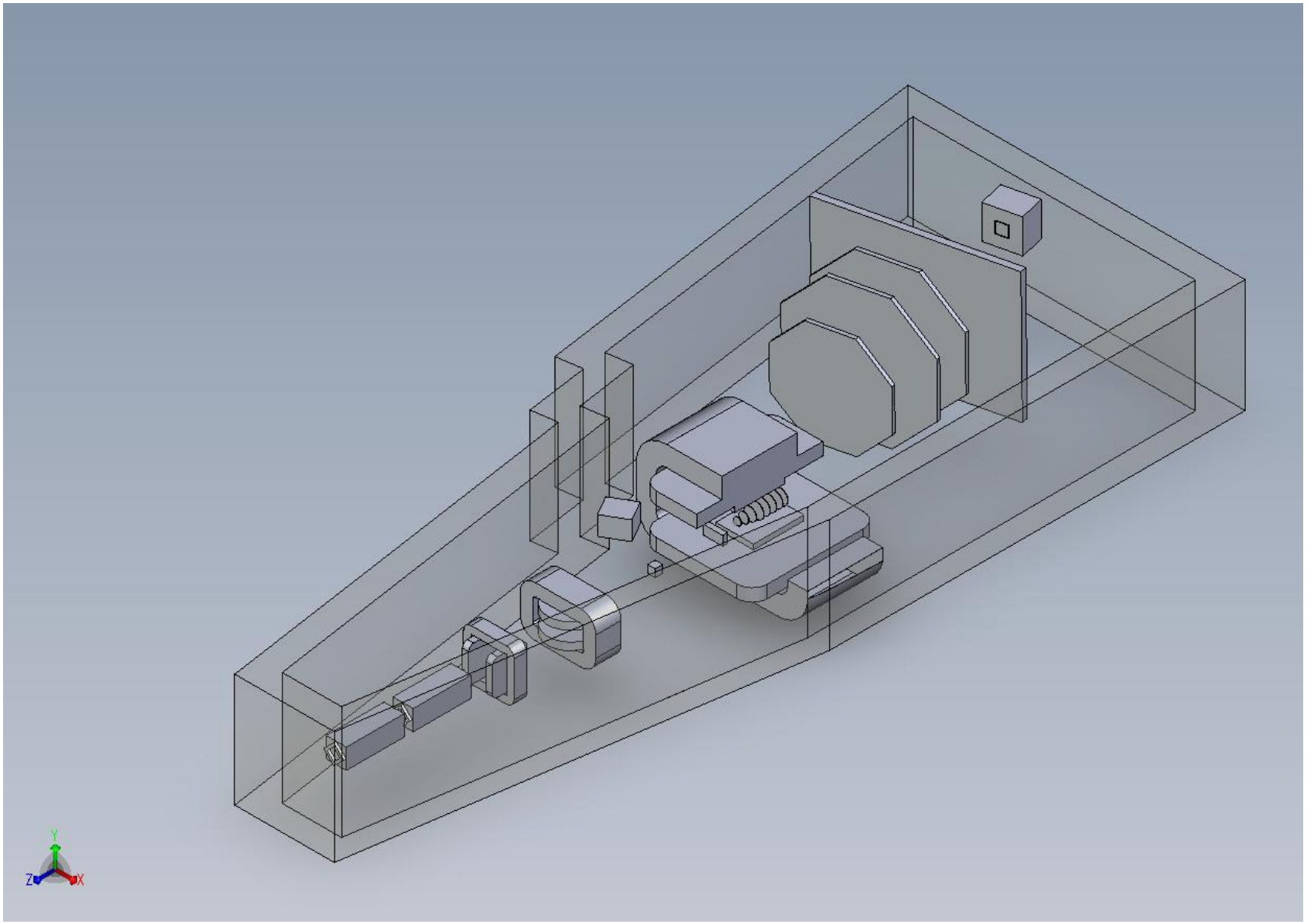

Выводы:

1) Предложена программа исследования ядро-ядерных и адрон- ядерных взаимодействий в диапазоне энергий ускорителя ИТЭФ
2) Существующие экспериментальные данные показывают возможность осуществления предложенной программы при реалистичных параметрах ускорителя и экспериментальной установки
3) Представлен статус коллаборации и проекта многоцелевой установки, соответствующей предложенной программе

Extra slides

Original physics idea+
Innnovations:

target

vertex detector

magnet

tof

Veto with APD

neutron detectors

Data quality cuts

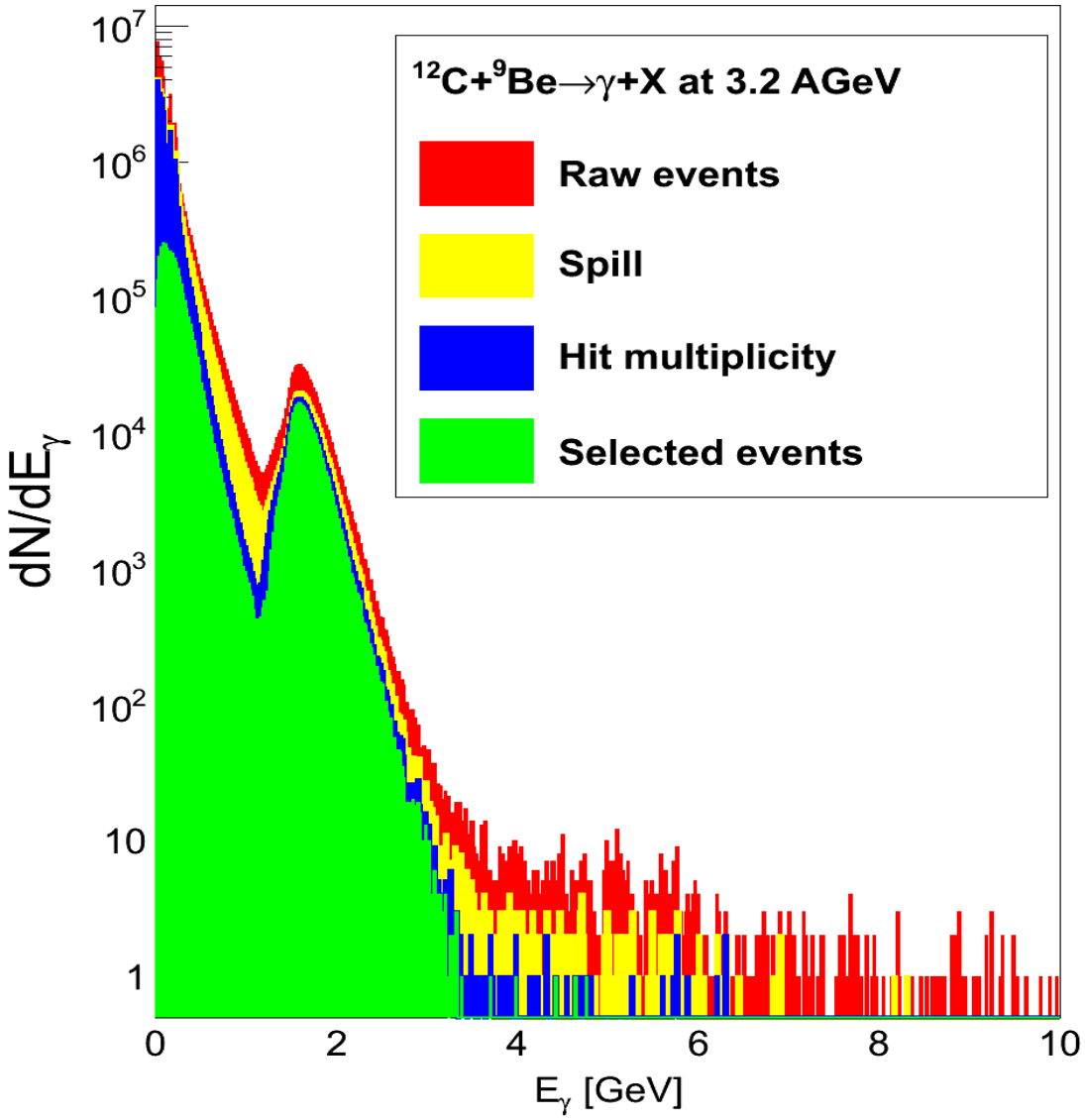

Three groups of cuts:

- Spill
- Hit Multiplicity
- Signal shape

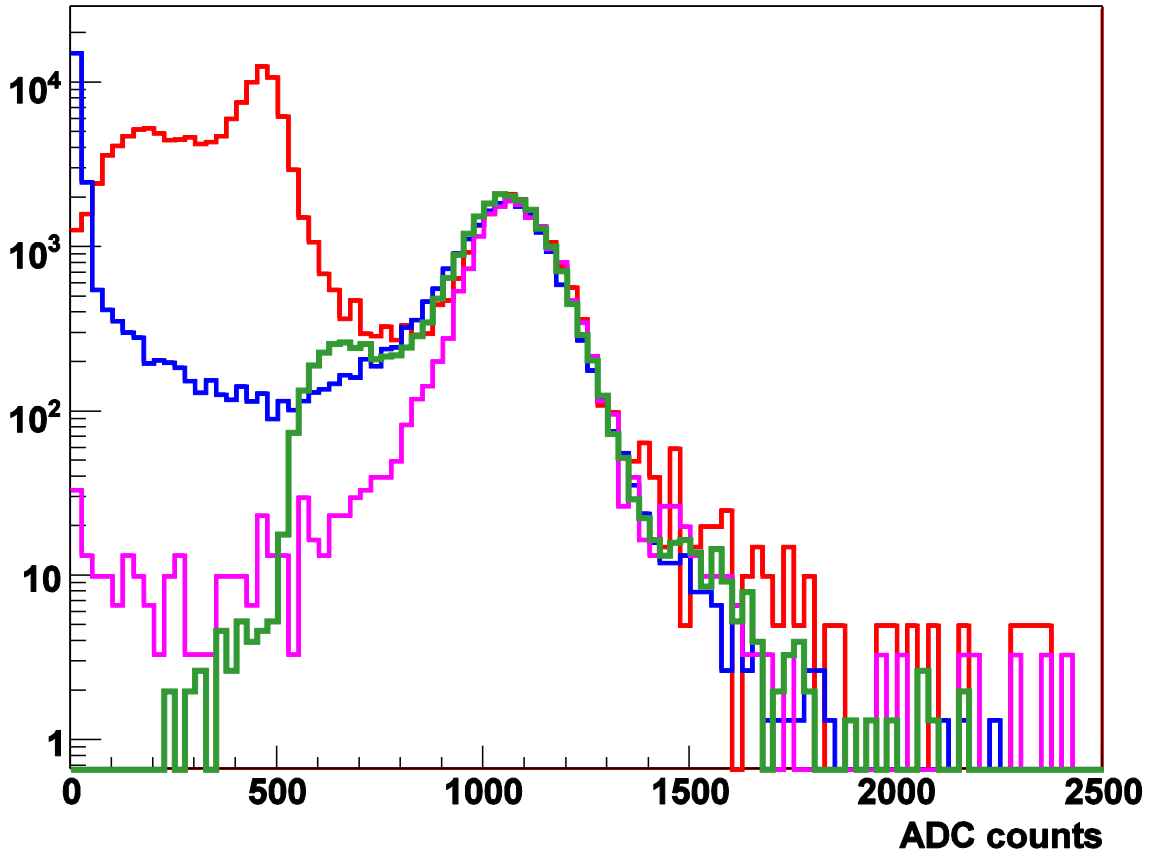

Рис. К+2. Спектр сигналов в калориметрическом счетчике при различных типах триггера(зеленый-самозапуск, синий-внешний триггер от порогового черенковского детектора, красный- внешний триггер от сцинтилляционного детектора площадью 100x100мм^2 , сиреневый- совпадение синего и красного.

hadron background simulation

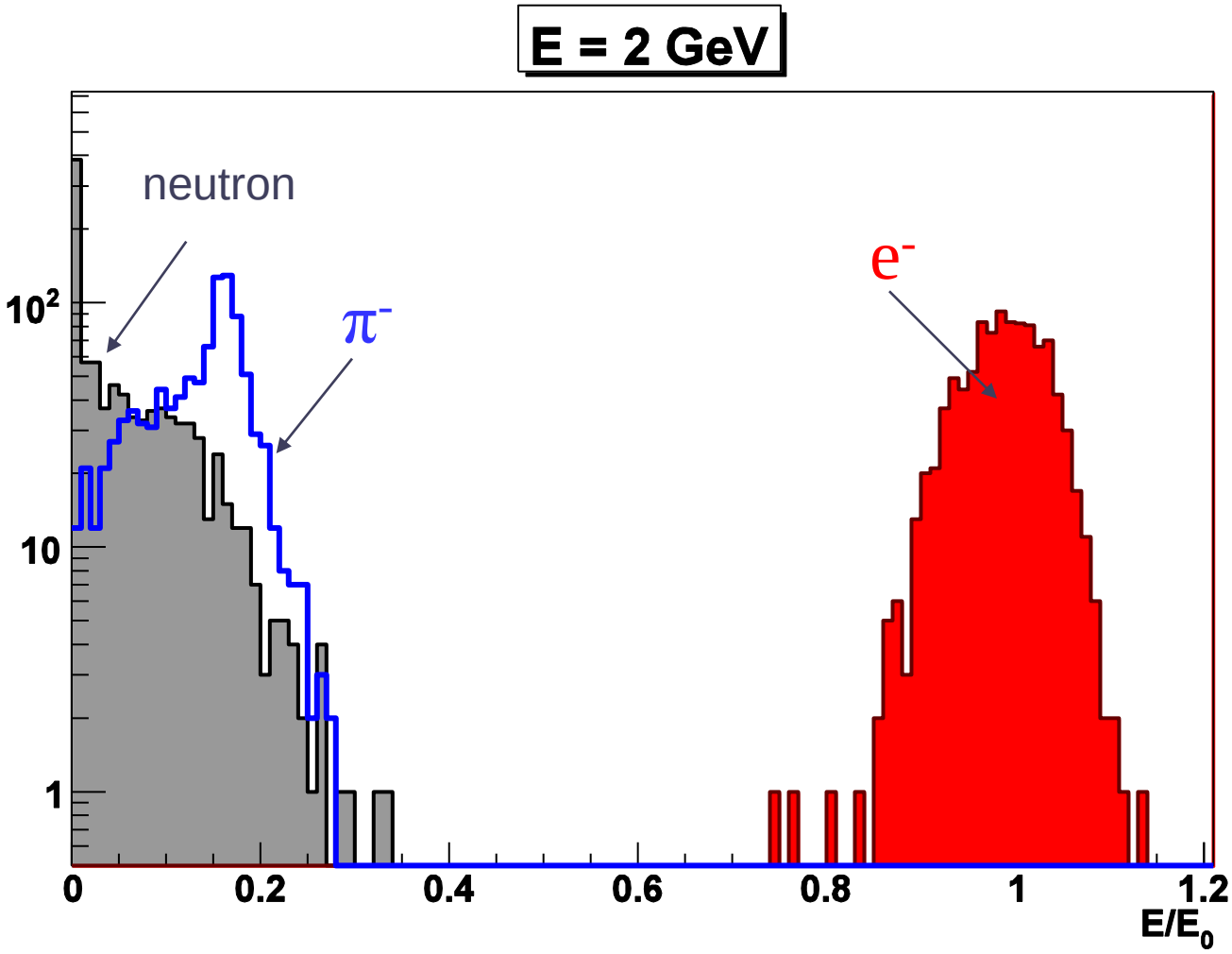

Flucton properties:

- Isosymmetry

Data:JINR, A.M.Baldin et al.,Yad.Fiz. **21**(1975) p.1008

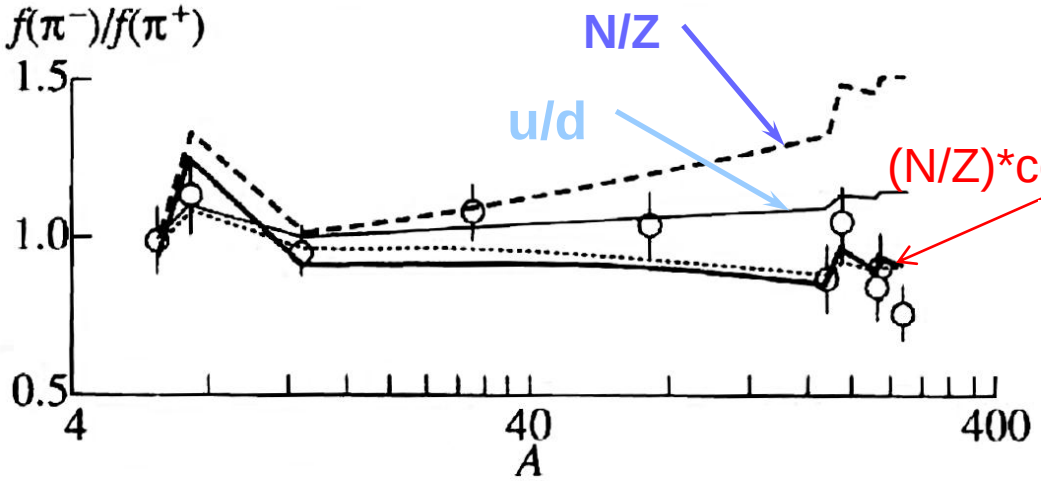

For isotopic effects see, also Yad.Fiz. 59 4 694 (1996)

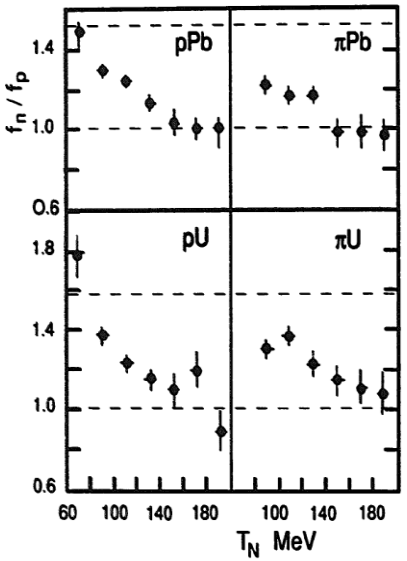

Figure 3 : Ratio of neutron to proton yields for various nuclei and various probes, as a function of the energy of the secondary hadron

G.A.Leksin at al.(ITEP)

3.Cumulative trigger-6

"local" mechanisms of cumulative processes

SRC configuration

Multiquark configuration

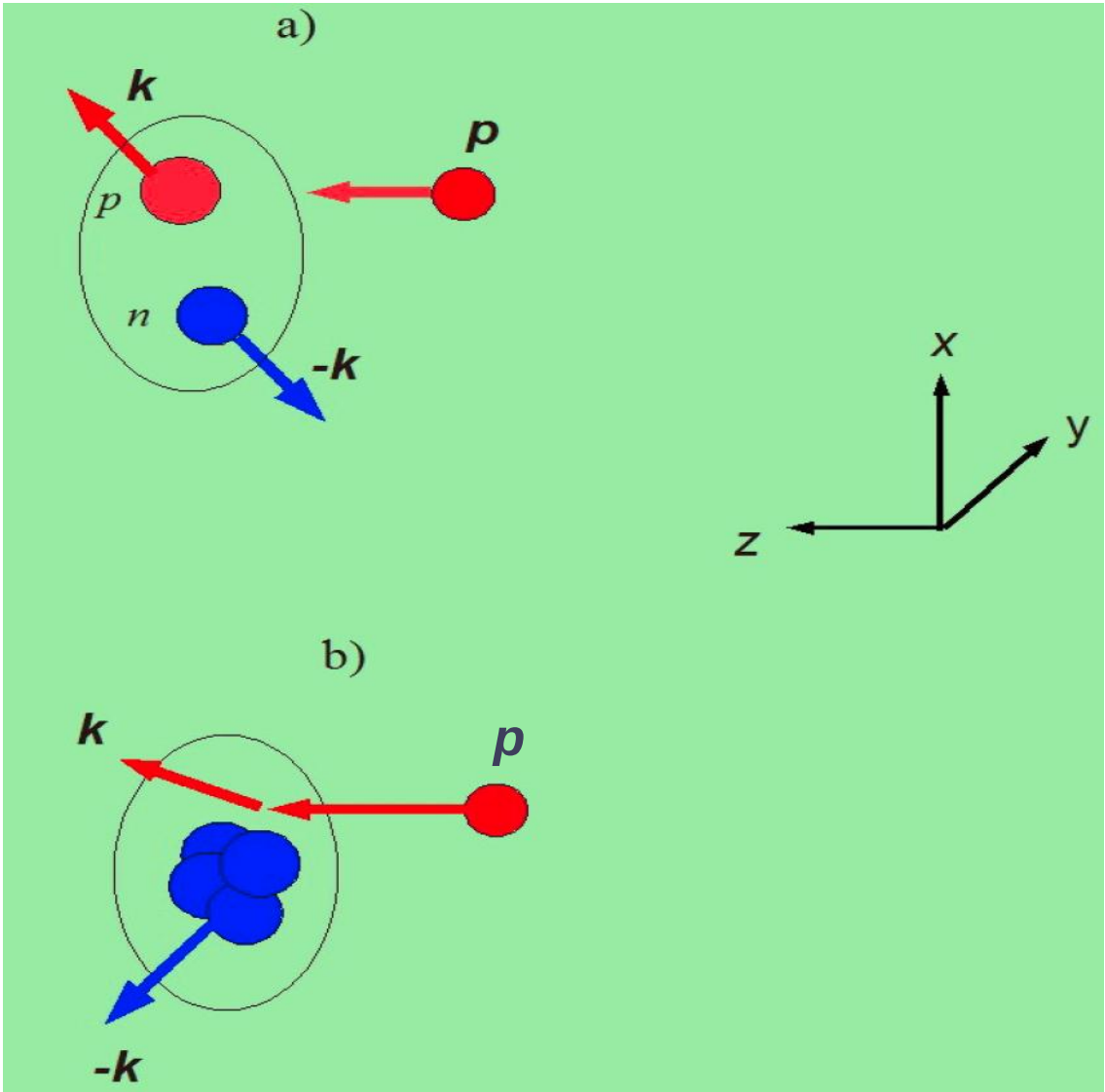

"nonlocal" mechanisms – multiple scattering

3.Cumulative trigger-4

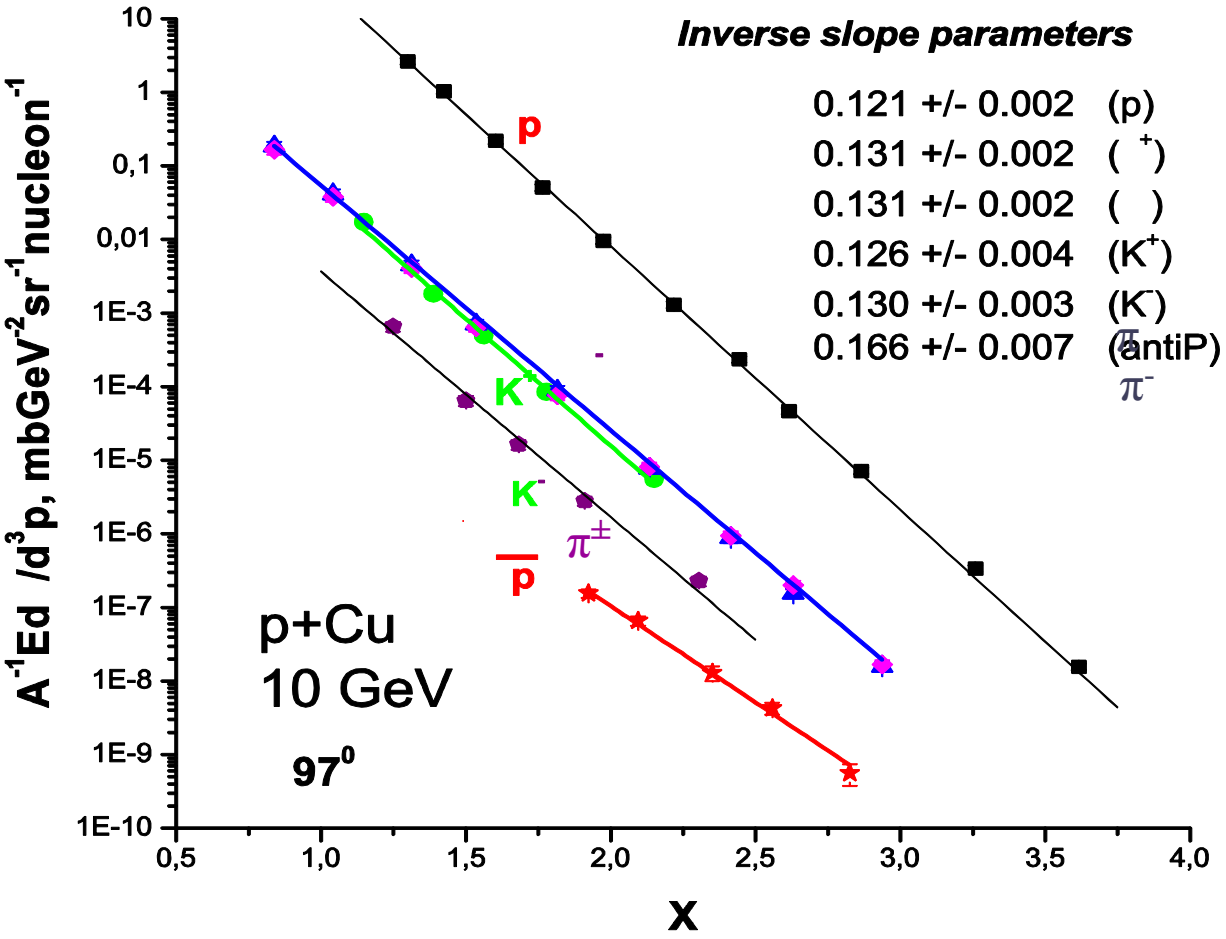

X – minimal target mass [m_N] needed to produce particle

FAS @ ITEP(Boyarinov et.alYad.Fiz 57(1994)1452)

Femtoscopy

Bose-Einstein statistics of identical bosons leads to short-range correlations in momentum space

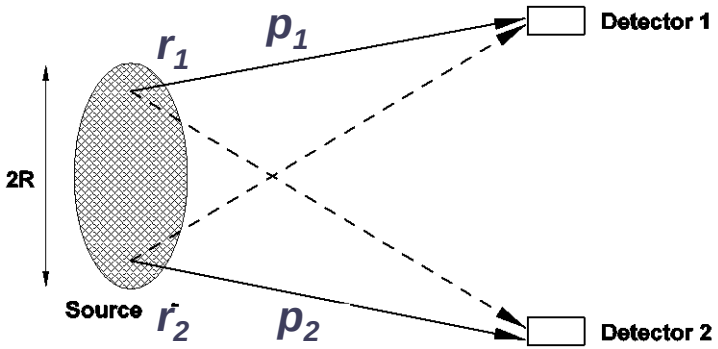

$$R\ (\vec{p}_1, \vec{p}_2) = \frac{P_2(\vec{p}_1, \vec{p}_2)}{P_1(\vec{p}_1) \cdot P_1(\vec{p}_2)}$$

First application with photons: size of stars (R. Hanbury-Brown, R.Q. Twiss, 1956)

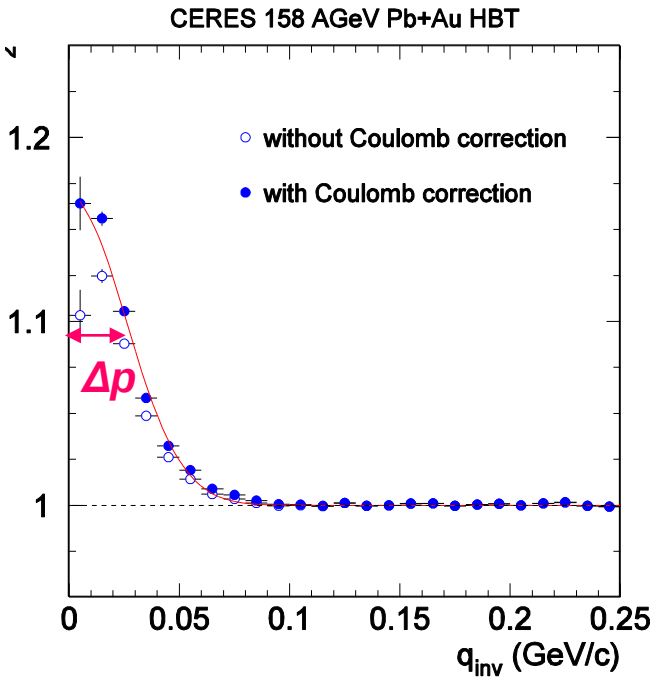

In heavy-ion reactions: pions, kaons, protons(Interferometry+strong FSI+Coulomb)…

$$\Delta r = \frac{\hbar c}{\Delta p} = \frac{197\ \mathrm{MeV/c}}{\Delta p}\ \mathrm{fm}$$

3.Cumulative trigger-3

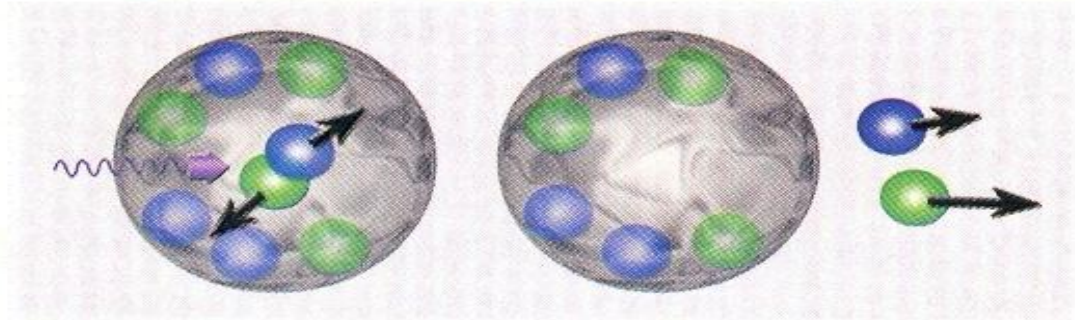

Fig. 1. Scattering of a virtual photon off a two-nucleon correlation, x > 1.5, before (left) and after (right) absorption of the photon.

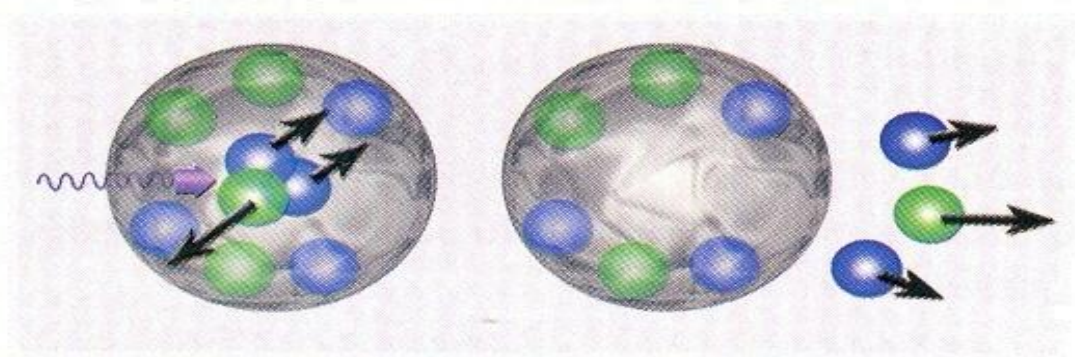

Fig. 2. Scattering of a virtual photon off a three-nucleon correlation, x > 2, before (left) and after (right) absorption of the photon.

Figure from: M.Strikman, CERN Courier Nov.2,2005

pp(ALICE, arXiv:1007.0516[hep-ex],K.Aamodt et al.)

$dN_{ch}/d\eta$	R_{inv}(fm)	Description
3.2	~0.9	Without hydro (arXiv:1106.1786[hep-ph] M.Nilsson et al.)
7.7	~1.1	
11.2	~1.2	With hydro (arXiv:1010.0400[nucl-th],K.Werner ety al.)

Criterium: r»l

	number of particles	Size(r), fm	free path, (l)fm
Heavy Ions:	1000	10	1
flucton-flucton	10	1	0.1

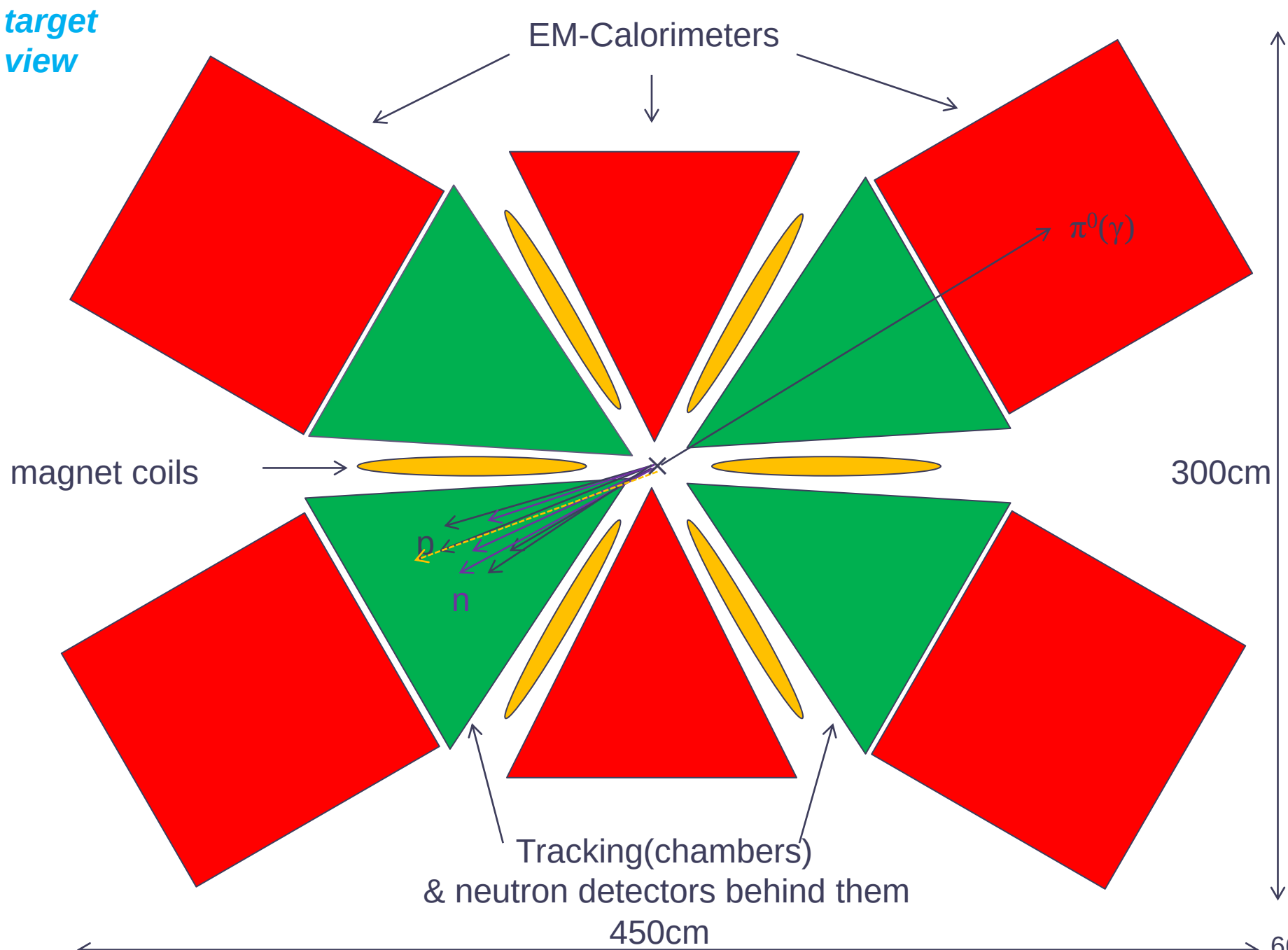
target view
EM-Calorimeters
$\pi^0(\gamma)$
magnet coils
300cm
n
n
Tracking(chambers)
& neutron detectors behind them
450cm

DCM detector position within ITEP experimental hall

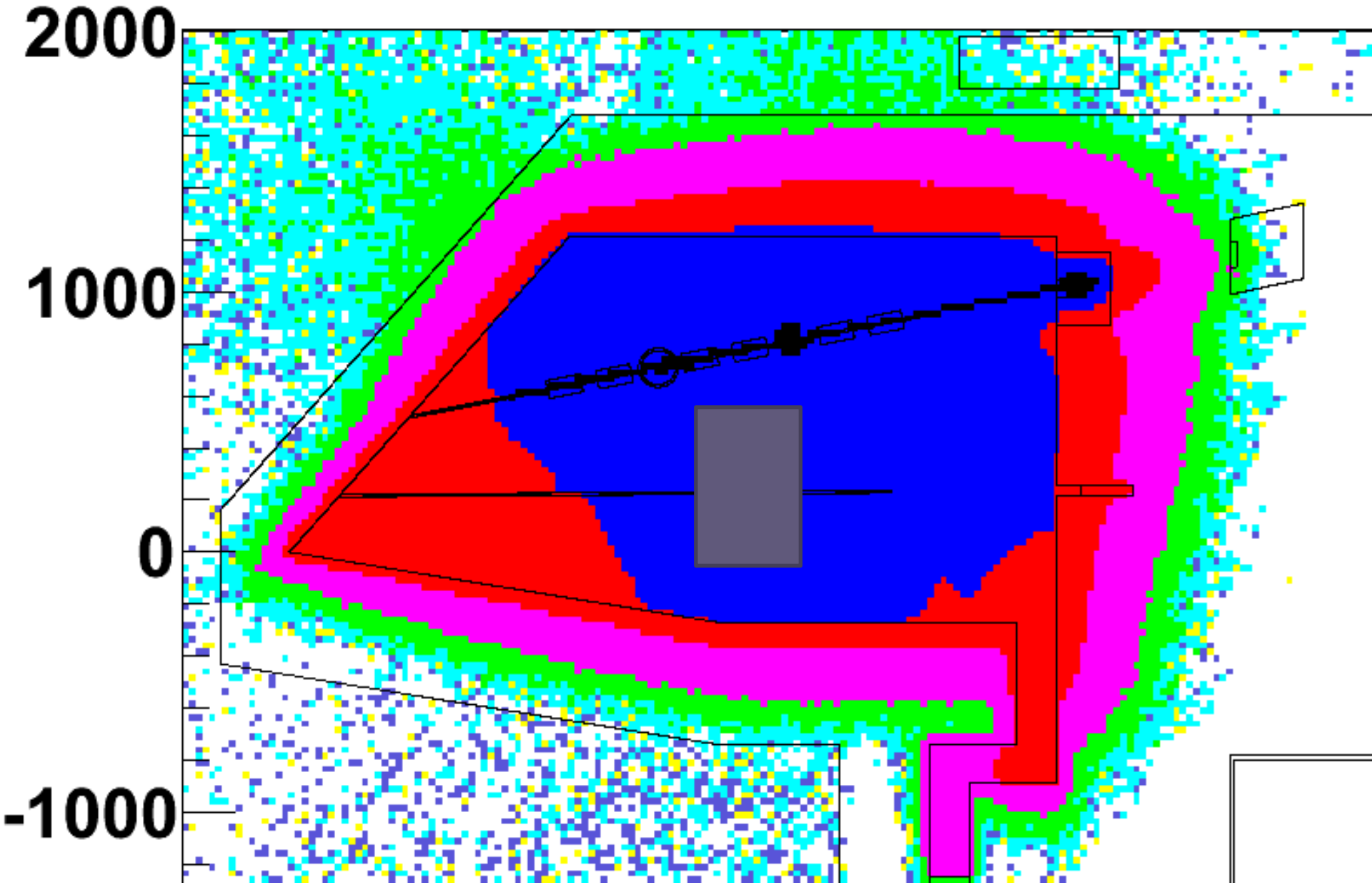

FLINT: X_1+X_2 as minimum

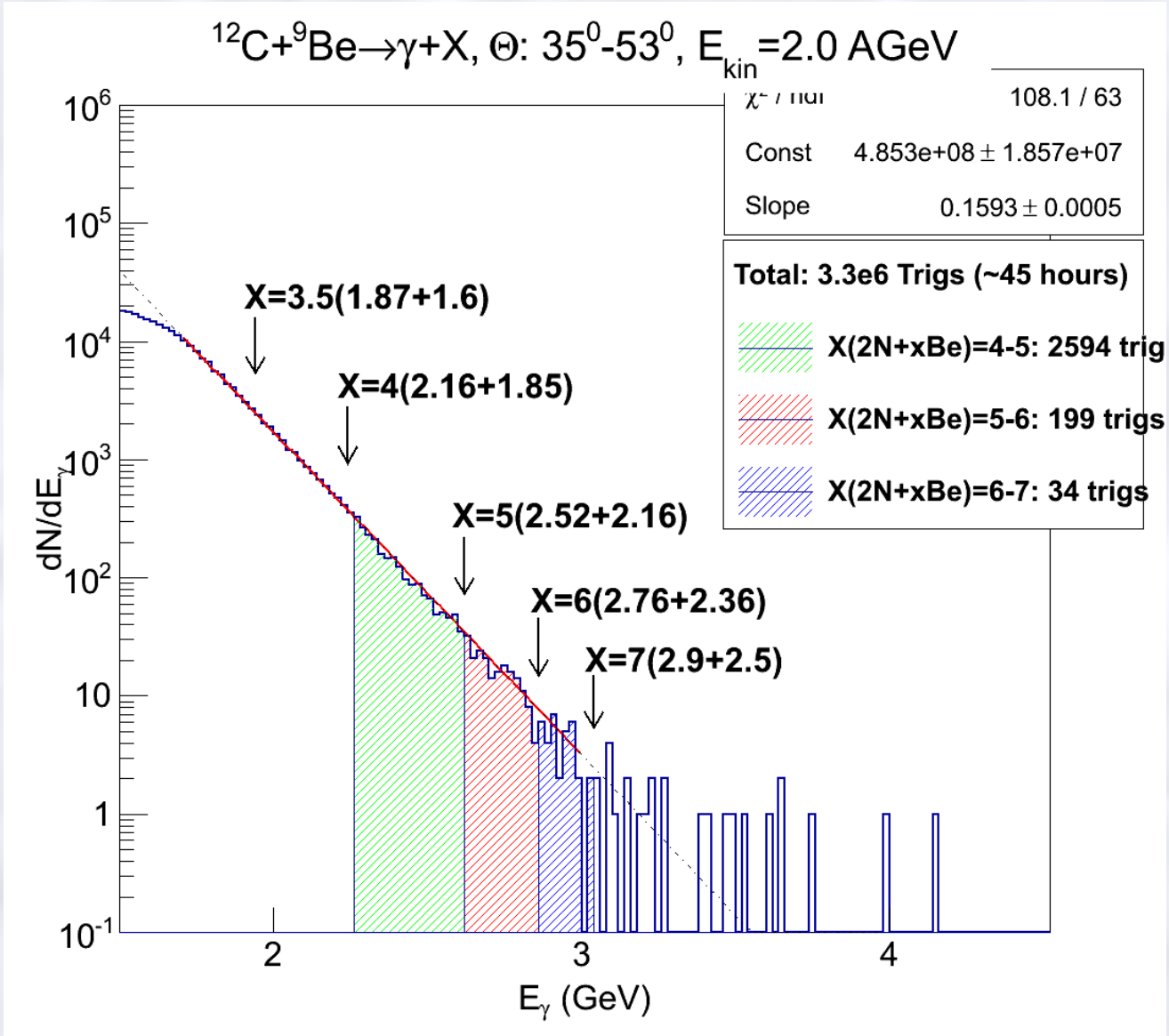

Cross-Talks

J.Pluta et al. NIM A411(1998) 417

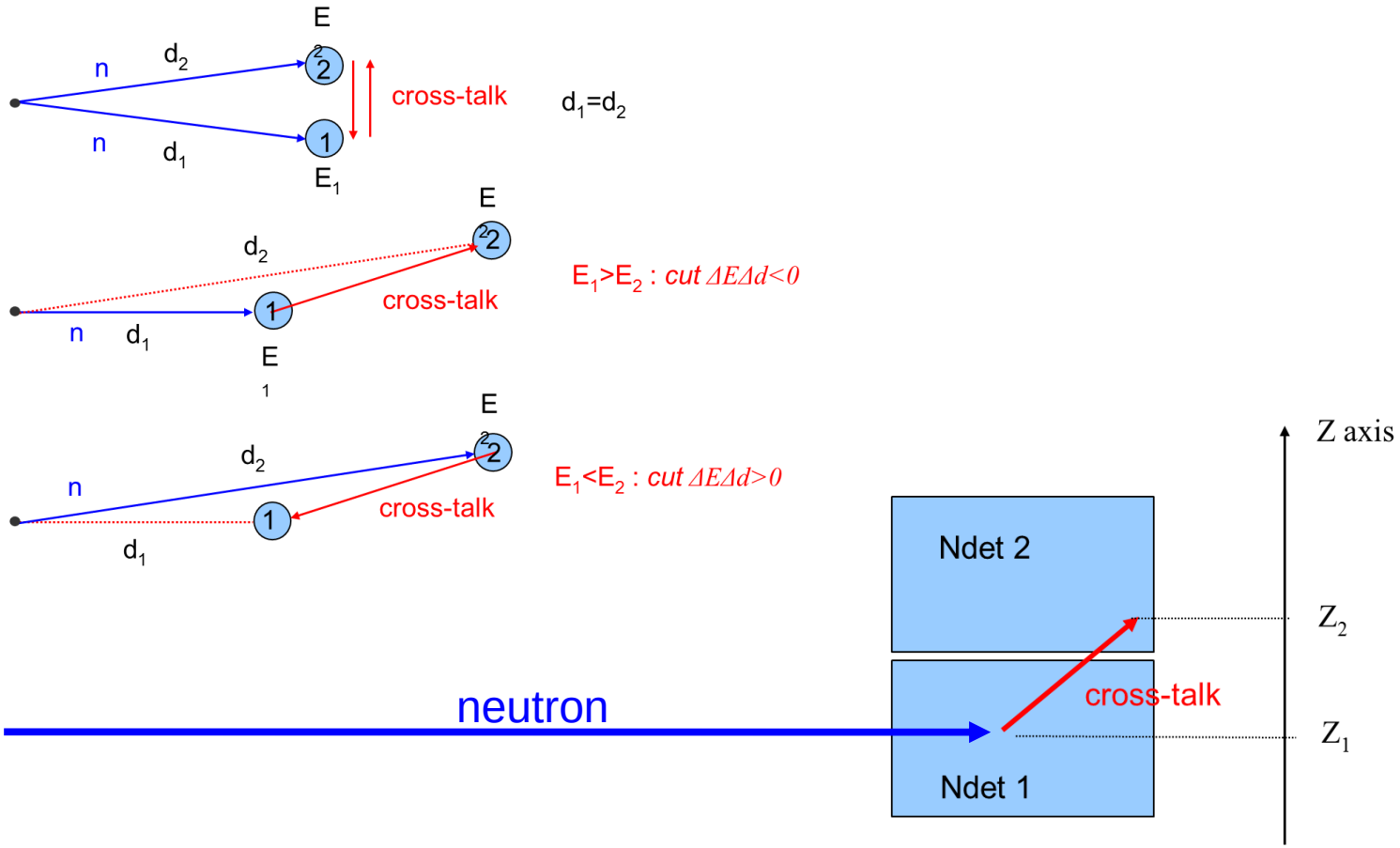

Position sensitive neutron detector could be help to reject cross-talk if we do the cut on coordinate?

Neutron detector (first prototype)-ITEP

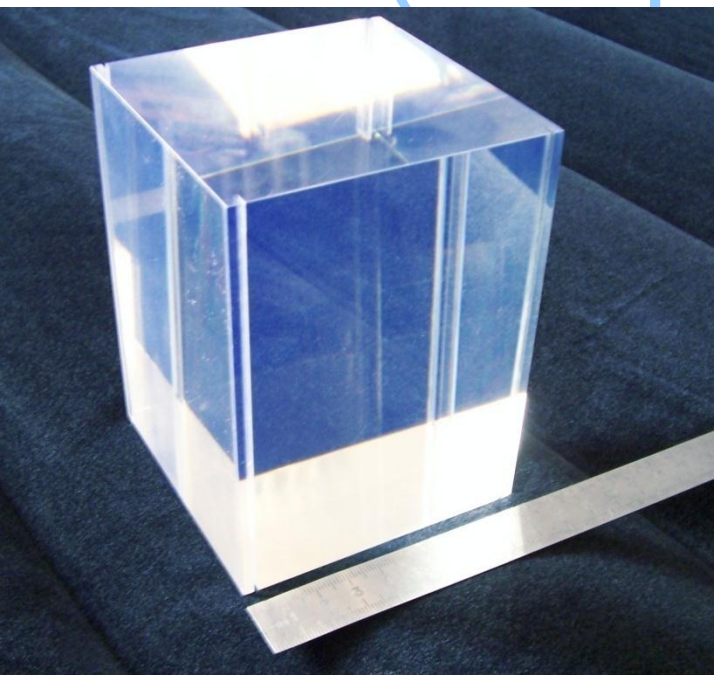

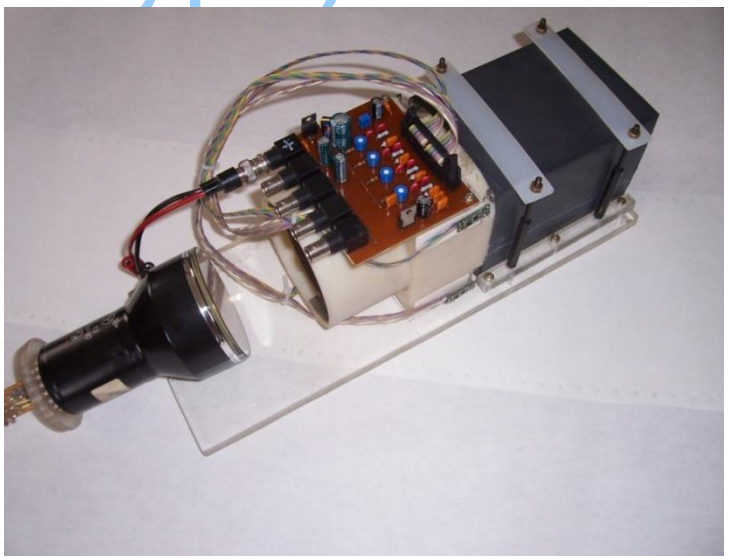

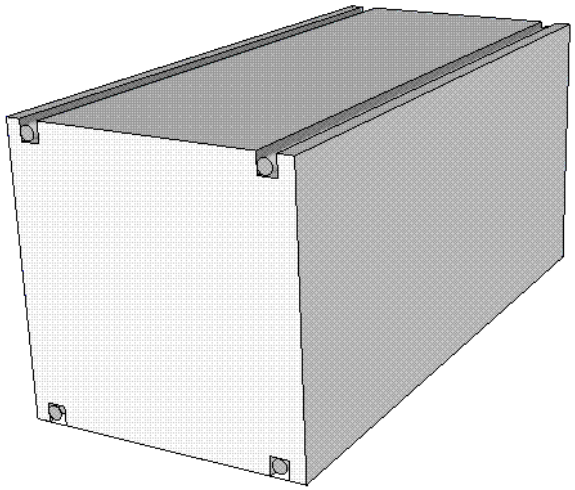

Plastic Scintillator 96 * 96 * 128 mr

Fiber: KYRARAY,Y-11,d =1mm,

wavelength shift

4 MRS APD & Amplifier - CPTA(Go

Efficiency (estimate) 15%

Beam tests of prototype

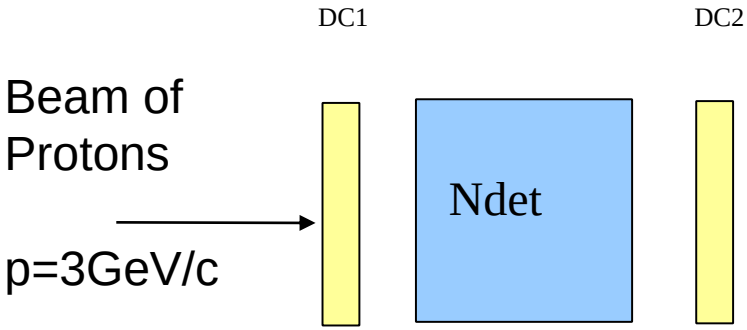

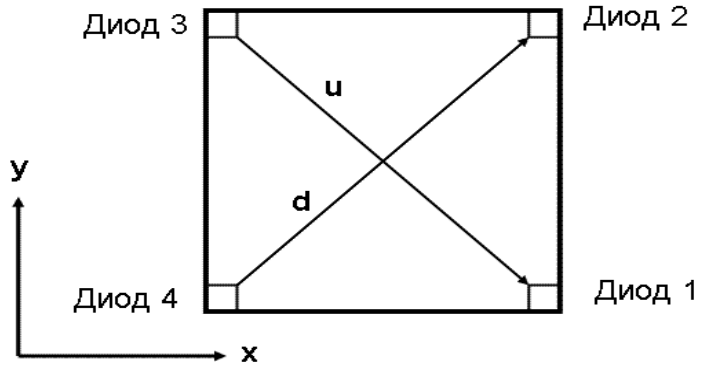

Ratio ($R=A_4/A_1$) of amplitude as exp(-R/d)

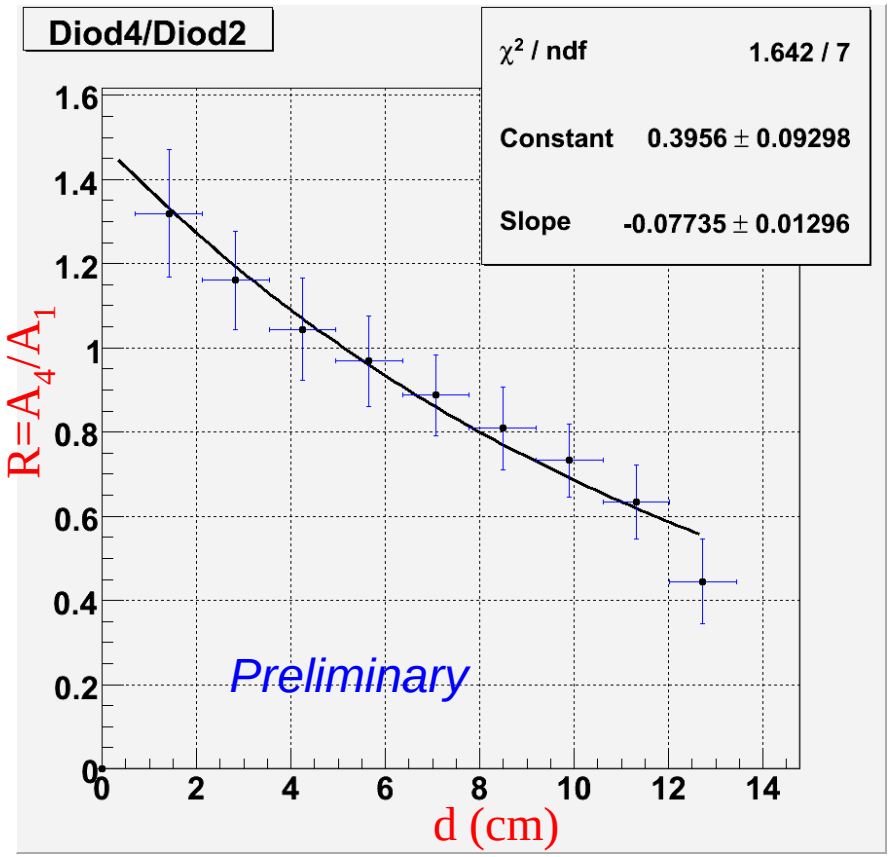

5. Detector for DCM study-12

AmpDiod 3

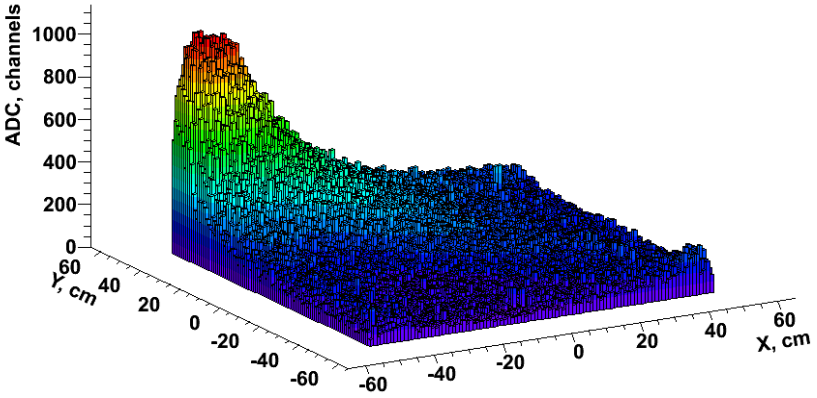

AmpDiod 2

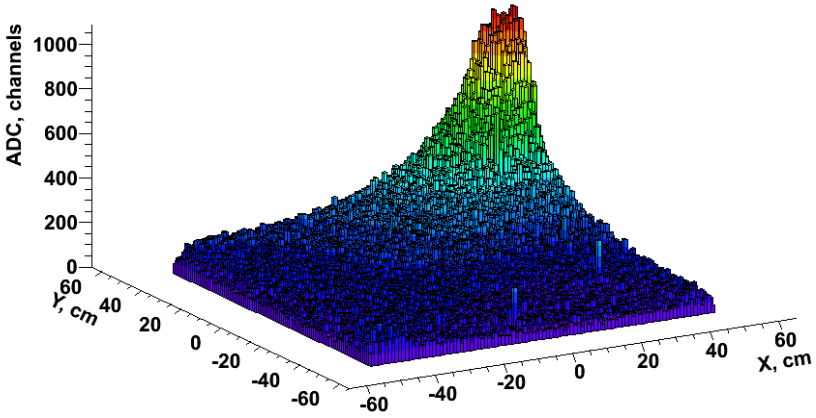

AmpDiod 4

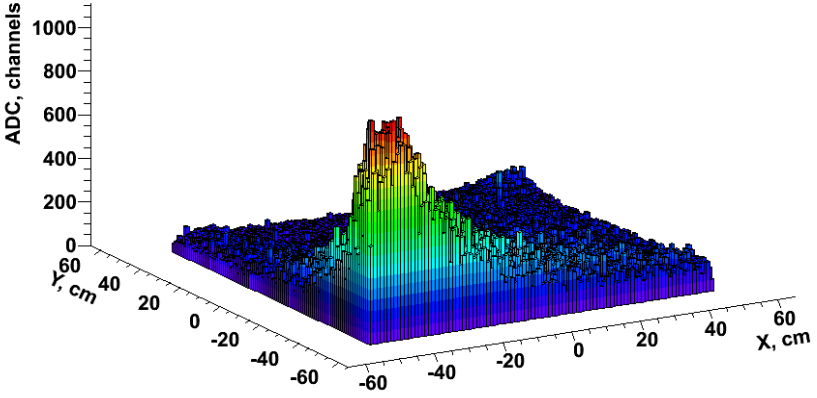

AmpDiod 1

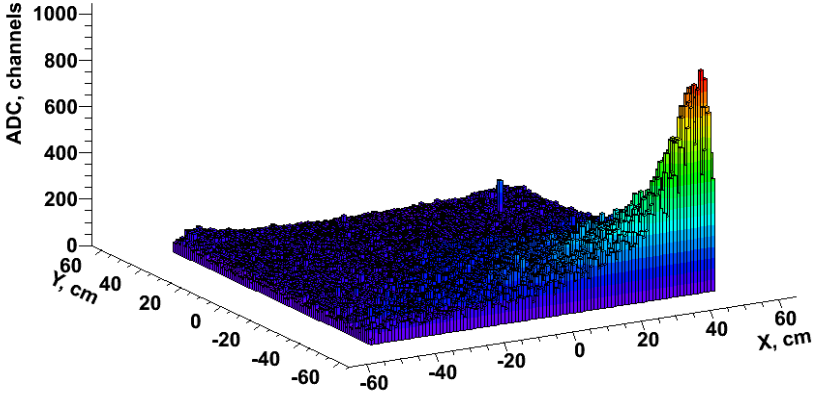

Does the theory of DCM really exist?

Lattice QCD at finite baryon density :

“The problem is that at μ≠0 the fermionic determinant is complex and the well known Monte-Carlo techniques cannot be applied”

For a review, see, for example, I.Barbour et al.,arXiv:9705042[hep-lat]

For resent reference, see, for example P.Huovinen and P.Petreczky,arXiv:1106.6227v1[nucl-th](QM2011,Annecy)

Color superconductivity:

See, for example,

M.Alford,K.Rajagopal,F.Wilczek,arXiv:9711395v4[hep-ph]

Diquark Bose Condensates:

See, for example,

R.Rapp,T.Schafer,E.Shuryak,M.Velkovsky,arXiv:9711396v1[hep-ph]

Opposite sign correlations

Our purpose here is to point out that if a manyboson or many-fermion system exhibits opposite sign correlations, then the state in question necessarily has a certain complexity. For example, consider a fermion gas. If the gas exhibits any positive pair correlations when it has been prepared in a certain state, then that state cannot be represented by a simple Slater determinant wavefunction. In general, if one probes a many-boson or many-fermion state and finds that it exhibits opposite sign correlations, then, even without any model for the unknown state, one may infer that it is not a “free” state, i.e., it does not have the form of a grand canonical ensemble for noninteracting indistinguishable particles. We believe that opposite sign correlations can be observed in current experimental setups and may even have already been observed and passed unnoticed.

Ref.:Alex D. Gottlieb and Thorsten Schumm, arXiv:0705.3491 [quant-ph]

Quantum Correlations with Metastable Helium Atoms

K.G.H. Baldwin

Helium in the long-lived metastable state (He*) has the unique property amongst other BEC species that single atoms can be detected with nanosecond temporal resolution (1). This enables experiments that measure the quantum statistical properties of atoms in the same way that quantum optics opened up a new way to study light following the development of the laser. The seminal work of Glauber (2) used quantum theory to describe the coherence properties of photon statistics beyond classical theory: distinguishing between classical, first-order coherence of the light intensity and the quantum coherence between n multiple photons (nth-order correlations) - a perfectly coherent source is coherent to all orders.

For example, measurement of the arrival time of individual photons at a detector enables the correlation between pairs (second-order), triplets (third-order), and higher-order groups of photons to be determined. An incoherent source of light will exhibit bosonic photon bunching— that is, an enhanced probability of groups of photons arriving within an interval that defines the coherence time of the source. Second-order correlations were first demonstrated in the famous Hanbury Brown and Twiss (HBT) experiment (3). Conversely, a highly coherent light source such as a laser will exhibit no bunching, with a uniform arrival-time probability for pairs, triplets, and larger groupings of photons; this indicates long-range coherence to all orders in the correlation functions.

The same concepts can be applied to the quantum statistics of matter waves. Specifically, incoherent sources of bosonic atoms have also been shown to exhibit HBT-like (second-order) bunching behavior (4), whereas incoherent fermionic sources exhibit anti-bunching (a reduced probability of particles being found close together) (5) as a consequence of the Pauli exclusion principle.

Fig. 1. Experimental setup for measuring atom correlations: An ensemble of He* atoms (red spheres) falls under gravity onto the MCP detector creating a series of detection events (yellow) separated in space and time. Third-order correlations measure arrival time differences between three atoms (right).

In this talk we will also present recent experiments in our laboratory which have measured atomic correlation functions to demonstrate the higher order coherence of a BEC (in analogy to the laser) [6], and which demonstrate the link between atomic speckle and temporal correlation functions [7].

References

[1] K.G.H. Baldwin, *Contemp. Phys.* ***46, 105 (2005).*** [2] R.J. Glauber, *Phys. Rev.* ***130, 2529 (1963).***
[3] R. Hanbury Brown and R.Q. Twiss, *Nature* ***177, 27 (1956).*** [4] M. Schellekens et al., *Science* ***310, 648 (2005).***
[5] T. Jeltes et al., *Nature* ***445, 402 (2007).*** [6] S.S. Hodgman et al., *Science* ***331, 1046 (2011).***
[7] R.G. Dall et al., *Nature Communications* ***2, article 291 (2011).***

Cumulative particle production

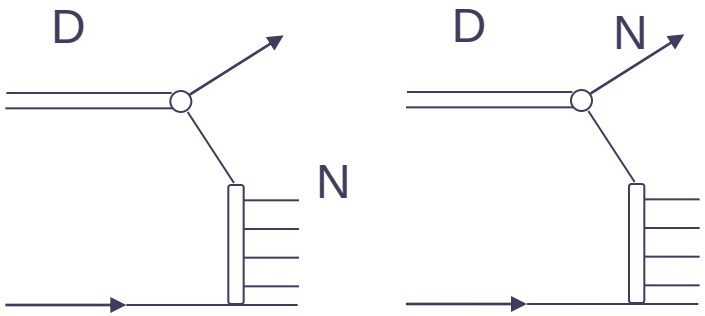

L. Frankfurt and Strikman
Phys. Let. 76B,3 (1978)

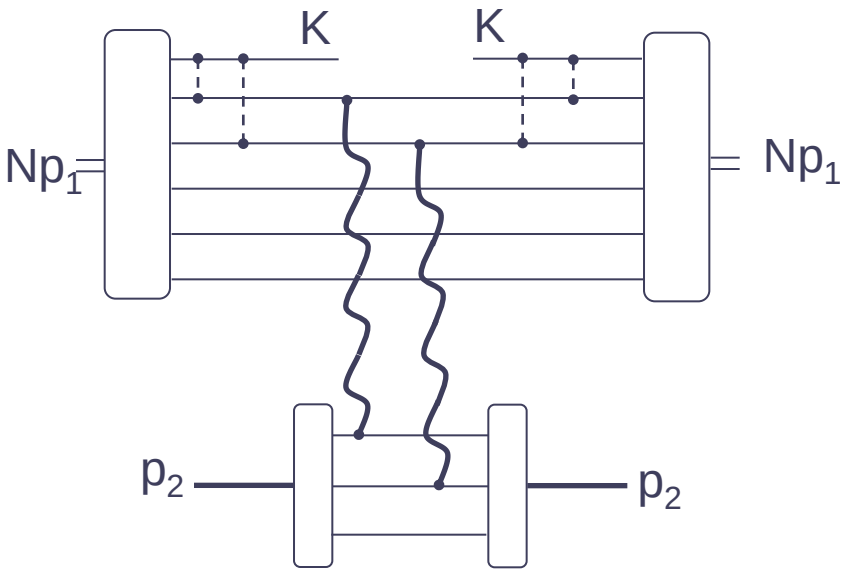

M. Braun and V. Vechernin,
Nucl. Phys. B **427**, 614 (1994)

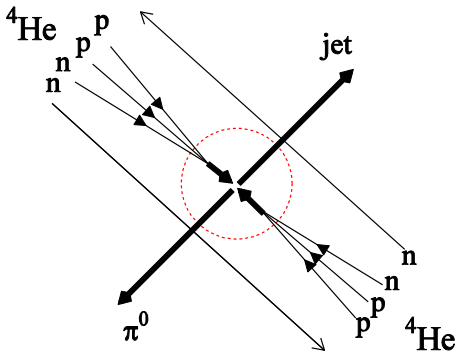

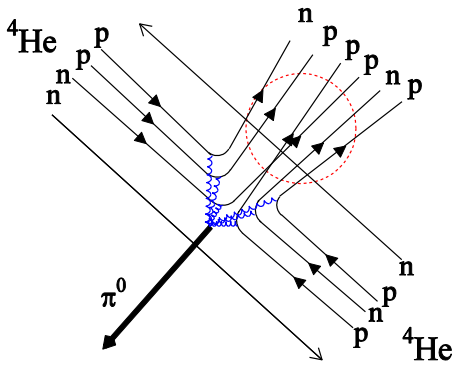

aA(flucton) N_{max} ~ 4

Possible solutions :

~~Fragments~~

~~Lower initial energy~~

not only formally large cumulative number, but also b_{ik}»1(A.M.Baldin)

AA(flucton+flucton): N_{max}~7-8

Cumulative number

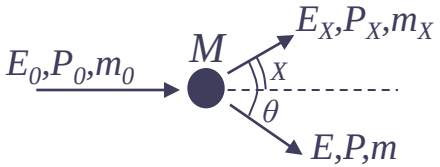

$$\begin{cases} E_0 + M = E + E_X \\ p_0 = p\cdot\cos\theta + p_X\cdot\cos X \\ 0 = p\cdot\sin\theta + p_X\cdot\sin X \\ m_X^2 = (m_0 + M)^2 \end{cases} \Rightarrow \begin{cases} E_X^2 = E_0^2 + M^2 + E^2 + 2E_0M - 2EM - 2E_0E \\ p_X^2 = p_0^2 + p^2 - 2p_0p\cos\theta \\ m_X^2 = (m_0 + M)^2 \end{cases}$$

$$X\cdot m_N = M = \frac{E_0E - p_0p\cos\theta - m^2/2}{T_0 - E}$$

1+N	4,0	1+(N+1)	5,0
2+N	1,9	2+(N+2)	3,9
3+N	1,6	3+(N+3)	4,6

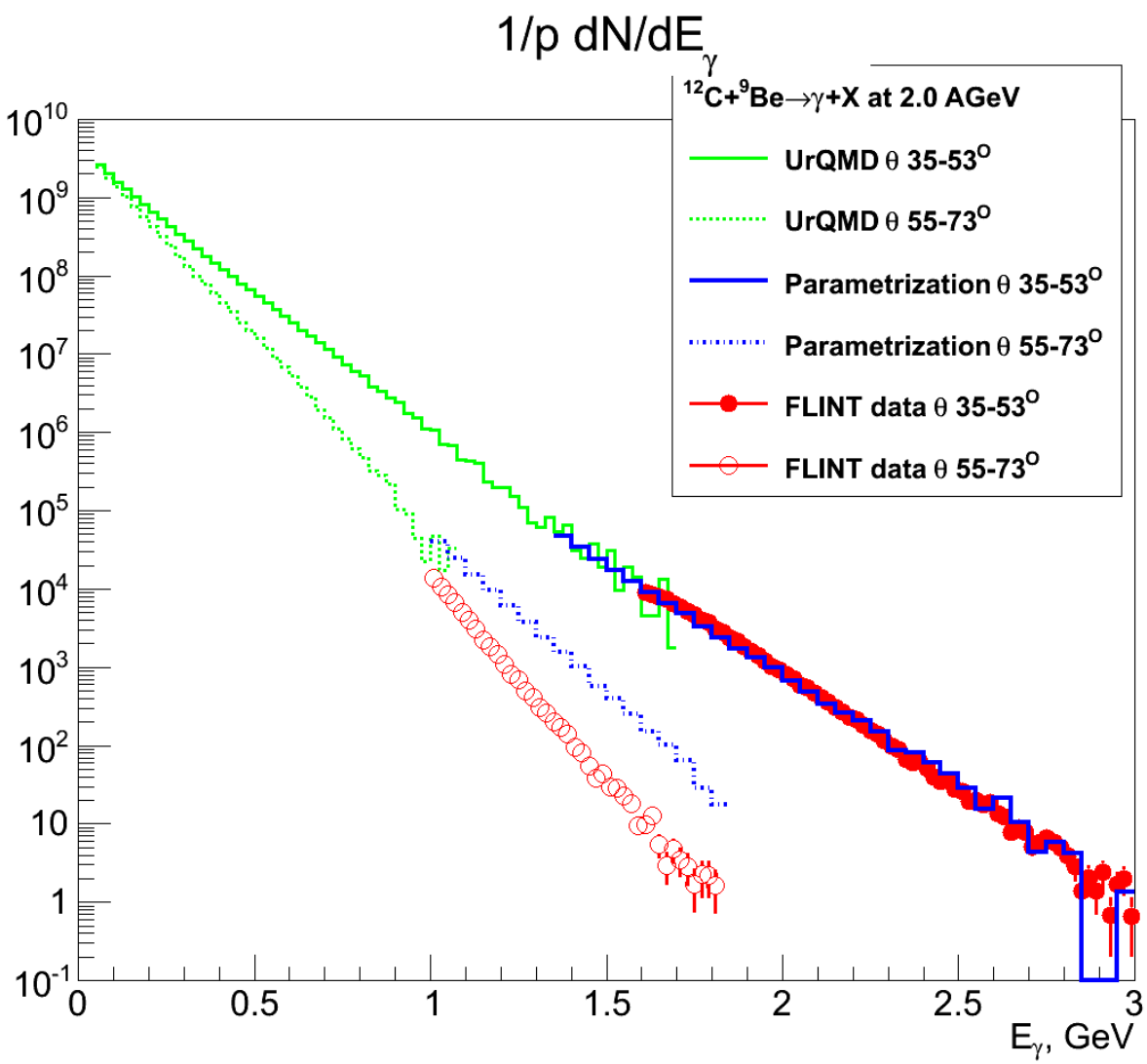
1/p dN/dE$_\gamma$
^{12}C+^{9}Be→γ+X at 2.0 AGeV
UrQMD θ 35-53°
UrQMD θ 55-73°
Parametrization θ 35-53°
Parametrization θ 55-73°
FLINT data θ 35-53°
FLINT data θ 55-73°
10^{10}
10^{9}
10^{8}
10^{7}
10^{6}
10^{5}
10^{4}
10^{3}
10^{2}
10
1
10^{-1}
0
0.5
1
1.5
2
2.5
3
E$_\gamma$, GeV

Fermi motion

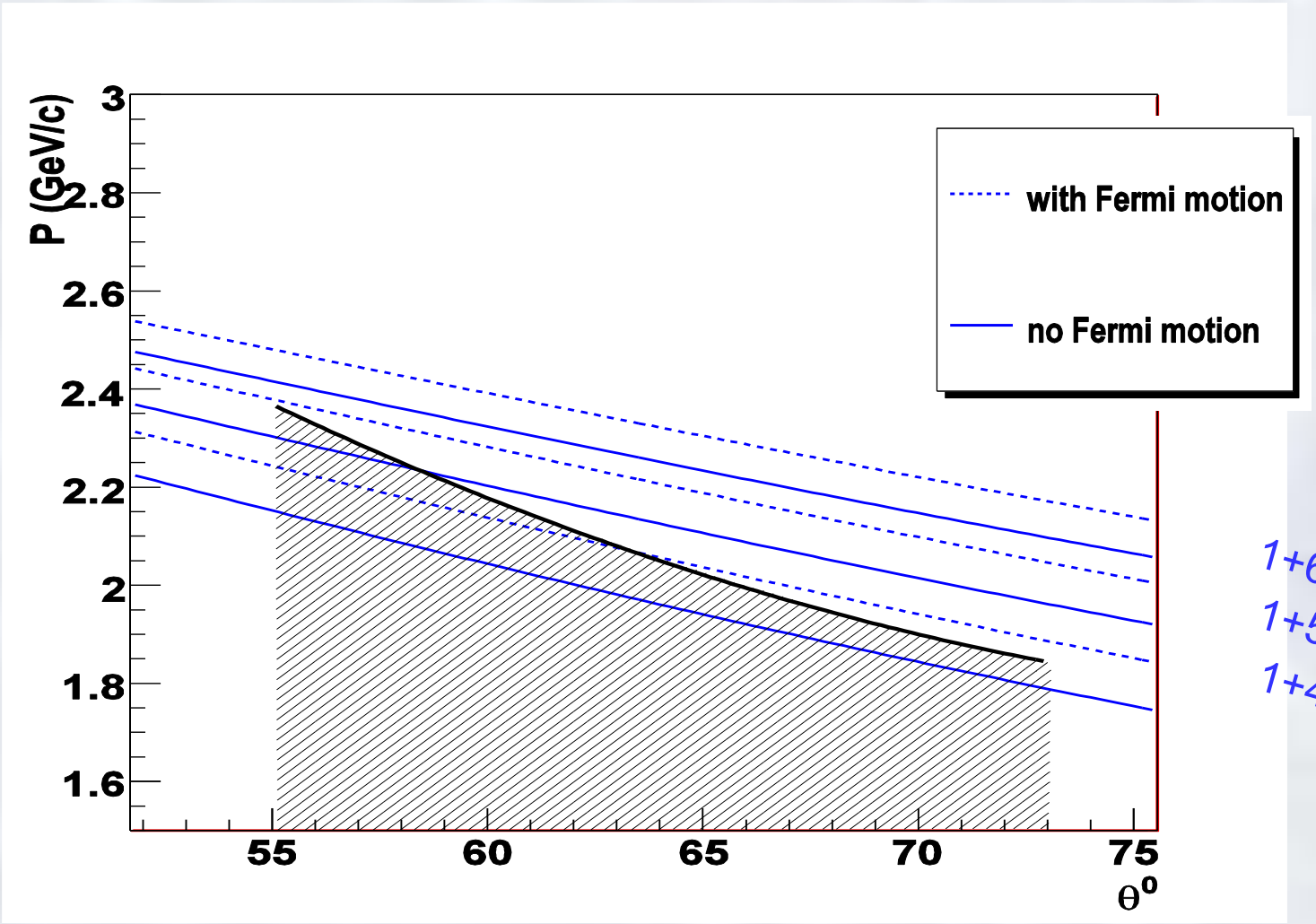

What is the difference between pion and photon cumulative number?

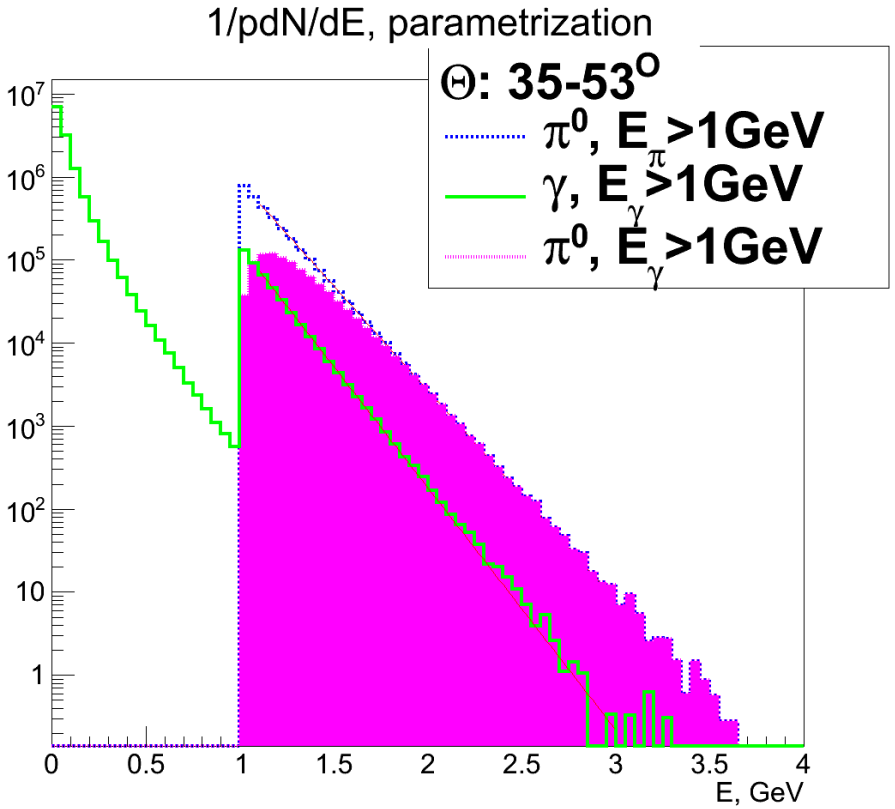

Using the empirical scaling for the beam energy dependence of the Lorentz-invariant cross sections

$$\sigma_I = E\frac{d^3\sigma}{d^3p} \quad (1)$$

found in [20] and parameterizing the angle dependence one can propose the following laboratory momentum dependence of the cross section for the reaction $C+C \rightarrow \pi X$

$$\sigma_I = Cexp(-\frac{p}{p_o}), \quad (2)$$

where C=3800 (mb GeV^{-2} c sr^{-1}) and

$$p_o = \frac{0.075\gamma}{1-\beta(cos\theta - cos45^0) - cos^2 45^0} \quad (3)$$

with β and γ are the Lorentz transformation factors which define the nucleon-nucleon c.m. frame relative to the laboratory frame and depend on the beam energy.

$E_\pi - E_\gamma \sim 0.3GeV \not\Rightarrow$ $Q_\pi - Q_\gamma \sim 1$

C(2GeV/nucleon)+Be→π^0+X, $\pi^0 \rightarrow \gamma\gamma$

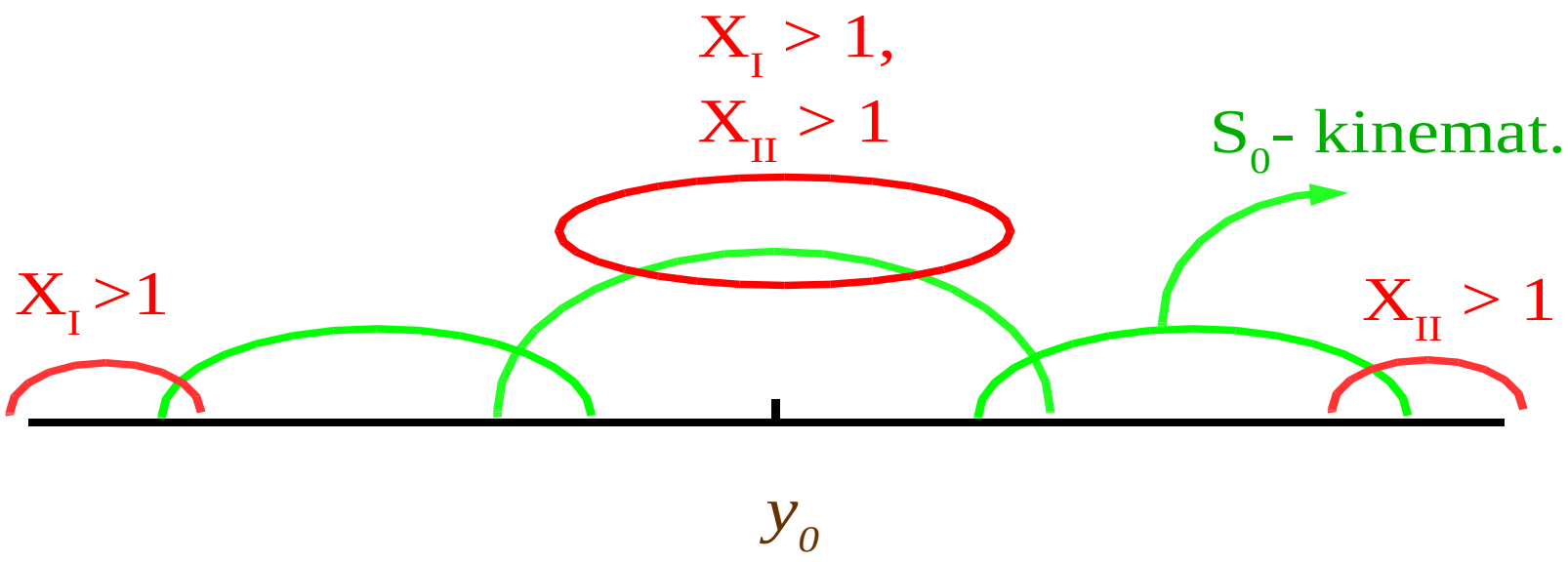

Cumulative processes:

1) $X_I = 1$ and $X_{II} > 1$ } Fragmentation
2) $X_{II} = 1$ and $X_I > 1$ } regions
3) $X_I > 1$ and $X_{II} > 1$ Central region

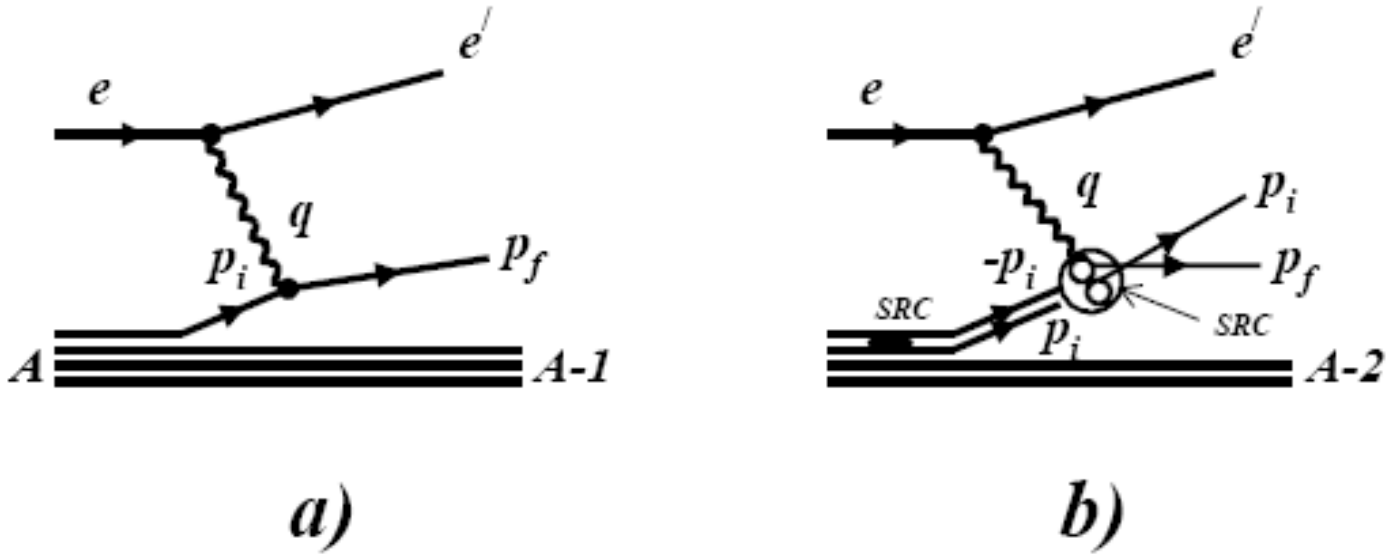

FIG. 1. Two mechanisms of $A(e,e')$ scattering. (a) Single nucleon model; (b) short range correlation model.

Investigation of Proton-Proton Sort-Range Correlations via the C(e,e'pp) Reaction; R.Shneor et al., Hall A JLAB, nucl-ex/0703023

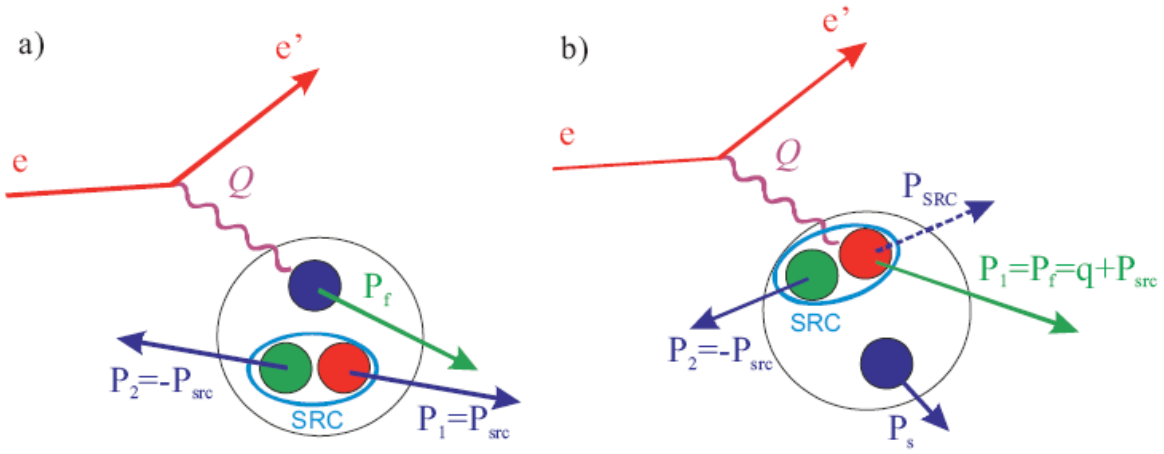

Figure 3. Kinematic diagrams for the two approaches to select SRC in the ^{3}He$(e, e'pp)n$ data. a) shows the approach from ref. [14], which has the constraints that $P_N > 250$ MeV$/c \geq P_{fermi}$, $T_{p1,p2} < 0.2\ \omega$ (ω is the energy transfered by the scattered electron) and $P_{f\perp} < 300$ MeV$/c$. b) shows the approach from ref. [13], which has the constraints that $P_s < 150$ MeV$/c$, $P_1 > 300$ MeV$/c$, and $\theta_{p_2q} > 100°$.

Nature of phase transition @ high baryon density

$$dN = g\frac{4\pi p^2 dpV}{(2\pi h)^3}, \bar{n}_p = \frac{1}{e^{(\varepsilon-\mu)/T}+1}; LL, vol.5, ch.5(1976)$$

$$E = \frac{3}{2}PV = \int_0^{\mu} pdN = g\frac{\mu^4 V}{8\pi^2 h^3}, P = g\frac{\mu^4}{12\pi^2 h^3}$$

$$h \to q \Rightarrow g = 2 \to g = 6$$

$$P_h = \frac{\mu^4}{6\pi^2 h^3} \to P_q = \frac{\mu^4}{2\pi^2 h^3} - B, B \approx\sim 0.17 GeV/fm^3$$

$$P_h = P_q \Rightarrow \mu_c \approx 7B^{1/4} \Rightarrow n_c \approx 5n_0$$

FLINT Experiment @ ITEP : C + Be→ γ + X, 3.2AGeV

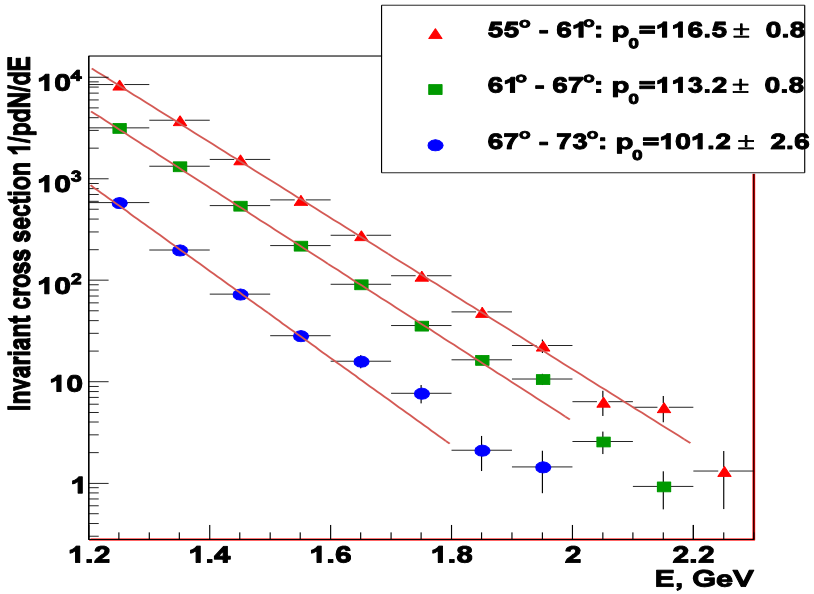

•$T_{0эксп}$=113±10 МэВ

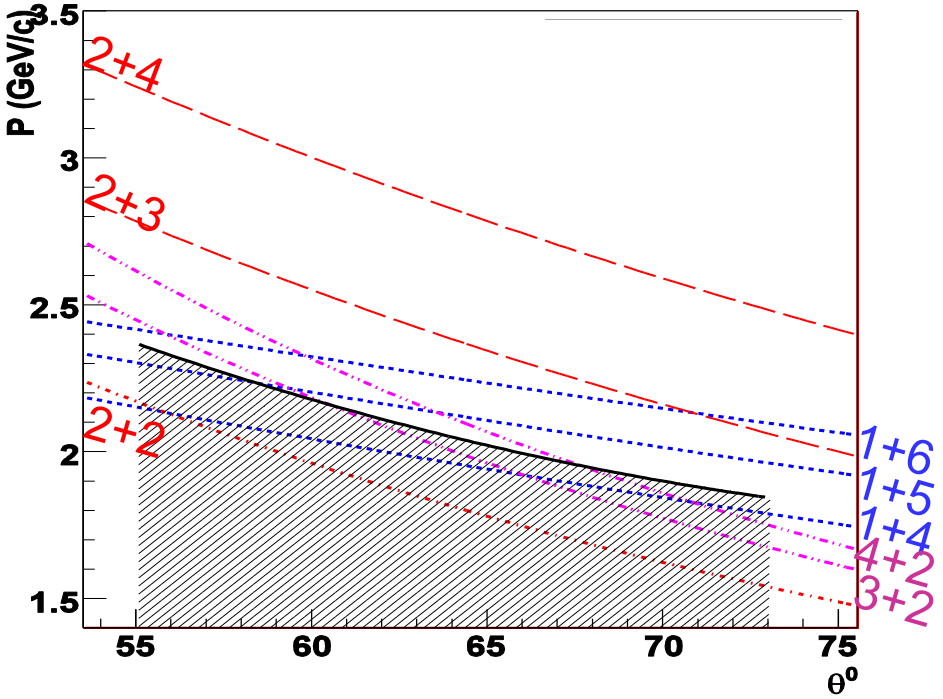

	Δp(X+1), MeV	T_0, MeV	T_0±σ(E), MeV
1N+jN	140±20	20±3	~ 34
iN+2N	160±80	23±11	~ 36
2N+jN	570±70	81±10	~ 83

•2+3 T_0
•close to T_{0exp}

Flucton-flucton interaction !

Cumulative particle production

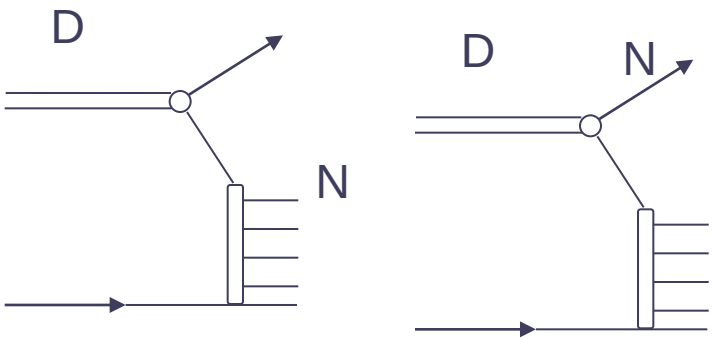

L. Frankfurt and Strikman
Phys. Let. 76B,3 (1978)

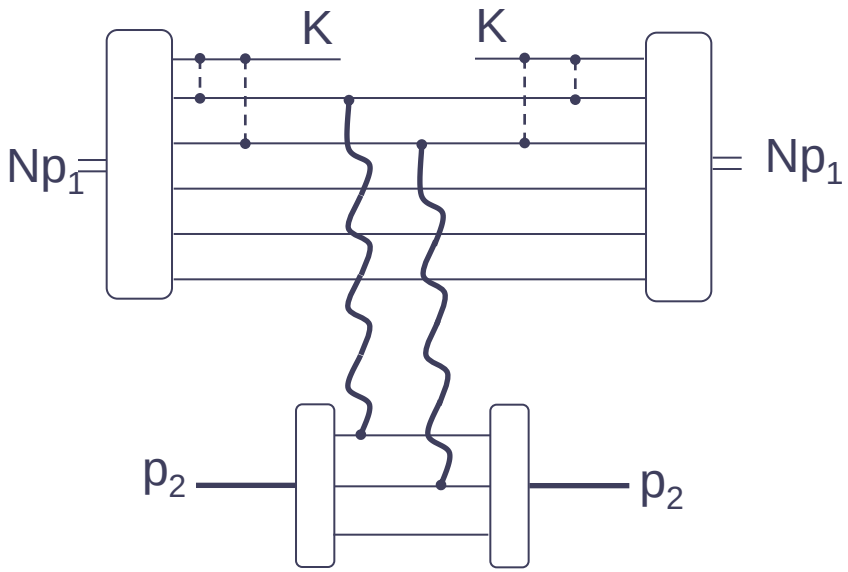

M. Braun and V. Vechernin,
Nucl. Phys. B **427**, 614 (1994)

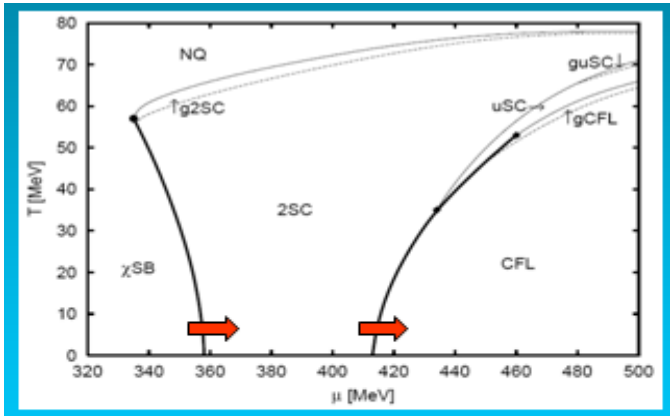

Rüster et al Phys.Rev.D 2005

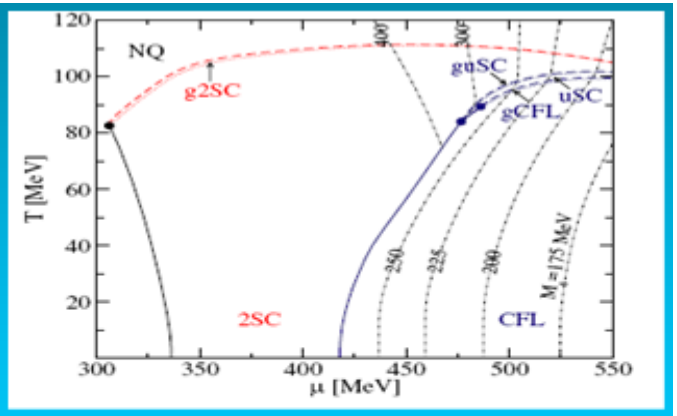

Blaschke et al Phys.Rev.D 2005

Two first order phase transitions:

Hadronic matter ➡ 2SC ➡ CFL

Ref.: Pagliara

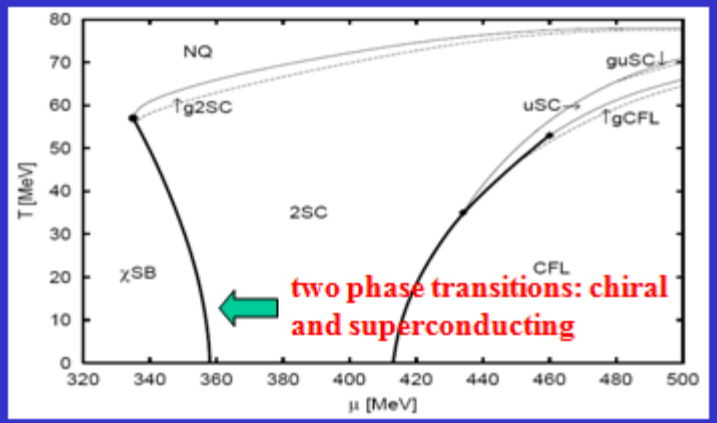

assumption that "deconfinement" and chiral symmetry restoration coincide (see also Bender et al. Phys.Lett.B 1998)

Is the diquark condensate a good order parameter for deconfinement at finite density ??

(see also Bentz et al Nucl.Phys.A 2002)

*Correlations between signatures could be a signal of the two phase transitions as the density increases and the temperature decreases

B decays to baryons

TORSTEN LEDDIG[a,*]
[a]Universität Rostock, Institut für Physik, Universitätsplatz 3, 18055 Rostock - Germany

Abstract. From inclusive measurements it is known that about 7% of all B mesons decay into final states with baryons. In these decays, some striking features become visible compared to mesonic decays. The largest branching fractions come with quite moderate multiplicities of 3-4 hadrons. We note that two-body decays to baryons are suppressed relative to three- and four-body decays. In most of these analyses, the invariant baryon-antibaryon mass shows an enhancement near the threshold. We propose a phenomenological interpretation of this quite common feature of hadronization to baryons.

arXiv:1211.1856v1[hep-ex]

A common feature observed in several B decays to baryons but also outside the B-physics sector is an enhancement at the invariant baryon-antibaryon mass threshold which can be seen for three examples in Fig. 1.

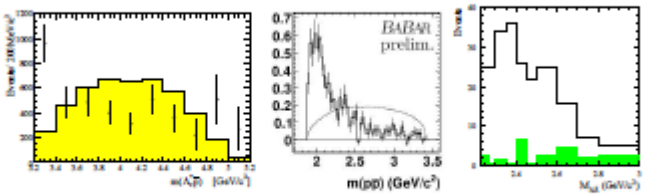

Figure 1. The enhancement observed at the baryon-antibaryon mass threshold in $B^0 \to \Lambda_c^+ \bar{p}\pi^0$ [1] (the yellow histogram represents the phase space expectation), $B^0 \to D^0 p\bar{p}$ [2] (the dotted line represents the phase space expectation) and $e^+e^- \to \Lambda\Lambda\gamma$ [3] (The shaded histogram shows fitted background).

Another feature of these decays is the multiplicity dependence of the branching fractions. Measurements from BABAR, Belle and CLEO show that the largest branching fractions for B decays to baryons come with quite moderate multiplicities. Comparing the

$$\mathcal{B}(\overline{B}^0 \to \Lambda_c^+ \overline{p})$$
$$\times 14$$
$$\mathcal{B}(B^- \to \Lambda_c^+ \overline{p}\pi^-)_{\text{non-res}}$$
$$\times 2.3$$
$$\mathcal{B}(\overline{B}^0 \to \Lambda_c^+ \overline{p}\pi^+\pi^-)_{\text{non-res}}$$
$$\times 3.4$$
$$\mathcal{B}(B^- \to \Lambda_c^+ \overline{p}\pi^-\pi^+\pi^-)$$

$$\mathcal{B}(B^- \to \Sigma_c^0(2455)\overline{p})$$
$$\times 4.3$$
$$\mathcal{B}(\overline{B}^0 \to \Sigma_c^0(2455)\overline{p}\pi^+)$$
$$\times 2.9$$
$$\mathcal{B}(B^- \to \Sigma_c^0(2455)\overline{p}\pi^+\pi^-)$$

$$\mathcal{B}(\overline{B}^0 \to \Lambda_c^+ \overline{p})$$
$$\times 9.5$$
$$\mathcal{B}(\overline{B}^0 \to \Lambda_c^+ \overline{p}\pi^0)$$
$$\times 9.5$$
$$\mathcal{B}(B^- \to \Lambda_c^+ \overline{p}\pi^-\pi^0)$$

Figure 2. Relative change of the branching fractions for a subset of baryonic B decays.

Figure 3. Effective Feynman diagrams for the initial meson-meson configuration.

Figure 4. Effective Feynman diagrams for the initial diquark-antidiquark configuration.

4. Kinematical trigger -3

Two possible scenarios of flucton-flucton interaction

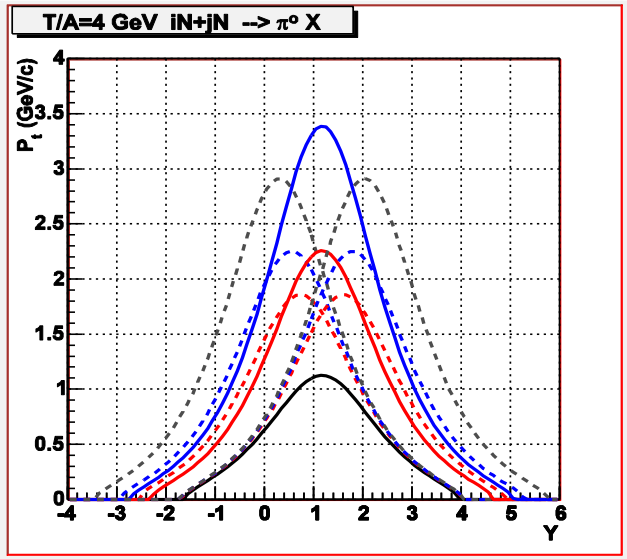

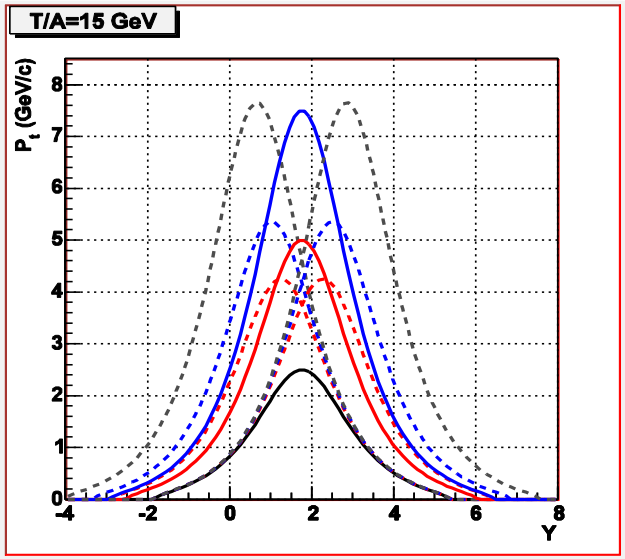

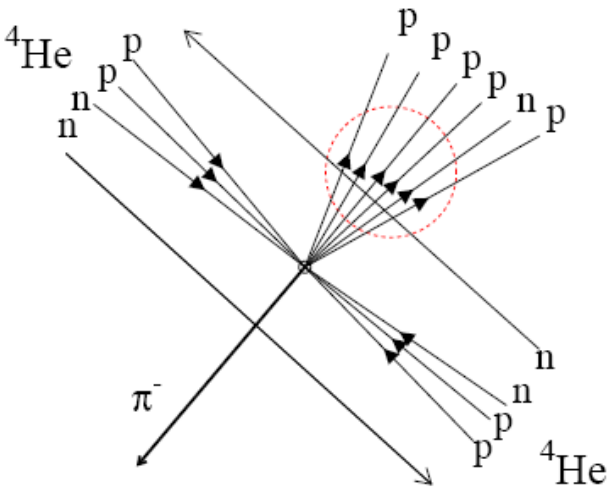

Dense baryon system with high p_t

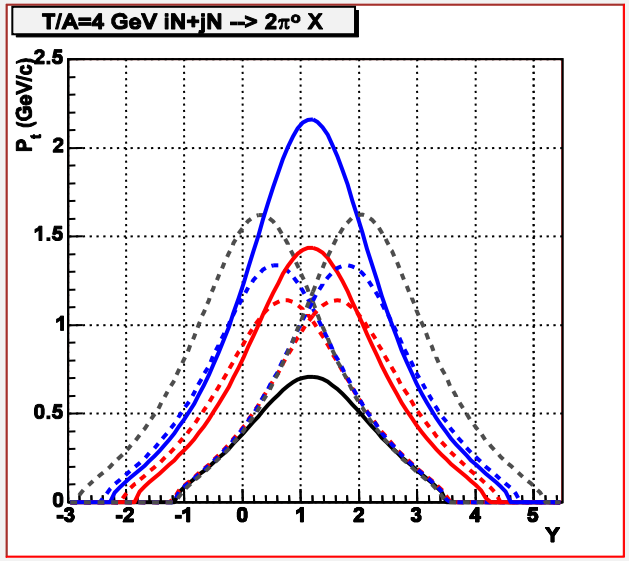

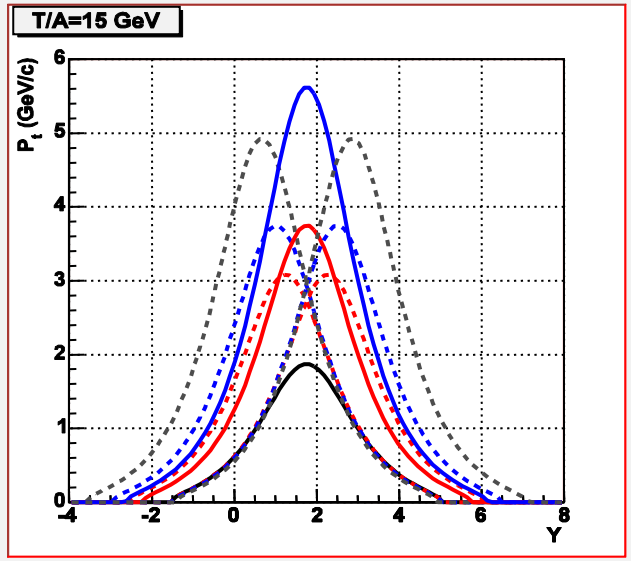

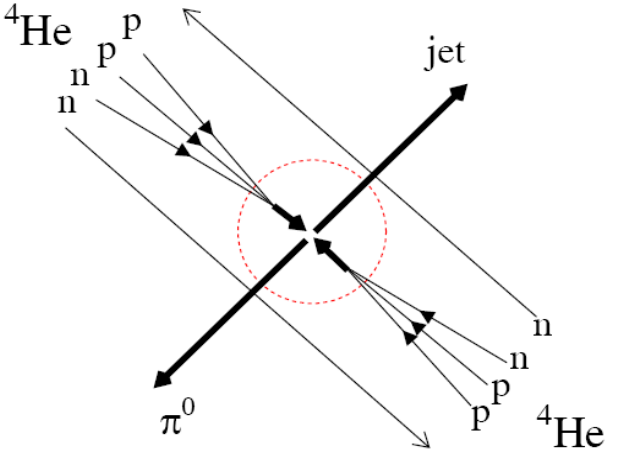

Dense baryon system with low p_t

Limits for N_i+N_j:1+1,1+3,1+5,1+12,2+2,3+3

Search for and study of cold dense baryonic matter
(Letter of intent)

I.G.Alexeeev[1], A.A.Golubev[1], V.S.Goryachev[1], A.G.Dolgolenko[1], N.M.Zhigareva[1], Yu.M.Zaitsev[1], K.R.Mikhailov[1], M.S.Prokudin[1], M.I.Katz[1], B.O.Kerbikov[1], S.M.Kiselev[1], N.A.Pivnyuk[1], P.A.Polozov[1], D.V.Romanov[1], D.N.Svirida[1], A.V.Stavinskiy[1], V.L.Stolin[1], G.B.Sharkov[1] , A.Andronenkov[2], A.Ya. Berdnikov[2] , Ya.A. Berdnikov[2], M.A. Braun[2], V.V. Vechernin[2], L. Vinogradov[2], V. Gerebchevskiy[2], S. Igolkin[2], A.E. Ivanov[2], V.T. Kim[3,2], A. Koloyvar[2], V.Kondrat'ev[2], V.A.Murzin[3], V.A. Oreshkin[3], D.P. Suetin[2] ,G. Feofilov[2],A.A.Baldin[4], V.S.Batovskaya[4], Yu.T. Borzunov[4], A.V. Kulikov[4],A.V. Konstantinov[4], L.V.Malinina[4],G.V.Mesheryakov[4],A.P.Nagaitsev[4], V.K. Rodionov[4], S.S.Shimanskiy[4], O.Yu.Shevchenko[4]

1). SSC RF ITEP , Moscow, 2). SPbSU, S.Peterburg, 3). SSC RF PINF, S.Peterburg, 4). LPHE,JINR,Dubna

Detector for DCM study-2

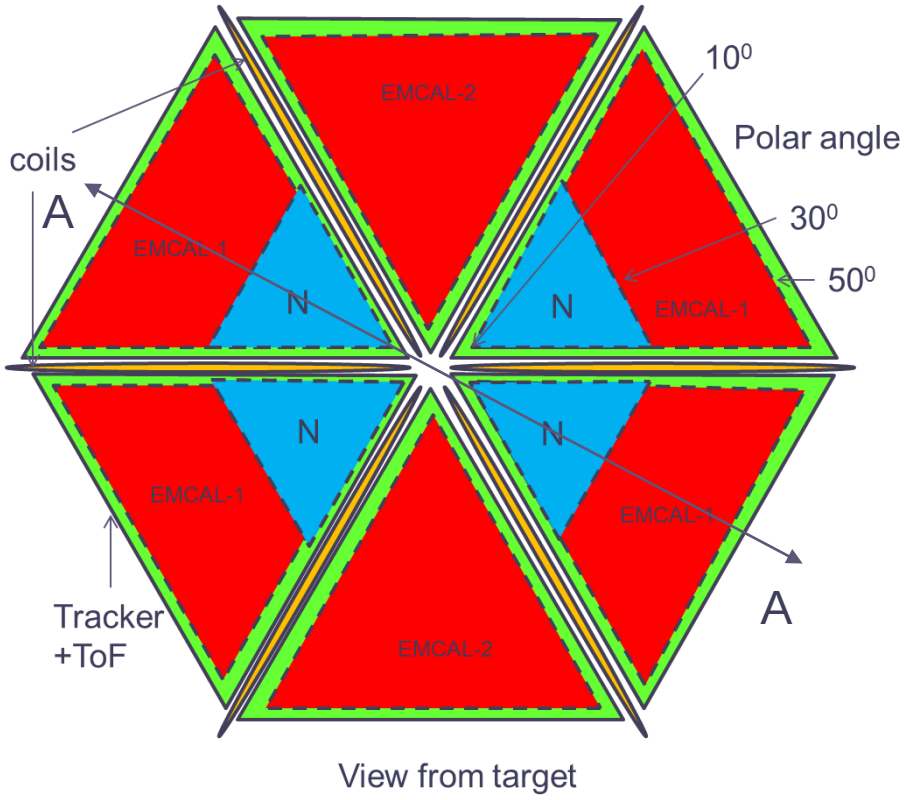

View from target